
Long-term bio-geomorphological modelling of the formation and succession of salt marshes

- MSc Thesis -



Author: Ype ATTEMA
Date: December 22, 2014

Long-term bio-geomorphological modelling of the formation and succession of salt marshes

By

Ype ATTEMA

in partial fulfilment of the requirements for the degree of

Master of Science

in Civil Engineering

DELFT UNIVERSITY OF TECHNOLOGY (TUD)

Faculty of Civil Engineering and Geosciences

Department of Hydraulic Engineering

NATIONAL UNIVERSITY OF SINGAPORE (NUS)

Faculty of Engineering

Department of Civil and Environmental Engineering

Graduation Committee:

Prof.dr.ir J.A. ROELVINK (TUD / IHE), Chairman

Dr.ir. B.C van PROOIJEN (TUD), Supervisor TUD

Dr.ir. R.J. LABEUR (TUD), Supervisor TUD

ir. G. DAM (Svašek), Supervisor Svašek

Dr.ir. V.P. CHUA (NUS), Supervisor NUS

Abstract

Salt marshes are complex and delicate coastal ecosystems that fulfil a variety of vital functions. For instance, they are of ecological importance and form an effective natural barrier that captures sediments and stabilizes the shoreline. In the past these values were not recognized and substantial loss of marsh areas occurred. Fortunately, nowadays these values are widely recognized and this has resulted in protective regulations and management. However, managing and protecting these tidal ecosystems is a complicated task due to the dynamic character and the complex feedback mechanisms between biology, ecology and geomorphology (Bouma et al., 2007). In view of this, numerical models can be a potential tool to identify important dynamic processes and feedback mechanisms to simulate long term geomorphological evolution.

This thesis aims to contribute to the understanding of the influence of vegetation on the salt marsh development. For this reason the objective is to assess to what extent vegetation modelling can contribute to the long-term morphodynamic prediction of salt marsh formation and succession.

The interaction between vegetation and the morpho-hydrodynamics is considered to be a crucial aspect of the salt marsh formation and development process. The vegetation alters the hydrodynamic forces, which can cause flow concentration and channel initiation (Temmerman et al., 2007), in addition to the ability of vegetation to capture and trap sediments (Wesenbeeck, 2007). It is hypothesised that the inclusion of a vegetation model in the process-based morphodynamic models is therefore essential to reproduce and predict the morphodynamic development of the formation and succession of salt marshes.

There are various ways of representing vegetation growth and the interaction with the morpho-hydrodynamics in a bio-geomorphological model. In this research two vegetation models are adopted, the population dynamics model based on the method developed by Temmerman et al. (2007) and the window of opportunity model, which is a newly developed method based on the window of opportunity concept (Balke et al., 2011). The essence of these vegetation methods is to capture the temporal and spatial vegetation growth characteristics in one normative variable, the vegetation stem density. This vegetation stem density is related to the morpho-hydrodynamics through the representative roughness and shear stress approach developed by Baptist (2005). These vegetation models have been implemented in the morpho-hydrodynamics modelling software FINEL2d, developed by Svašek Hydraulics.

The assessment of the bio-geomorphological models in a sensitivity analysis contributes to gain insight in the functioning, performance and sensitivity of the models. A comparison of the baseline simulations reveals that both models are capable of representing salt marsh characteristic morphological and hydrodynamic phenomena, i.e. overgrown marsh platform dissected by tidal creeks, realistic flow velocities and characteristic sedimentation/erosion patterns. Whereas the purely morphological simulations show barely any morphological activity. In addition, the importance of certain processes, parameters or numerical/theoretical assumptions in the bio-geomorphological models have been assessed in the sensitivity simulations. Therefore a selection of parameters have been varied separately. The results of the sensitivity simulations are compared to the baseline simulation to identify qualitative and quantitative differences. From this comparison, it is found that the vegetation patterns are inherently sensitive to changes in the input parameters, but that the quantitative vegetation growth characteristics and the global patterns appear to be rather robust.

To evaluate the practical applicability and the performance of the bio-geomorphological models in a case study, they have been deployed to hindcast the formation and succession of 'The drowned land of Saeftinghe' over 100 years. The starting point of this long-term hindcast is the bathymetry of 1905, when no salt marsh or tidal flat was present in Saeftinghe. The results of the case study simulations demonstrate that the models are capable of reproducing the development of channels, tidal creeks and tidal flats in Saeftinghe, although not at the exact locations. Further, the simulations show characteristic overgrown vegetated marsh platforms dissected by tidal creek systems on the tidal flats. The performance of the models is reflected in a positive Brier-Skill Score of around 0.8, which indicates that the model has a good skill in this case study. The differences observed in the location of the main channel and the larger tidal creek pattern between the bio-geomorphological simulations and the purely morphological model results are relatively small, which indicate that the morphology, and not the vegetation, is determining the overall pattern.

As a general conclusion, it is found that the contribution of vegetation modelling on the long-term morphodynamic prediction of salt marsh formation and succession depends on the type of system under consideration. Two types of systems have been identified, one in which vegetation is leading and one in which morphology is leading. For the situation that vegetation is leading, like in the sensitivity simulations, vegetation modelling is essential, but when the vegetation follows the morphological development, as in the 'Saeftinghe' case, the contribution is less important.

Acknowledgements

This research concludes the double degree Master of science programme 'Hydraulic Engineering and Water Resources Management' at Delft University of Technology and National University of Singapore. The research project was conducted during nine months at the consultancy firm Svašek Hydraulics in Rotterdam.

I would like to express my gratitude to professor J.A Roelvink and my supervisors R.J. Labeur and B.C. van Prooijen at Delft University of Technology, and V.P. Chua at the National University Singapore for their critical feedback, helpful input and the lively discussions. Also, I would like to give a special thanks to my supervisor at Svašek Hydraulics, G. Dam for his help and guidance during my research, and to B. van Leeuwen for his input and sharing his knowledge. Further, I am grateful for the opportunity to do my research at Svašek Hydraulics and for the wonderful time with my colleagues there.

Finally, I could not have done this without the encouragement and support of my family, friends and my girlfriend Nanda.

Ype Attema, Delft December 22, 2014

Contents

Abstract	v
Acknowledgements	ix
Contents	x
List of Figures	xv
List of Tables	xix
Symbols	xxi
1 Introduction	1
1.1 Background	1
1.2 Problem definition	3
1.3 Research objective	4
1.3.1 Sub-questions	4
1.4 Research methodology	4
1.5 Thesis outline	5
2 Theory of salt marsh formation	7
2.1 General introduction on salt marshes	7
2.2 Formation and development of salt marshes	9
2.2.1 Stage 1: Stem establishment	10
2.2.2 Stage 2: Tussock development	11
2.2.3 Stage 3: Marsh platform succession	13
2.3 Salt marsh characteristics	13
2.3.1 Hydrodynamic characteristics	13
2.3.2 Morphological characteristics	14
2.4 Concluding remarks	15
3 Vegetation growth models	17
3.1 Interplay between vegetation and morpho-hydrodynamics	18
3.1.1 Introduction	18
3.1.2 Theoretical background	18
3.1.3 Representative roughness	20
3.1.4 Representative bed shear stress	21

3.1.5	Influence on sediment transport	23
3.2	Vegetation growth models	23
3.2.1	General overview	23
3.2.2	Governing equations	24
3.2.3	Stage 1: Stem establishment	25
3.2.4	Stage 2: Stem density growth	27
3.2.5	Stage 3: Marsh platform succession	28
3.2.6	Vegetation decay processes	29
3.3	Discussion	30
4	Numerical implementation	31
4.1	Description FINEL2d	32
4.1.1	Hydrodynamics	32
4.1.2	Morphodynamics	33
4.2	Implementation of representative roughness and shear stress	34
4.3	Implementation vegetation models	35
4.3.1	Governing equation	35
4.3.2	Stage 1: Stem establishment	36
4.3.3	Stage 2: Stem density growth	38
4.3.4	Stage 3: Marsh platform succession	39
4.3.5	Vegetation decay processes	41
4.4	Bio-geomorphological acceleration factor	42
4.4.1	Governing equations	42
4.4.2	Establishment	43
4.5	Discussion	43
5	Sensitivity analysis	45
5.1	Simple numerical simulations	46
5.1.1	Influence of vegetation on the hydrodynamics	46
5.1.2	Grid cell size dependency	50
5.1.3	Conclusion	51
5.2	2D Sensitivity analysis	52
5.2.1	Model setup	52
5.2.2	Baseline simulations	55
5.2.3	Parameter sensitivity simulation	68
5.3	Discussion	81
6	Case study	
	'The drowned land of Saeftinghe'	83
6.1	Introduction	83
6.2	Case study setup	83
6.2.1	Model setup	84
6.2.2	Input parameters	85
6.3	Model results	87
6.3.1	Vegetation	87
6.3.2	Morphology	93
6.4	Hydrodynamics	98

6.5	Conclusions	100
7	Discussion	101
8	Conclusions and recommendations	105
8.1	Conclusions	105
8.2	Recommendations	106
A	Vegetation growth models	109
A.1	Rewriting the representative roughness equation	109
B	Numerical implementation	111
B.1	Vegetation decay processes, population dynamics model	111
C	Case study results	115
C.1	Development of Saeftinghe, window of opportunity model	115
C.2	Development of Saeftinghe, population dynamics model	121
C.3	Development of Saeftinghe, measured	126
C.4	Saeftinghe results for different sediment grain sizes, window of opportunity	130
	Bibliography	133

List of Figures

1.1	Saeftinghe, a typical salt marsh in the Western Scheldt Estuary	2
1.2	Interaction of vegetation with the morpho-hydrodynamics	3
2.1	Typical cross-section of a salt marsh	8
2.2	The development of a bare tidal flat to a marsh platform	8
2.3	Vegetation and sedimentation feedback process	9
2.4	Formation and development processes in salt marshes	10
2.5	Sedimentation feedback process in and around tussocks	11
2.6	Ssedimentation and erosion in and around tussocks as a function of the stem density	12
2.7	Alternative stable state consisting of tussocks of <i>Spartina</i>	12
2.8	Water level flow velocity curves	14
2.9	Sedimentation pattern after a semi-diurnal tidal cycle	15
3.1	Schematic framework for the vegetation model	17
3.2	Fluid forces for steady uniform steady flow with vegetation	19
3.3	Vertical profile of horizontal velocity for vegetation	21
3.4	Stem density growth described by a logistic growth function	28
4.1	Interaction of vegetation with the morpho-hydrodynamics	31
4.2	Discontinuous Galerkin method	33
4.3	Schematisation of the stem density flux for triangular grid discretisation	39
5.1	The 1D model setup	46
5.2	Depth averaged velocity and representative friction coefficient for different stem densities	48
5.3	Depth averaged velocity and bed shear stress for different stem densities	49
5.4	Comparison of lateral expansion for different grid refinements of a vegetation platform	51
5.5	Sensitivity case study	52
5.6	Comparison of the bed level after 30 years for the two bio-geomorphological models and the morphological model	56
5.7	Vegetation patterns after 30 years for the bio-geomorphological models	57
5.8	Vegetation growth characteristics for the sensitivity baseline simulations throughout 30 years	58
5.9	Vegetation mortality characteristics for the sensitivity baseline simulations throughout 30 years	58
5.10	Shear stress mortality patterns after 30 years for the bio-geomorphological models	59
5.11	Inundation mortality patterns after 30 years for the bio-geomorphological models	60

5.12	Establishment process highlighted for the two bio-geomorphological models throughout 30 years	60
5.13	Establishment height graph for the window of opportunity model	61
5.14	Establishment height graph for the population dynamics model	61
5.15	Vegetation pattern after 9 years for the window of opportunity model	62
5.16	Vegetation pattern after 9 years for the population dynamics model	62
5.17	Bed level and vegetation pattern after 30 years for the window of opportunity model	63
5.18	Erosion/sedimentation pattern after 30 years for the window of opportunity model	63
5.19	Bed level and vegetation pattern after 30 years for the population dynamics model	64
5.20	Erosion/sedimentation pattern after 30 years for the population dynamics model	64
5.21	Erosion and sedimentation characteristics after 30 years for the two bio-geomorphological models	65
5.22	Maximum flow velocity and patterns during falling tide for window of opportunity model	66
5.23	Maximum flow velocity and patterns during falling tide for window of opportunity model	66
5.24	Computed flow velocity during a M2 Tidal cycle for the window of opportunity model	67
5.25	Computed flow velocity during a M2 Tidal cycle for the window of opportunity model	67
5.26	Vegetation growth characteristics for different acceleration factors throughout 30 years, window of opportunity model	69
5.27	Bed level and vegetation patterns after 30 years, window of opportunity model	70
5.28	Bed level and vegetation patterns and the vegetation growth characteristics for different acceleration factors after/throughout 30 years, population dynamics model	71
5.29	Bed level and vegetation patterns for different grid cell sizes after 30 years, window of opportunity model	73
5.30	Growth characteristics for different grid cell sizes after 30 years, window of opportunity model	74
5.31	Bed level and vegetation patterns, and the bed level difference pattern for different sediment diameters after 30 years, window of opportunity model. In the bed level difference plot, the red colour indicates a higher bed level elevation for the $D50 = 30 \mu m$ simulation.	76
5.32	Growth and erosion/sedimentation characteristics for different sediment diameters throughout 30 years, window of opportunity model	77
5.33	Vegetated and bare bed level pattern for different value for $n_{b,threshold} C_{fr}$ and for different establishment approaches after 30 years, window of opportunity model	78
6.1	Location of 'Saeftinghe'	84
6.2	Model setup	85
6.3	Measured and modelled bed level and vegetation pattern for Saeftinghe after 100 years (in 2004)	88
6.4	Modelled bed level and vegetation pattern for Saeftinghe after 100 years (in 2004)	89
6.5	Vegetation growth characteristics for Saeftinghe throughout 100 years (1905-2004)	90
6.6	Comparison of the modelled and measured vegetated area for Saeftinghe throughout 100 years (1905-2004)	90
6.7	Establishment characteristics for Saeftinghe throughout 100 years (1905-2004)	91

6.8	Establishment characteristics for Saeftinghe throughout 100 years (1905-2004) . . .	91
6.9	Elevation changes in the areas that shifted from bare to vegetated tidal flat at Saeftinghe, window of opportunity model	92
6.10	Measured and modelled Erosion/sedimentation patterns for Saeftinghe after 100 years (in 2004)	94
6.11	Modelled Erosion/sedimentation patterns for Saeftinghe in after 100 years (in 2004)	95
6.12	Elevation difference between the bio-geomorphological models and the morphological model for Saeftinghe after 100 years (in 2004)	96
6.13	Measured and modelled cumulative erosion/sedimentation and the performance of the models regarding the erosion/sedimentation patterns expressed in terms of the BSS	98
6.14	Flow characteristics for Saeftinghe after 100 years (in 2004), window of opportunity model	99
6.15	Flow characteristics for Saeftinghe after 100 years (in 2004), window of opportunity model	99
B.1	Difference between the online and offline coupling approach	112
B.2	Adjusted mortality coefficient for the online coupling method	112
C.1	Bed level and vegetation pattern for Saeftinghe after 26 years (in 1931), window of opportunity model	115
C.2	Bed level and vegetation pattern for Saeftinghe after 58 years (in 1963), window of opportunity model	116
C.3	Bed level and vegetation pattern for Saeftinghe after 87 years (in 1992), window of opportunity model	117
C.4	Bed level and vegetation pattern for Saeftinghe after 99 years (in 2004), window of opportunity model	118
C.5	Bed level and vegetation pattern for Saeftinghe after 122 years (in 2027), window of opportunity model	119
C.6	Bed level and vegetation pattern for Saeftinghe after 148 years (in 2053), window of opportunity model	120
C.7	Bed level and vegetation pattern for Saeftinghe after 26 years (in 1931), population dynamics model	121
C.8	Bed level and vegetation pattern for Saeftinghe after 58 years (in 1963), population dynamics model	122
C.9	Bed level and vegetation pattern for Saeftinghe after 87 years (in 1992), population dynamics model	123
C.10	Bed level and vegetation pattern for Saeftinghe after 99 years (in 2004), population dynamics model	124
C.11	Bed level and vegetation pattern for Saeftinghe after 122 years (in 2027), population dynamics model	125
C.12	Measured bed level and vegetation pattern for Saeftinghe after 26 years (in 1931)	126
C.13	Measured bed level and vegetation pattern for Saeftinghe after 58 years (in 1963)	127
C.14	Measured bed level and vegetation pattern for Saeftinghe after 87 years (in 1992)	128
C.15	Measured bed level and vegetation pattern for Saeftinghe after 99 years (in 2004)	129
C.16	Bed level and vegetation pattern for Saeftinghe after 148 years (in 2053), window of opportunity model	130
C.17	Bed level and vegetation pattern for Saeftinghe after 148 years (in 2053), window of opportunity model	131

C.18 Bed level and vegetation pattern for Saeftinghe after 148 years (in 2053), window of opportunity model	132
--	-----

List of Tables

5.1	The input parameters	46
5.2	Numerical example, lateral expansion isolated tussock	50
5.3	Numerical example, refinement of vegetation platform	51
5.4	Sensitivity case grid properties	53
5.5	Morpho-hydrodynamic parameters	53
5.6	Vegetation input parameters: Population dynamics model	54
5.7	Vegetation input parameters: Window of opportunity model	55
5.8	Vegetated area	59
5.9	Bio-geomorphological acceleration factor sensitivity simulations	69
5.10	Grid cell size sensitivity simulation	72
5.11	Sediment grain size sensitivity simulation	75
5.12	$n_{b,threshold} C_{fr}$ sensitivity simulation	79
5.13	Establishment representation sensitivity simulation	80
6.1	Morpho-hydrodynamic parameters	85
6.2	Vegetation input parameters: Population dynamics model	86
6.3	Vegetation input parameters: Window of opportunity model	86
6.4	BSS classification	97
B.1	Numerical example, online and offline coupling vegetation inundation mortality	111

Symbols

c_e	Equilibrium sediment concentration in the water	$[kg \cdot m^{-3}]$
C_{Dv}	Drag coefficient vegetation	$[-]$
C_{fb}	Bed friction coefficient	$[-]$
$C_{fr \text{ submerged}}$	Bed friction coefficient submerged vegetation	$[-]$
$C_{fr \text{ unsubmerged}}$	Bed friction coefficient unsubmerged vegetation	$[-]$
D	Water depth	$[m]$
D_{50}	Uniform median sediment grain size	$[m]$
f_c	Coriolis coefficient	$[s^{-1}]$
F_g	Gravitational force	$[N]$
F_S	Shear stress force	$[N]$
F_D	Drag force	$[N]$
g	Gravitational acceleration	$[m \cdot s^{-2}]$
h	Water depth	$[m]$
h_i	Computed water depth	$[m]$
h_{crit}	Critical inundation water depth	$[m]$
i	Friction slope	$[m \cdot m^{-1}]$
$I_{\%, i}$	Average submergence percentage	$[-]$
$I_{\%, crit}$	Critical submergence percentage	$[-]$
k	Uniform vegetation height	$[m]$
k_n	Nikuradse bed roughness	$[m]$
K	Uniform radial growth rate	$[m \cdot yr^{-1}]$
n_b	Stem density	$[m^{-2}]$
$n_{b, crit \text{ diff}}$	Threshold mature stem density for lateral expansion	$[m^{-2}]$
$n_{b, establishment}$	Initial establishment density	$[m^{-2}]$
$n_{b,j}$	Stem density in neighbouring grid cell	$[m^{-2}]$
$n_{b,i}$	Stem density in grid cell under consideration	$[m^{-2}]$

$n_{b, max}$	Maximum carrying capacity stem density	$[m^{-2}]$
$n_{b, seedling}$	Initial establishment density of seedlings	$[m^{-2}]$
$n_{b, threshold\ bare}$	Threshold bare grid cell	$[m^{-2}]$
$n_{b, threshold\ C_{fr}}$	Threshold hydrodynamic influence stem density	$[m^{-2}]$
m	Number of measurements	$[-]$
P_{est}	Establishment chance of vegetation on bare soil	$[yr^{-1}]$
PE_h	Plant mortality coefficient for inundation stress	$[m^{-3} \cdot s^{-1}]$
PE_τ	Plant mortality coefficient for shear stress	$[N \cdot s^{-1}]$
q_x	Sediment flux in x direction	$[m^2 \cdot s]$
q_y	Sediment flux in y direction	$[m^2 \cdot s]$
r	Intrinsic growth rate of stem density	$[yr^{-1}]$
S	Magnitude of the equilibrium sand transport	$[m^2 \cdot s]$
t	Time	$[s]$
T_A	Characteristic time scale	$[s]$
$T_{I\%, avg}$	Inundation relaxation time	$[s]$
$T_{Ph:1}$	Inundation free period required	$[s]$
$T_{Ph:2}$	Duration of phase 2	$[s]$
$T_{Ph:3}$	Duration of phase 3	$[s]$
$T_{Rec:1, i}$	Recorded inundation free period	$[s]$
$T_{Rec:2, i}$	Recorded duration in phase 2	$[s]$
$T_{Rec:3, i}$	Recorded duration in phase 3	$[s]$
T_t	Occurring window of opportunity	$[s]$
u	Depth average uniform flow velocity	$[m \cdot s^{-1}]$
u_c	Depth average uniform flow velocity within vegetation	$[m \cdot s^{-1}]$
z_b	Bottom level	$[m]$
Γ_j	Interface length between the two cells under consideration	$[m]$
$\Delta n_{b, establishment, i}$	Stem density increase due to establishment	$[m^{-2}]$
$\Delta n_{b, expansion, i}$	Stem density increase due to lateral expansion	$[m^{-2}]$
$\Delta n_{b, flow, i}$	Reduction in stem density due to shear stress	$[m^{-2}]$
$\Delta n_{b, growth, i}$	Stem density increase due to stem density growth	$[m^{-2}]$
$\Delta n_{b, inundation, i}$	Reduction in stem density due to inundation stress	$[m^{-2}]$
Δt	Time step	$[s]$
Δt_{yr}	Time step converted to years	$[yr]$

κ	Von karman constant	$[-]$
λ	Bio-geomorphological acceleration factor	$[-]$
ρ	Volumetric mass density of water	$[kg \cdot m^{-3}]$
τ_b	Bed shear stress	$[N \cdot m^{-2}]$
$\tau_{b,crit}$	Maximum shear stress resistance of mature vegetation	$[N \cdot m^{-2}]$
$\tau_{b,crit, phase 2}$	Critical bed shear stress resistance seedling	$[N \cdot m^{-2}]$
$\tau_{b, ph:1}$	Shear stress resistance of seedlings after phase 1	$[N \cdot m^{-2}]$
$\tau_{b, ph:3}$	Maximum shear stress resistance of mature vegetation	$[N \cdot m^{-2}]$
τ_{bv}	Total bed shear stress for vegetated soil	$[N \cdot m^{-2}]$
$\tau_{bv, i}$	Computed instantaneous bed shear stress	$[N \cdot m^{-2}]$
τ_r	Radiation stress	$[N \cdot m^{-2}]$
τ_w	Wind shear stress	$[N \cdot m^{-2}]$
ϕ	Stem diameter	$[m]$
χ	Number from pseudo-random number generator	$[-]$
∇n_b	Stem density gradient	$[m^{-3}]$

Chapter 1

Introduction

1.1 Background

Salt marshes are complex and delicate coastal ecosystems in intertidal areas between land and sea, typically occurring at sheltered low-energy shorelines, such as embankments, estuaries or sand spits. These ecosystems are regularly flooded during tides and storm surges and are characterized by dense stands of salt tolerant vegetation. The vegetation, typically dissected by tidal creeks, mostly consists of herbs and grasses that are essential for the stability and preservation of these marshes (Fagherazzi et al., 2011). This gives salt marshes their distinctive pattern that can be seen in figure 1.1.

In the coastal system, these salt marshes fulfil a variety of vital functions and are particularly of ecological importance. The importance can be substantiated by the fact that the marshes are among the most productive ecosystems on earth, providing a habitat for the feeding and breeding of fish, shellfish, birds and other organisms (Temmerman et al., 2005b). In addition, the marshes also have a bio-geochemical function by filtering sediments, nutrients and contaminants. Besides the ecological importance, the marshes also form an effective natural barrier that captures sediments and stabilizes the shoreline, as they reduce erosion from wave impacts (Wang et al., 2013). Finally, they also have an aesthetic value and a recreational function. In the past, however, the value of salt marshes was not recognized and substantial loss of marsh areas occurred through human activities such as land reclamation for agriculture, industry, urbanization, navigation and recreation. Nowadays, fortunately, the importance of salt marshes is widely recognized which has resulted in protective regulations and management for tidal marshes and estuarine ecosystems (Temmerman et al., 2005b).

Managing and protecting these tidal ecosystems, on the other hand, is still a complex task due to the dynamic character, with on-going sedimentation and/or erosion processes and complex feedback mechanisms between biology, ecology and geomorphology (Bouma et al., 2007). In view of this, numerical models can be a potential tool, as they can help to identify important dynamic processes and feedback mechanisms to simulate long term geomorphological evolution (Fagherazzi et al., 2011). The potential of numerical models has also drawn the attention of various researchers and institutions which has led to research and development of process-based models. One of these models is developed by D'Alpaos et al. (2005). This model combines the hydrodynamic model of Rinaldo et al. (1999) with a morphodynamic model to assess channel

initiation and early development of salt marshes. This model was, subsequently, employed by D'Alpaos et al. (2007) to model the long term development of salt marshes in terms of sedimentation rates and platform elevation. A different numerical model was proposed by Temmerman et al. (2005a). He presented a three dimensional modelling approach accounting for the influence of vegetation on the hydrodynamics to reproduce flow and sedimentation patterns for short-term single inundation cycles. Temmerman et al. (2007) further developed this model and coupled it with a conceptual vegetation growth method to take into account the dynamic character of salt marsh vegetation. The purpose of this model was to demonstrate that vegetation can trigger channel initiation.

This thesis aims to contribute to the understanding of the influence of vegetation on the salt marsh formation and succession. Therefore, it focusses on the modelling of vegetation establishment and growth and the link with the geomorpho-hydrodynamics, also referred to as bio-geomorphological modelling.



FIGURE 1.1: Saeftinghe, a typical salt marsh in the Western Scheldt Estuary

1.2 Problem definition

Salt marshes are nowadays recognized as valuable but vulnerable ecosystems that require protective management. This has resulted, as mentioned in the previous section, in research and development of process-based models. The aim is to understand the dynamic character of salt marshes with its dynamic processes and feedback mechanisms, and to shed a light on long term geomorphological evolution. The vegetation in these tidal marshes is often considered to have an important influence on this dynamic character, as vegetation on bare tidal flats can cause flow concentration and channel initiation (Temmerman et al., 2007). Moreover, it has the ability to capture and trap sediments (Wesenbeeck, 2007). These interaction processes between the different processes are schematised in figure 1.2.

Up till now, the development of process-based models primarily focussed on the hydrodynamic and morphodynamic processes in tidal marshes, i.e. left column in figure 1.2. Temmerman et al. (2007) demonstrated with a conceptual bio-geomorphological model that the feedback between vegetation and the morpho-hydrodynamics does have an important control on the salt marsh formation and development. However, an assessment of the influence of these process-based bio-geomorphological models on the large scale and long term geomorphological development of salt marshes has not been carried out yet. Hence, it can be concluded that the inclusion of a vegetation growth model in these geomorphological models is still a new territory, where more research and development is still required (Ye, 2012).

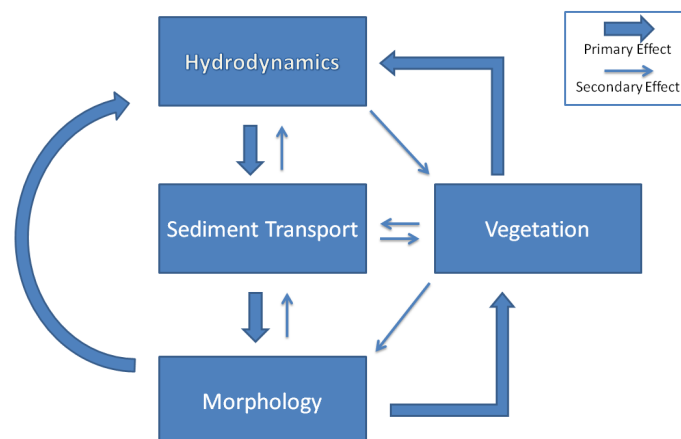


FIGURE 1.2: Interaction of vegetation with the morpho-hydrodynamics (Baptist, 2005)

1.3 Research objective

In this thesis it is hypothesized that the inclusion of a vegetation model in the process-based morphodynamic models is essential to reproduce and predict the morphodynamic development during the formation and succession of salt marshes. Therefore a vegetation growth model will be developed and implemented in morphodynamic modelling software to assess this hypothesis.

This leads to the following main research question:

”To which extent can vegetation modelling contribute to the long-term morphodynamic prediction of salt marsh formation and succession?”

1.3.1 Sub-questions

In order to answer this research question a couple of sub-questions have to be answered concerning the current situation of bio-geomorphological modelling and with respect to the results of the sensitivity analysis and case study.

Current situation

- What are the important processes that influence salt marsh formation and succession?
- Which conditions determine where salt marsh vegetation establishes and grows?
- What bio-geomorphological models are available?
- What are the limitations of the current models?
- How can the interaction between vegetation and the geomorpho-hydrodynamics be accounted for in the model?

Sensitivity analysis and case study

- Which processes have a significant effect on the results of the bio-geomorphological model?
- What are the timescales and length scales of the important processes?
- How sensitive is the model to variations in the input parameters?
- What is the predictive capability of the bio-geomorphological model?

1.4 Research methodology

The research methodology will be presented individually for each phase of the research process. This research project will consist of the following phases:

- Literature study
- Implementation vegetation-growth module in FINEL2d
- Sensitivity analysis
- Case study

The first phase of this research project is the literature study. This is necessary to get familiar with the problem, to analyse the current situation and to enhance the understanding of the bio-geomorphological processes. Furthermore, insight should be gained in the functioning of the current vegetation models.

Phase two consists of developing and implementing the vegetation models in the modelling software FINEL2d. This will firstly require the understanding of the FINEL2d code with the underlying assumptions and ideas.

In the third phase a sensitivity analysis will be performed with these vegetation models. Therefore, the models will firstly be tested on a simplified small tidal basin in order to investigate the importance of certain processes and assumptions. Secondly, it will shed a light on the model sensitivity to certain variations in the input parameters and initial conditions.

In the final phase, the model will be applied and tested in a case study to show the applicability of the model. To this end, the model will be employed to hindcast the formation and succession of 'The drowned land of Saeftinghe'. For this test case the model performance will be analysed and compared to field data.

With this approach the research aims to, firstly, develop and implement theory-based bio-geomorphological models and, secondly, to assess the applicability, sensitivity and performance of these models on the basis of a combination of theory and evidence. This should give an insight into the value of bio-geomorphological modelling of the formation and succession of salt marshes in terms of geomorphodynamic development.

1.5 Thesis outline

Chapter 2 describes the theoretical background of salt marsh formation and development, and the observed morphodynamic and hydrodynamics phenomena. Base on the theory, the vegetation models are adjusted and developed in chapter 3 and discretised and implemented in the numerical modelling software FINEL2d in chapter 4. Chapter 5 presents a sensitivity analysis to gain insight in the functioning, performance and sensitivity of the bio-geomorphological models. Subsequently, these models are deployed in chapter 6 to evaluate the practical applicability and the performance in the Saeftinghe case study. Finally, the results are discussed in chapter 7, and in chapter 8 the conclusions and recommendation are presented for this thesis.

Chapter 2

Theory of salt marsh formation

The aim of this chapter is to give insight in the formation and development of salt marshes, and to describe some related hydrodynamic and morphodynamic processes. To this end, this chapter starts with a general and broad overview of salt marshes in section 2.1. Subsequently, section 2.2 will discuss the physical and biological aspects of the formation and succession of salt marshes in more detail. This will be done based on the different stages that can be identified during salt marsh development. Finally, section 2.3 will address some physical characteristics of salt marshes in terms of flow patterns and sedimentation patterns.

2.1 General introduction on salt marshes

As mentioned in the introduction, salt marshes are coastal ecosystems in intertidal areas between land and sea. These systems, covered with dense stands of salt tolerant vegetation, typically occur at sheltered low-energy shorelines where fine sediments, i.e. sand, silt and/or mud, can accumulate. At these shorelines the presence of the tide is crucial, since suspended and dissolved sediments are transported by the tide and deposited during regular flooding. It is this accumulation, together with the requirement for sufficient sediment input, that is necessary for the formation and succession of salt marshes. Therefore, salt marshes often occur at embankments, sand spits or estuaries near large rivers or deltas, as the river can provide the necessary sediment input (Fagherazzi et al., 2011).

A typical cross-section of a salt marsh is presented in figure 2.1. In this cross-section, the salt marsh ecosystem is divided into different types of marshes depending on its maturity. It shows that the more mature salt marsh is located at higher elevations and that the formation of new marshes starts at the interface of the tidal flat and the pioneer marsh, where the vegetation invades and colonizes the bare tidal flats. These different types of salt marshes each have their own characteristics, which is illustrated in figure 2.2. The left picture shows a bare tidal flat where colonization of vegetation can occur under favourable conditions. The middle picture represents a pioneer marsh with tussocks and some initial merging of tussocks. Moreover, it shows local morphological development and initial creek formation next to the vegetation. The final picture on the right side depicts a middle marsh and/or a mature marsh where an overgrown marsh platform is dissected by tidal creeks with small levees on either sides.

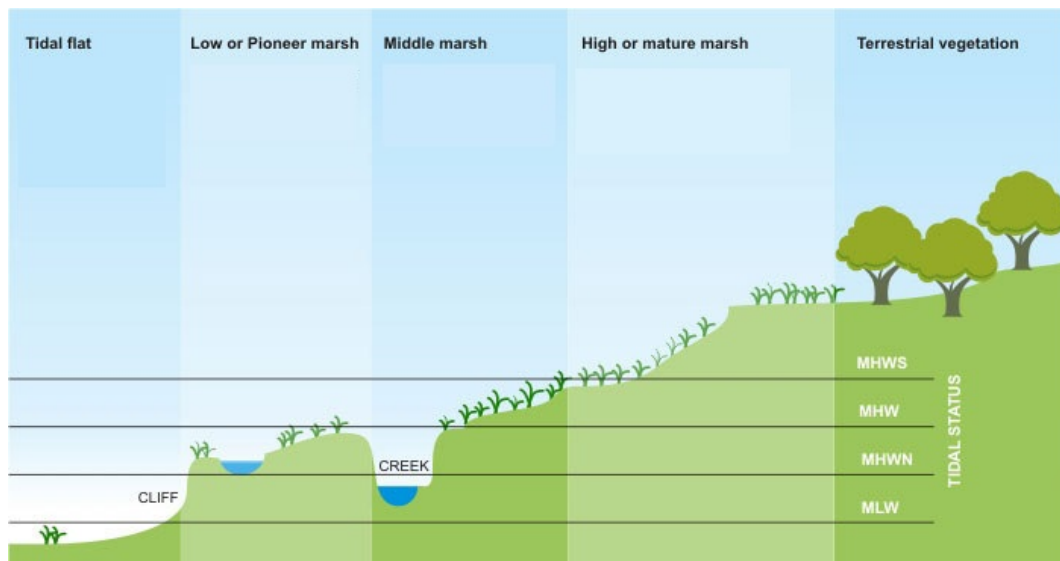


FIGURE 2.1: Typical cross-section of a salt marsh (Royal Haskoning 2010)

These different types of marshes can be linked to three different stages that can be distinguished in salt marsh formation and succession process. These stages are:

- Stage 1: Stem establishment
 - This is the process that describes the transition from bare tidal flat to pioneer marsh.
- Stage 2: Tussock development
 - This is the process that describes the evolution of pioneer marshes.
- Stage 3: Marsh platform succession
 - This is the process that describes the transition from pioneer marsh to a middle and ultimately to a mature marsh.

The formation and succession of salt marshes according to these stages will be discussed in more detail in the next sections.

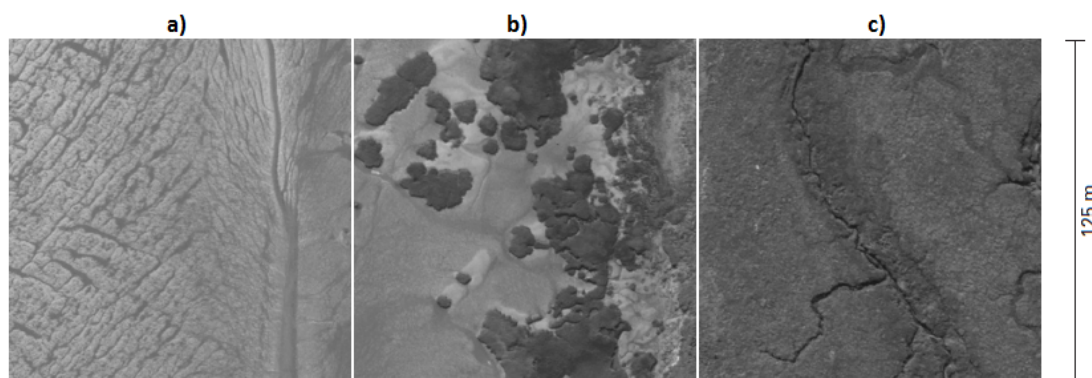


FIGURE 2.2: The development of a bare tidal flat to a marsh platform (Wesenbeeck, 2007)

a) Bare tidal flat

b) Pioneer marsh

c) middle marsh and mature marsh

2.2 Formation and development of salt marshes

The formation of a salt marsh ecosystem is a result of the interaction between physical and biological processes (Dijkema et al., 2001), since vegetation has the ability to change its environment by interacting with the abiotics (i.e. morphology and hydrology). Organisms that interact with their environment are also known as ecosystem engineers (Jones et al., 1994). This interaction with the surrounding environment improves the development and survival conditions for itself and for others, thus causing a positive biophysical feedback.

This positive feedback is an essential process throughout the different formation and development stages in salt marshes, which starts once vegetation settles and the first vegetation stems arise. The stems and their leaves interact with the hydrodynamics and reduce the current velocities. These lower velocities, in turn, reduce erosion and increase sedimentation of sediments. The result is bottom elevation at the location of vegetation, which positively affects vegetation growth by reducing submersion times thus increasing light availability for photosynthesis (Wesenbeeck, 2007). This positive biophysical feedback loop is illustrated in figure 2.3. Moreover, vegetation also provides improved conditions for other vegetation, since the current velocities in the wake of vegetation are reduced as well.

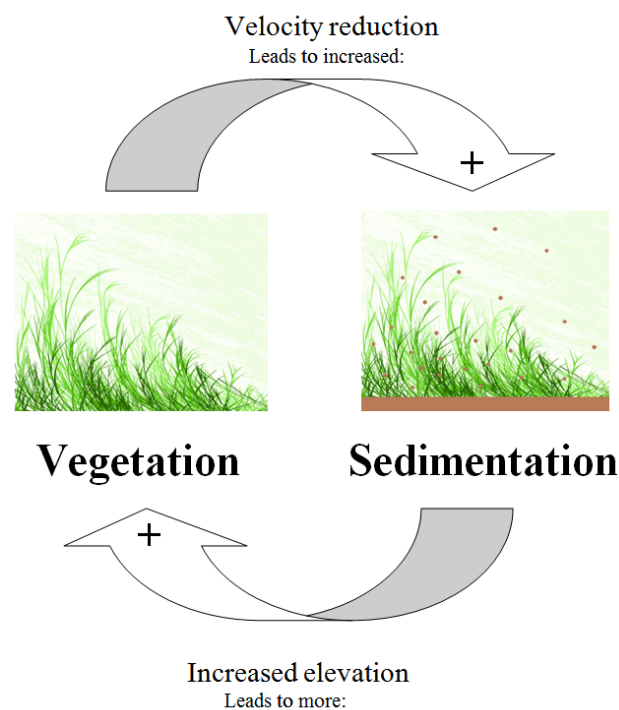


FIGURE 2.3: Vegetation and sedimentation feedback process (Wesenbeeck, TU Delft presentation)

The three stages in salt marsh formation and development, i.e. stem establishment, tussock development and marsh platform succession, can again be subdivided into several sub-stages that each have their own time scale and spatial scale at which the ecosystems engineering vegetation interact with their surrounding environment, see figure 2.4. This formation and development will be discussed in more detail based on of these three stages.

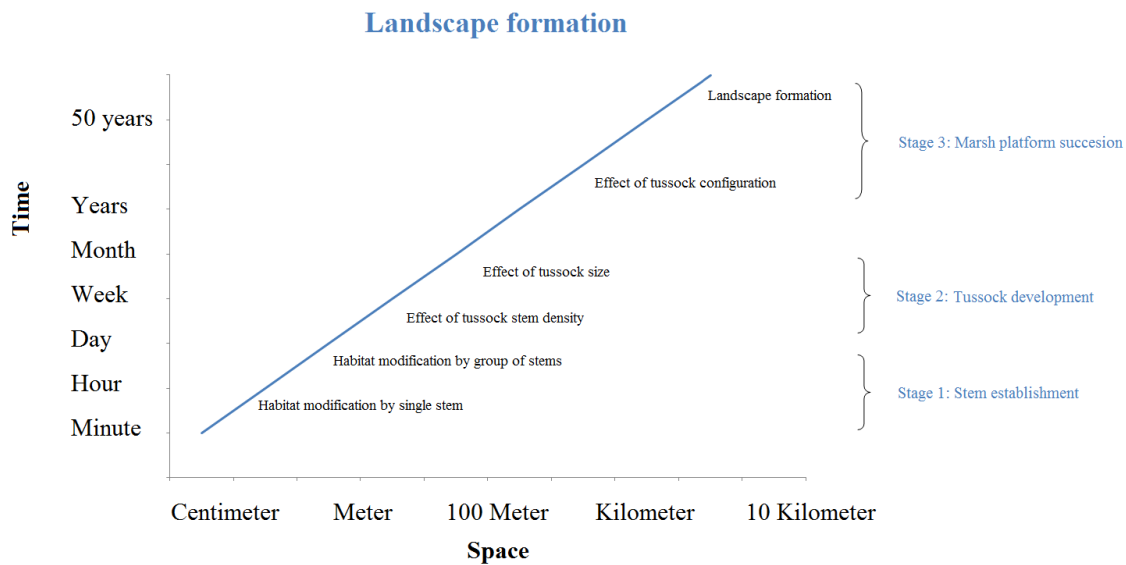


FIGURE 2.4: Formation and development processes in salt marshes with time and spatial scales (Modified after Wesenbeeck, TU Delft presentation)

2.2.1 Stage 1: Stem establishment

Establishment or colonisation of vegetation on bare tidal flats is not only dependent on physical processes, but also hindered by it. The relation between these two is crucial for understanding the colonisation process. Balke et al. (2011) describes this relation on the basis of the window of opportunity concept. According to this concept, colonisation can occur if there is a window of opportunity with favourable hydrodynamic conditions. Experiments and observations on mangrove seedlings, which go through a similar establishment process as salt marsh vegetation (Wesenbeeck, personal communication), identified that such a window of opportunity is similar to surviving a sequence of physical thresholds. The three thresholds that have been identified by Balke et al. (2011) are:

- Threshold 1: Displacement by flooding.
 - This requires an inundation free period for development of the first roots.
- Threshold 2: Dislodgement by hydrodynamic forces (i.e. currents and waves).
 - This requires a hydrodynamic calm period for further development of the roots.
- Threshold 3: Dislodgement by extreme hydrodynamic forces and sheet erosion.
 - This requires surviving also the high energy events.

The first two thresholds indicate that successful colonisation requires a window of opportunity with an inundation free period followed by a period of relative calm hydrodynamic conditions. This is necessary for the development of the roots system of the seedlings, as the roots prevent the seedlings from floating up when inundated and from dislodgement under bed shear stresses imposed by the hydrodynamics. Additionally, the third threshold requires the stems to survive the high energy events. These events generally occur during storms or spring tide and can cause high shear stresses on the vegetation, possibly in combination with reduced resistance due to a smaller effective root length caused by sheet erosion.

Although the occurrence of such a window of opportunity, where an inundation free period is followed by calm conditions, is likely to occur at neap tides, it is also dependent on the geometrical properties of the establishment location. Given that the surface elevation influences the submergence times and a sheltered location affects the hydrodynamic forces, which is favourable for establishment. This has also been identified by Wang et al. (2013), since they observed that the shift from bare tidal flat to salt marsh indeed has a higher chance of occurrence if located above a certain threshold elevation.

Besides hydrodynamic and geometrical requirements, establishment also depends on other local biotic and abiotic conditions, i.e. soil state, temperature and the availability of seeds, pieces of broken off rhizomes (part of the root system) or ramets (small clonal fragments). Especially the dispersal of seeds is important, as it is the dominant mechanism for new establishments.

In conclusion, successful establishment requires suitable geometrical features and favourable abiotic conditions, while the dispersal of seeds should coincide with the occurrence of a window of opportunity. Only under these conditions can the seeds establish, grow into stems and develop into patches or tussocks.

2.2.2 Stage 2: Tussock development

The plant species in Europe that are capable of invading and establishing on the bare tidal flats are *Spartina anglica* and *Salicornia*. Their capability to establish on these bare tidal flats can be attributed to the fact that they are both stiff plant species. Stiff plant species have the property to cause higher drag forces that lead to a higher velocity reduction and better sediment capture and erosion protection capabilities. However, only *Spartina anglica* is able to trigger the positive biophysical feedback loop needed to modify its habitat in such a way that formation of a salt marsh is possible. This can, in turn, be attributed to the rapid establishment potential and the patchy vegetation colonisation structure with high stem density (Bouma et al., 2009).

The patchy vegetation colonisation structure of *Spartina*, consisting of round shaped tussocks, can generally be found in the pioneer zone. It is within these tussock structures, with high stem density, that sedimentation can occur and that the positive feedback loop is triggered. However, the vegetation also sets off a negative feedback around the tussocks. This is caused by contraction of water around the tussocks, which leads to local erosion of gullies and prevents further lateral expansion of the vegetation (see figure 2.5).

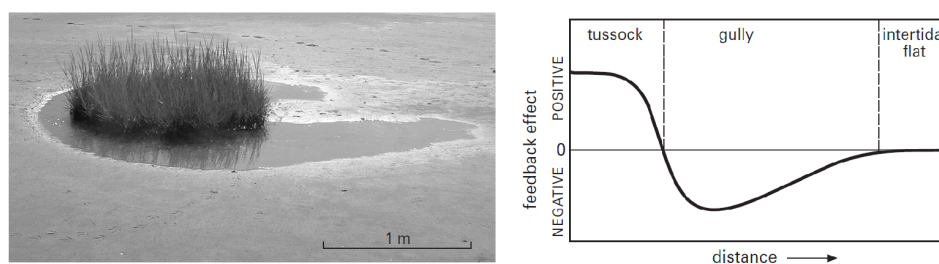


FIGURE 2.5: Sedimentation feedback process in and around tussocks (Wesenbeeck, 2007)

Bouma et al. (2009) found that the magnitudes of the positive feedback and of the negative feedback, respectively, depend on the stem density, see figure 2.6. In addition, they found that below a certain threshold density the positive feedback could change into a negative effect. This negative effect presents itself as erosion around the stems, which is caused by an increase in flow velocity and turbulence. However, the exact value of this threshold and the magnitude of the negative effects depends on the hydrodynamic forcing. In fact, in areas with low flow velocities the positive feedback can occur even without causing a significant negative effect, which results in favourable conditions for lateral expansion of the tussocks.

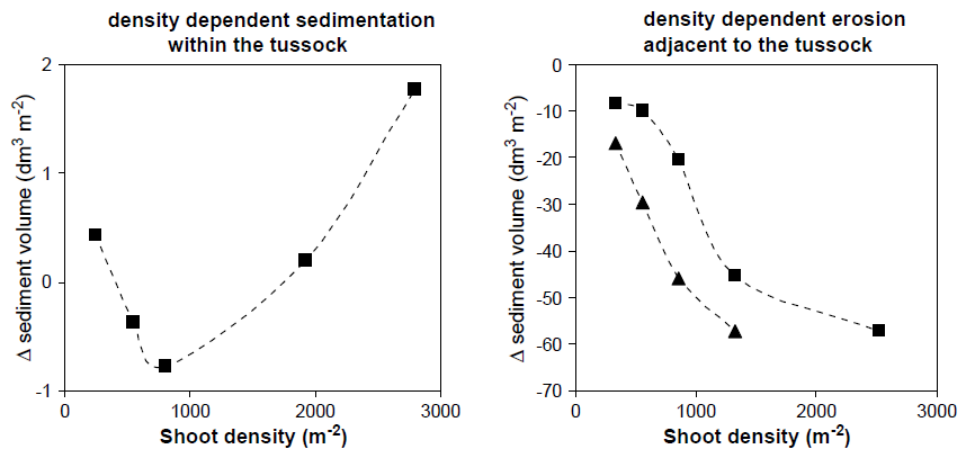


FIGURE 2.6: Sedimentation and erosion in and around tussocks as a function of the stem density. Bouma et al. (2009) obtained these results from flume experiments under a free stream current velocity of 0.3 m/s (\triangle) and 0.4 m/s (\square).

The patchy distribution that can be found on intertidal flats (see figure 2.7) indicates that a potential for an alternative stable state exists (Wesenbeeck, 2007). This might be because of the negative feedback around the tussocks, which prevents a shift to a marsh platform. Experiments have confirmed that this patchy tussock landscape state can indeed exist on a local and short time scale, however the landscape-scale and the long term observation suggest otherwise. Additionally, Wesenbeeck (2007) suggests that the alternative stable state may actually be an 'almost stable state', which slows down the development into a marsh platform.



FIGURE 2.7: Alternative stable state consisting of tussocks of *Spartina* (Wesenbeeck, 2007)

2.2.3 Stage 3: Marsh platform succession

The next stage describes the development of the patchy tussock landscape to a mature marsh platform. This is a transition that can occur slowly, but a sudden changes of state has also been observed. This shift in landscape from a bare/patchy to a vegetated state seems to be related to the coupling between local and global scale effects. The local effect of the vegetation, as mentioned, is the deflection of water around the tussock. However, in the presence of a configuration of tussock patches, the local effects can start to develop into a global effect on the morpho-hydrodynamics. The emerged tussocks can cause a reduction of available path area for water entering the pioneer zone (Temmerman et al., 2005b). This reduction in turn influences the amount of water entering, which results in reduced hydrodynamic forces and promotes expansion and merging opportunities for some tussocks. As a reduction in hydrodynamic forces on the tussock edges occurs, it gives the opportunity for lateral expansion. However, the expansion and merging of tussocks also leads to the concentration of flow, increase in hydrodynamic forces and thus increase in erosion in some other gullies. These processes constitute a positive feedback mechanism between increasing vegetation expansion and decreasing global hydrodynamics forces. Finally resulting in an equilibrium situation consisting of marsh platforms dissected by a creek system (Wesenbeeck, 2007).

The reduction in hydrodynamic conditions is crucial for the succession of the marsh platform, as a reduction in the hydrodynamics means lower flow velocities and lower bed shear stresses adjacent to the tussocks. The importance of lower bed shear stresses becomes evident when one considers that mechanisms for lateral expansion can be attributed to the sprouting of new stems from the laterally expanding rhizomes (root) system. As this, naturally, requires sufficiently calm flow conditions, in addition to the requirement for sufficient submergence times for photosynthesis.

2.3 Salt marsh characteristics

The previous section focussed on the vegetation formation and succession, the interaction of vegetation with the local morpho-hydrodynamics and the mechanisms that trigger the formation of tidal creeks. However, the global morphodynamic development of salt marshes are better understood and explained from overall sedimentation patterns. This can be substantiated by the fact that formation and succession of salt marshes, as mentioned before, is dependent on the influx and accumulation of sediments and nutrients. These sedimentation patterns are in turn influenced by the hydrodynamics and forced by the tidal oscillations. Therefore, this section will focus on global morpho-hydrodynamic characteristics, starting with a description of the flow patterns.

2.3.1 Hydrodynamic characteristics

The tidal creeks that typically dissect the marsh platform are traditionally regarded as the main supplier of water and constituents. However, research by Temmerman et al. (2005b) revealed that this is not necessarily true. The share of water supplied by tidal creeks is in fact dependent on the inundation height and the state of development of the creek network, adjoining levees and basins. Therefore, different cases can be identified; one for young marshes and two more for mature marshes during high and low water.

The traditional view, where the tidal creeks are the main supplier, is valid for mature, developed marshes under shallow inundation heights. The flow patterns for this case can be described using the simulation results from Temmerman et al. (2005a). It shows that firstly the tidal creeks start to fill up with water till bank full discharge is reached. Once the water level starts to exceed the levees around the tidal creeks, flooding of the marsh platform begins. The flow pattern at that moment shows flow directions perpendicular to the tidal creek and thus indicates that the water is indeed mainly supplied by the creeks. Furthermore, a velocity pulse in the tidal creeks can be identified (see, figure 2.8), which is caused by the sudden flooding of the levees. However, when the inundation height exceeds the vegetation height, this pattern starts to change. The flow directions become more or less perpendicular to the open marsh boundary and sheet flow starts to develop. This significantly reduces the share of water transported by the tidal creeks. On the other hand, for young, low marshes the role of tidal creeks is less important. In these younger marshes the flooding predominantly take place perpendicular to the marsh edge (Temmerman et al., 2005b). This is due to the gently seawards sloping topography and an undeveloped creek network.

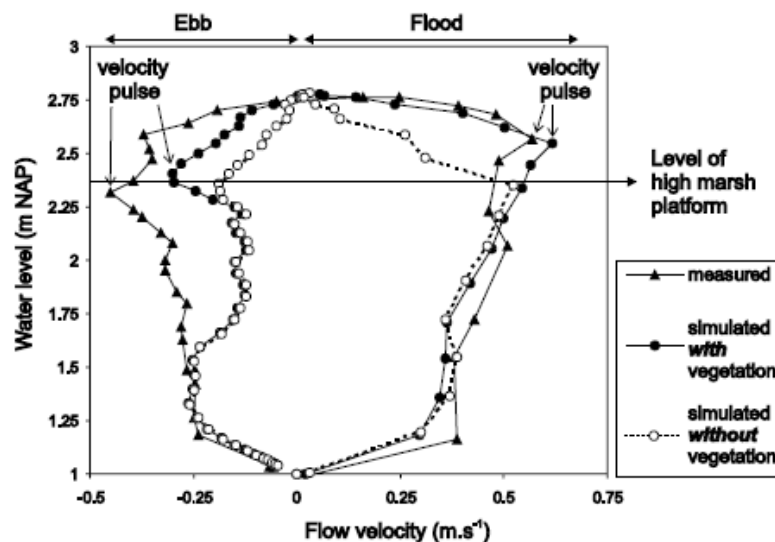


FIGURE 2.8: Water level flow velocity curves with a velocity pulse around bankfull (Temmerman et al., 2005a)

Figure 2.8 also gives a good indication of the current velocities within salt marsh gullies, as the upper range is generally around 0.3 or 0.4 m/s. Marshes with relatively low current velocities also occur (Temmerman et al., 2005a).

2.3.2 Morphological characteristics

The morphological and topographical characteristics of tidal marshes are determined by the supply, the deposition and erosion of sediments. The supply, as said before, is dependent on the flow patterns, while sedimentation and erosion rates are coupled to the flow velocities. This leads to different sedimentation patterns for pioneer and mature salt marshes, see figure 2.9.

The figure shows that for the low marsh the sedimentation primarily takes place close to the marsh edge and reduces further marsh inward. This was to be expected from the flow pattern,

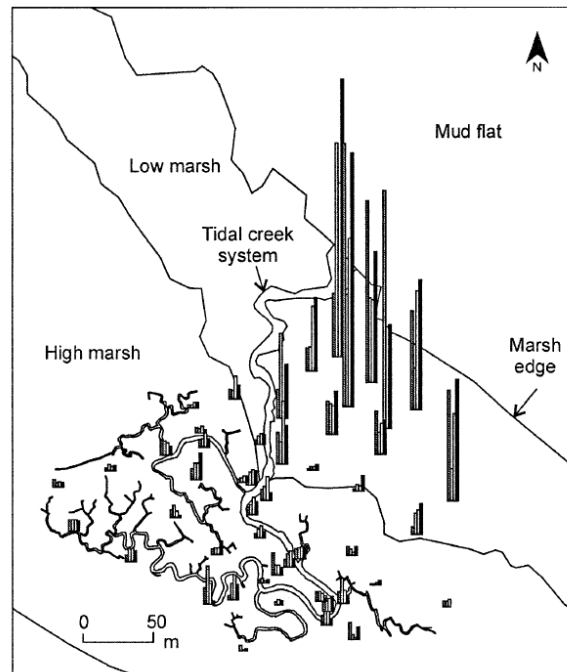


FIGURE 2.9: Sedimentation pattern after a semi-diurnal tidal cycle (Temmerman et al., 2005b)

since the water and thus the sediment supply enters the young marsh from the edge side. Once it reaches the marsh vegetation the velocity is reduced and sedimentation takes place. Further into the marsh the flow approximates the equilibrium sediment concentration again, resulting in less sedimentation. The sedimentation in the high marsh, on the other hand, shows a different pattern. The first thing that can be noted is that the sedimentation rates are significantly lower due to less frequent inundation (higher elevation) and less sediment supply (mainly from creeks). Secondly, it shows that sedimentation rates are higher close to the creeks which causes the formation of the levees on either side. This is again a result of the velocity reduction and the adjustments to the equilibrium sediment concentration that are initially accompanied by higher sedimentation rates.

2.4 Concluding remarks

This chapter presents the background of the formation and succession of salt marshes in terms of vegetation growth and morpho-hydrodynamics. Moreover, it reveals that the interaction between vegetation and the morpho-hydrodynamics is a crucial aspect in this development process. These insights can subsequently be utilized in the next chapter to evaluate the existing vegetation models and as a theoretical basis for adjustments and further development of these models. Finally, it also provides a good basis for the assessment of the performance of these models.

Chapter 3

Vegetation growth models

This chapter presents two vegetation-growth models that utilize the theory on salt marsh formation and succession described in chapter 2 as a starting point. The first model, that is based on the method developed by Temmerman et al. (2007), represents the processes described in the theory through a population dynamics model. Whereas, the second model is based on the 'window of opportunity' concept by Balke et al. (2011). Descriptions of these models are presented in section 3.2 where the background and the equations will be discussed. However, this chapter will start with section 3.1 that discusses the interaction between the vegetation-growth model, the hydrodynamics and the morphology, since this gives an idea of the bigger picture and the importance of vegetation modelling.

Figure 3.1 gives a schematic framework of the vegetation model with the different components that will be discussed in this chapter.

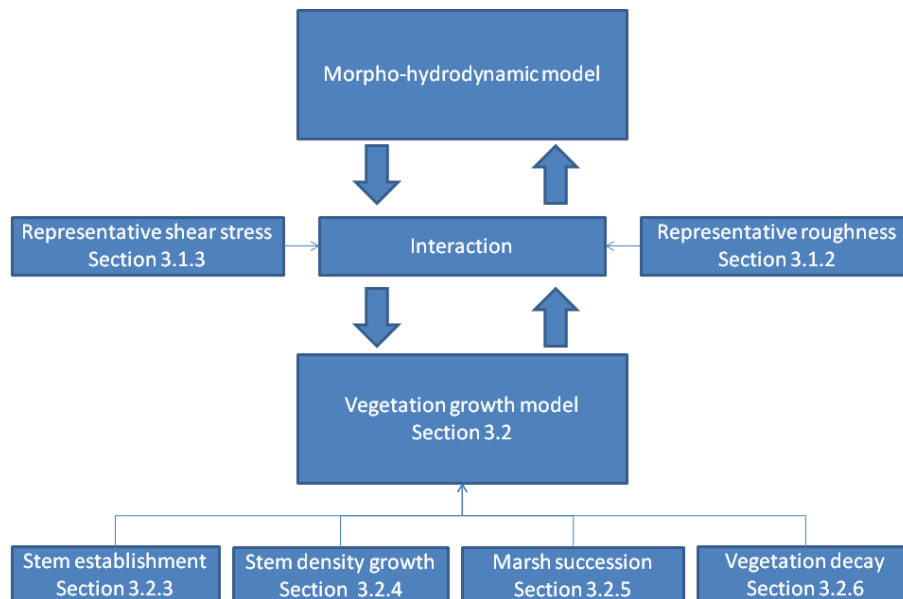


FIGURE 3.1: Schematic framework for the vegetation model

3.1 Interplay between vegetation and morpho-hydrodynamics

The theory described in section 2.3 revealed that the positive biophysical feedback between the vegetation and the morpho-hydrodynamics is an essential process for salt-marsh development and succession. One side of this feedback mechanism is the influence of the vegetation on the morpho-hydrodynamics, which is a result of increased hydraulic resistance and associated flow retardation caused by vegetation. This in turn affects flow patterns and thus the morphological processes, as the hydrodynamics is the driving force behind the morphodynamics. Thus, indicating that the interaction between the vegetation and the morpho-hydrodynamic is a crucial aspect of bio-geomorphological modelling. Therefore, this section will discuss and present an approach to describe the interaction between vegetation and the hydrodynamics, which in turn affects the morphodynamics.

3.1.1 Introduction

The influence of the vegetation on the hydrodynamics has also been a topic of interest for various fields within hydrodynamic modelling. One of these field is river engineering, where the modelling of bio-geomorphological processes in river floodplains is an important topic for modelling river floods. It is for this purpose that Baptist (2005) studied the interaction process between vegetation and hydrodynamics. In his research he derived, compared and validated expressions to represent the effect of vegetation on the hydrodynamic flow and shear stresses for two dimensional depth averaged flow situations. The applicability and the physical background of these expressions will be discussed in more detail in the subsections below.

3.1.2 Theoretical background

The flow of water through and over vegetation differs from steady uniform flow over a bare bed due to additional body force resistance caused by drag forces exerted on the vegetation. An overview of the forces on a fluid element Δx in a situation with flow over and through vegetation is given in figure 3.2, where the additional resistance due to vegetation is given by F_D and the bed shear stress is given by F_S .

Therefore the balance of forces for uniform flow becomes,

$$F_g \cdot \sin \beta = F_S + F_D \quad (3.1)$$

Since $\sin \beta$ is small and approximates the bottom or friction slope, i_b , this can be given as,

$$F_g \cdot i_b = F_S + F_D \quad (3.2)$$

Where,

F_g	=	Gravitational force	[N]
F_S	=	Shear stress force	[N]
F_D	=	Drag force	[N]

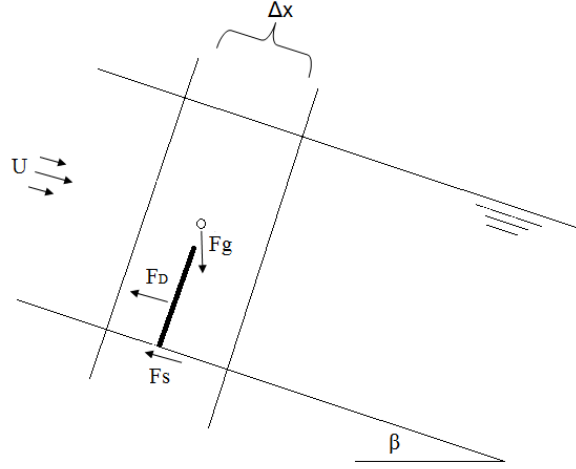


FIGURE 3.2: Fluid forces for steady uniform steady flow with vegetation (Baptist, 2005)

In this equation, the force exerted on the vegetation is generally approximated by the force on a group of rigid vertical cylinders with homogeneous properties. Resulting in the following expression for F_D ,

$$F_D = \frac{1}{2} \cdot \rho \cdot C_D \cdot n_b \cdot \phi \cdot \min\{h, k\} \cdot u^2 \quad (3.3)$$

Therefore, the force balance can be written as,

$$\rho h g i = \tau_b + \frac{1}{2} \cdot \rho \cdot C_D \cdot n_b \cdot \phi \cdot \min\{h, k\} \cdot u^2 \quad (3.4)$$

Or,

$$h g i = \left(1 - n_b \cdot \frac{\pi}{4} \cdot \phi^2\right) \cdot C_{fb} \cdot u^2 + \frac{1}{2} \cdot C_{Dv} \cdot n_b \cdot \phi \cdot \min\{h, k\} \cdot u^2 \quad (3.5)$$

Where,

ρ	= Volumetric mass density of water	$[kg \cdot m^{-3}]$
g	= Gravitational acceleration	$[m \cdot s^{-2}]$
h	= Water depth	$[m]$
i	= Friction slope	$[m \cdot m^{-1}]$
τ_b	= Bed shear stress	$[N \cdot m^{-2}]$
C_{Dv}	= Drag coefficient vegetation	$[-]$
n_b	= Stem density	$[m^{-2}]$
ϕ	= Stem diameter	$[m]$
k	= Uniform vegetation height	$[m]$
u	= Uniform depth average flow velocity	$[m \cdot s^{-1}]$
C_{fb}	= Bed friction coefficient	$[-]$

3.1.3 Representative roughness

Based on this theoretical background, several expressions have been derived to describe the influence of the vegetation on the depth average flow velocity. Baptist (2005) assessed these different approximations in his research and compared them to measurements. He concluded that the relative compact and practical representative roughness approach, consisting of two separate equations, yields the better results.

The first equation describes the situations for flow through unsubmerged vegetation, thus when the water depth is smaller than the vegetation height. In this situation the expression for the representative friction coefficient follows from the momentum balance for uniform flow through the vegetation, equation 3.5. Therefore, it contains a part accounting for the bed shear stress plus the additional term for the vegetation resistance, which results in the following equation,

$$C_{fr, unsubmerged} = C_{fb} + \frac{1}{2} \cdot C_{Dv} \cdot n_b \cdot \phi \cdot h \quad \text{for } h \leq k \quad (3.6)$$

This is valid under the assumption that $n_b \cdot \frac{\pi}{4} \cdot \phi^2 \ll 1$

Where,

$$C_{fr, unsubmerged} = \text{Representative bed friction coefficient for unsubmerged vegetation} \quad [-]$$

The second equation represents the flow through and over submerged vegetation and has been derived through genetic programming by Uthurburu (2004). This equation basically consists of a combination of equation 3.6, describing the flow resistance within the vegetation, and the theoretical logarithmic profile describing the flow above the vegetation (see figure 3.3). For more details see Baptist (2005) and Keijzer et al. (2005).

The equation that approximates the flow for this second situation, which is originally derived by Uthurburu (2004) to approximate the representative Chézy coefficient, is rewritten in terms of the dimensionless friction coefficient (see appendix A) and is given by,

$$C_{fr, submerged} = \left(\frac{1}{\frac{1}{\kappa} \cdot \log\left(\frac{h}{k}\right) + \sqrt{\frac{1}{C_{fb} + \frac{1}{2} \cdot C_{Dv} \cdot n_b \cdot \phi \cdot k}}} \right)^2 \quad \text{for } h \geq k \quad (3.7)$$

This is valid under the assumption that $n_b \cdot \frac{\pi}{4} \cdot \phi^2 \ll 1$

Where,

$$C_{fr, submerged} = \text{Representative bed friction coefficient for submerged vegetation} \quad [-]$$

$$\kappa = \text{Von karman constant} \quad [-]$$

These two separate equation can also be represented in a compact and practical way, this is given by,

$$C_{fr} = \left(\frac{1}{\frac{1}{\kappa} \cdot \log\left(\frac{\max\{h,k\}}{k}\right) + \sqrt{\frac{1}{C_{fb} + \frac{1}{2} \cdot C_{Dv} \cdot n_b \cdot \phi \cdot \min\{h,k\}}}} \right)^2 \quad (3.8)$$

This is valid under the assumption that $n_b \cdot \frac{\pi}{4} \cdot \phi^2 \ll 1$

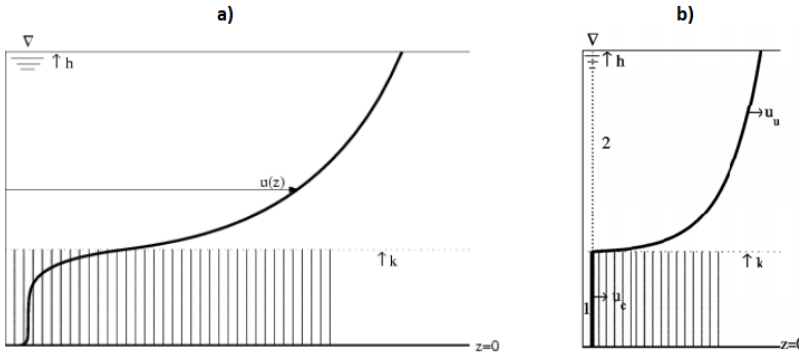


FIGURE 3.3: Vertical profile of horizontal velocity for vegetation
a) Theoretical flow profile (Keijzer et al., 2005) b) Approximated flow profile (Baptist, 2005)

3.1.4 Representative bed shear stress

In addition, Baptist (2005) also elaborated on the influence of vegetation on the total bed shear stress. Although the interest in his research initially was on the effect of vegetation on the hydrodynamic resistance, the assessment of the bed shear stress on vegetated soil is also of use in this thesis. This is due to the fact that the bed shear stress is used in the literature as a measure for the force exerted on the vegetation stems, i.e. Temmerman et al. (2007) relates the vegetation mortality rate to the bed shear stress and Balke et al. (2011) the eradication of seedlings. Therefore, the effect of vegetation on the bed shear stress is assessed here as well.

The need for this assessment is that the use of equation 3.9 would lead to an overestimation of the total bed shear stress for submerged vegetation.

$$\tau_b = \rho \cdot C_{fb} \cdot u^2 \quad (3.9)$$

Where,

$$u = \text{Depth average uniform flow velocity} \quad [m \cdot s^{-1}]$$

The reason for this is that the flow velocity within submerged vegetation is significantly lower than the depth average uniform flow velocity u , see figure 3.3. Therefore, Baptist (2005) developed two approaches to calculate the total bed shear stress within submerged vegetation. He

derived these approaches on the basis of the general formulae for the forces balance and showed that they yielded relatively good results when compared to experimental data. In this thesis, however, only the more convenient and relatively simple reduction factor approach is applied and presented.

The underlying assumption for this reduction factor approach is that the flow profile for submerged vegetation can be considered as two non-interacting flow layers where the flow within the vegetation is uniform (see figure 3.3), which is only valid in situation with dense and relatively high vegetation. Therefore, the shear stress within submerged vegetation can be determined by,

$$\tau_{bv} = \rho \cdot C_{fb} \cdot u_c^2 \quad (3.10)$$

Where,

$$\begin{aligned} u_c &= \text{Depth average uniform flow velocity within vegetation} && [m \cdot s^{-1}] \\ \tau_{bv} &= \text{Total bed shear stress for vegetated soil} && [N \cdot m^{-2}] \end{aligned}$$

Thus, the first step in this reduction factor approach is to determine the uniform flow velocity, u_c , within the vegetation. This follows from the balance of forces, equation 3.5, for the situation that the water depth equals the vegetation height:

$$u_c = \sqrt{\frac{ghi}{C_{fb} + \frac{1}{2} \cdot C_{Dv} \cdot n_b \cdot \phi \cdot k}} \quad (3.11)$$

Combining equation 3.10 and 3.11 finally gives,

$$\tau_{bv} = \frac{1}{1 + \frac{1}{2} \cdot C_{Dv} \cdot k \cdot \phi \cdot n_b \cdot C_{fb}} \rho ghi \quad (3.12)$$

However, more convenient is to express the total bed shear stress within submerged vegetation in terms of the representative friction coefficient value and since ρghi is equivalent to $\rho \cdot C_{fr} \cdot u^2$ this results in:

$$\tau_{bv} = \frac{1}{1 + \frac{1}{2} \cdot C_{Dv} \cdot k \cdot \phi \cdot n_b \cdot C_{fb}} \cdot \rho \cdot C_{fr} \cdot u^2 \quad (3.13)$$

Note, that using this equation in the situation with non-submerged vegetation would result in the well know formula for bed shear stress. Since in that situation the uniform flow velocity within the vegetation is equal to the mean velocity. This also follows from combining the representative friction coefficient equation 3.6 with equation 3.13 for the total bed shear stress.

$$\tau_{bv, unsubmerged} = \rho \cdot C_{fb} \cdot u_c^2 = \rho \cdot C_{fb} \cdot u^2 \quad (3.14)$$

3.1.5 Influence on sediment transport

The previous section described the effect of vegetation on the hydrodynamics, which in turn affects the transport capacity. However, the effect of vegetation on the sediment transport is even more complex. For starters, the correction for the bed shear stress can also be applied for the sediment transport formulae, but additionally, the vegetation is also thought to affect the morphodynamics through:

- Increased sediment transport due to turbulence around vegetation
- Increased resistance against erosion due to a network of roots
- Increased sedimentation due to direct capture of sediment by the vegetation

Research into the relevance of these effects is still being conducted and a formulation to describe these processes in a 2D depth averaged model still requires more development. Therefore, these effects are left outside the scope of this research and only mentioned to give a short overview for the correct general understanding of the process in reality. In conclusion, the effect of vegetation on sediment transport is only taken into account through the increase in hydrodynamic resistance and the corresponding reduction in flow velocity.

3.2 Vegetation growth models

This section discusses two different vegetation growth models on the basis of the different stages identified in chapter 2, i.e. stage 1: stem establishment, stage 2: tussock development and stage 3: marsh platform succession. However, this section will start with a general overview of the models and the underlying assumptions and principles on which they are based.

3.2.1 General overview

The purpose for development of vegetation models in this research, to briefly recall the objective, is to assess the value of bio-geomorphological modelling on the long term and large scale geomorphodynamic development for tidal marshes. This implies that short term fluctuations, such as seasonal variations, and secondary processes, such as competition among species, the influence of salinity concentrations and nutrient availability, are not considered in the model. In addition, the model is only applicable for tidal dominated situations and does not account for the influence of wind or storm waves, as salt marshes generally occur at sheltered low-energy shorelines where the morphological development is dominated by tidal motion.

The normative variable used in the vegetation models to describe vegetation growth is the stem density. This stem density is a good measure for the age and maturity of the vegetation, and can be used to express the influence of the vegetation on the hydrodynamics, as was explained in the previous section. The logical next step is to develop a vegetation growth model capable of describing the temporal and spatial changes in the vegetation density. This in turn requires equations that can describe the important growth and mortality processes. According to the theory described in chapter 2, the important process that could be identified were growth through establishment, stem density growth, lateral expansion and mortality as a consequence

of inundation and shear stresses due to tidal oscillations. A process that is not included is the growth of the stem dimensions (i.e. in diameter or in the vertical), since this growth process is considered to be less important for the long term and large scale growth characteristics. Therefore, it is assumed to be a constant and a characteristic of the vegetation under consideration.

3.2.2 Governing equations

Population dynamics model

The first vegetation-growth model is based on the method developed by Temmerman et al. (2007). This method, describing the vegetation density, can be classified as a population dynamics model. These type of models consider the change of a population per unit of time. In this particular model the change can be obtained by combining the contributions of all these growth and decay processes. The idea behind this model is that vegetation can establish and grow throughout the whole study domain, but that the distribution of bare and vegetated areas is ultimately the result of the prevailing process, i.e. growth or decay. This is described by the following equation,

$$\frac{dn_b}{dt} = \left(\frac{dn_b}{dt}\right)_{\text{establishment}} + \left(\frac{dn_b}{dt}\right)_{\text{growth}} + \left(\frac{dn_b}{dt}\right)_{\text{expansion}} - \left(\frac{dn_b}{dt}\right)_{\text{flow}} - \left(\frac{dn_b}{dt}\right)_{\text{inundation}} \quad (3.15)$$

Where,

$$\begin{aligned} n_b &= \text{Stem density} && [m^{-2}] \\ t &= \text{Time} && [s] \end{aligned}$$

Window of opportunity model

The other model discussed in this sections is based on the window of opportunity concept described by Balke et al. (2011). According to this concept, colonisation of vegetation can occur when a window of opportunity arises. Balke et al. (2011) showed that for the establishment of mangrove seedlings on tidal flats, this window of opportunity implies surviving several physical threshold. Although Balke et al. (2011) only discussed this for mangrove seedlings, Wesenbeeck (personal communication) suggests that a similar concept can be applied to describe the establishment of salt marsh vegetation.

In addition to the use of a different establishment concept, this model also deviates from the population dynamics model in the way the vegetation mortality is represented. Since this model does not consider any vegetation decay processes. Instead, settlement only occurs if a window of opportunity arises, lateral expansion only occurs under favourable hydrodynamic conditions and an area only stays vegetated as long as the conditions stay favourable. This ultimately results in a model that considers either a bare state or a vegetated state, where the latter only occurs at suitable locations. This is represented by the following equation,

$$\frac{dn_b}{dt} = \left(\frac{dn_b}{dt}\right)_{\text{establishment}} + \left(\frac{dn_b}{dt}\right)_{\text{growth}} + \left(\frac{dn_b}{dt}\right)_{\text{expansion}} \quad (3.16)$$

The reason for introducing this second model is that the population dynamics model, seen from a theoretical point of view, can be improved. In particular, since it assumes unbounded vegetation growth should be balanced or countered through the use of vegetation decay functions. To this end, the theoretically supported window of opportunity concept is applied in the new model, which ensures that vegetation only establishes and grows on suitable locations. Therefore, making the use of vegetation decay function redundant. The result is a model that, although maybe less dynamic, is more transparent and practical, as the use of these decay rates is less insightful, difficult to quantify, and theoretical harder to justify.

3.2.3 Stage 1: Stem establishment

Population dynamics model

The colonization of vegetation on bare tidal flats, as described in section 2.2.1 ('Stage 1: stem establishment'), starts with the establishment of vegetation stems that, after surviving the physical thresholds, develop into tussocks or patches of vegetation. These physical thresholds represent the favourable hydrodynamic conditions that are required for settlement, however, they are not considered in this particular formulation, instead these processes are approximated by the decay processes. Therefore, the establishment processes are simplified and can be represented by a relatively simple stochastic formulation describing the establishment of these patches as if the conditions are favourable throughout the whole study domain. Meaning that the establishment chance, P_{est} , depends on the coincidence of favourable abiotic conditions, like the soil conditions, temperature and the dispersal of seeds or rhizomes, in the study area. This is given by,

$$\left(\frac{dn_b}{dt}\right)_{establishment} = P_{est} \cdot n_{b,establishment} \quad (3.17)$$

Where,

$$\begin{aligned} P_{est} &= \text{Establishment chance of vegetation on bare soil} && [yr^{-1}] \\ n_{b,establishment} &= \text{Initial establishment density} && [m^{-2}] \end{aligned}$$

According to Ye (2012), it is quite realistic to assign such a stochastic function to model the random distribution of seeds, parts of rhizomes or ramets over the study domain. Since the dispersal length scale can be in the order of a 100 meters.

Window of opportunity model

The establishment process in the window of opportunity model considers the three physical thresholds identified by Balke et al. (2011), which have been represented in three phases. The idea behind the window of opportunity concept is that establishment of seedlings and development into permanent vegetation is only successful if the vegetation manages to pass through these three phases.

This final step into permanent vegetation, after surviving the three stages, is represented by the governing establishment equation:

Governing establishment equation:

$$\text{For } T_t = T_{\text{phase 1}} + T_{\text{phase 2}} + T_{\text{phase 3}} : \quad dn_{b, \text{establishment}} = n_{b, \text{seedling}} \quad (3.18)$$

Where,

$$\begin{aligned} T_t &= \text{Occurring window of opportunity} && [s] \\ T_{\text{phase 1, 2, 3}} &= \text{Required window of opportunity for the different phases} && [s] \\ n_{b, \text{seedling}} &= \text{Initial establishment density of seedlings} && [m^{-2}] \end{aligned}$$

Phase 1: *Establishment of seedlings*

The first phase describes the initial establishment of vegetation stems, which requires an inundation free period. If such a period occurs then there is a chance that establishment can take place. In this formulation, the establishment chance represents the occurrence or coincidence of an inundation free period with other necessary abiotic conditions. This chance is described using a stochastic function.

Establishment of seedlings possible after inundation free period throughout phase 1:

$$\text{For } T_t > T_{\text{phase 1}} : \quad \left(\frac{dn_b}{dt} \right)_{\text{seedling}} = P_{\text{est}} \cdot n_{b, \text{establishment}} \quad (3.19)$$

Phase 2: *Development of the root system*

The second phase describes the development of the roots system of the newly established seedlings. This development is essential for the vegetation in order to increase their resistance against bed shear stresses imposed by the hydrodynamics. Initially, just after establishment, the stems are still vulnerable to higher energy events. Therefore, the stems require a period with relative calm hydrodynamic conditions to further develop their roots and increase their resistance. This increase in root length, and thus the increase in shear stress resistance, of the seedlings in time can be approximated by a linear function according to the measurement done by Balke et al. (2011). This process is given by,

Increase in shear stress resistance and perseverance throughout phase 2:

$$\text{For } T_{\text{phase 2}} > T_t > T_{\text{phase 1}} : \quad \begin{aligned} \tau_{b, \text{crit, phase 2}} &= a_\tau \cdot [T_t - T_{\text{phase 1}}] + b_\tau \\ \tau_{b, \text{crit, phase 2}} &> \tau_b \end{aligned} \quad (3.20)$$

Where,

$$\begin{aligned} \tau_{b, \text{crit, phase 2}} &= \text{Critical bed shear stress resistance seedling} && [N \cdot m^{-2}] \\ \tau_b &= \text{Bed shear stress} && [N \cdot m^{-2}] \end{aligned}$$

Phase 3: Perseverance throughout extreme energy events

The final phase describes the period after the root system reaches maturity, which is characterized by an increased bed shear stress resistance. During this period the seedlings need to survive exposure to extreme energy events that generally occur during storms and/or spring tide. These events can cause high shear stresses on the vegetation, probably in combination with reduced resistance due to a smaller effective root length caused by sheet erosion, although the effect of sheet erosion is not explicitly taken into account. This is given by,

Perseverance throughout phase 3:

$$\text{For } T_{\text{phase 3}} > T_t > T_{\text{phase 1}} + T_{\text{phase 2}} : \quad \tau_{b, \text{crit}} > \tau_b \quad (3.21)$$

Where,

$$\tau_{b, \text{crit}} = \text{Maximum shear stress resistance of mature vegetation} \quad [N \cdot m^{-2}]$$

This phase generally has a duration in the order of a spring-neap cycle. In case that the shear stresses remain below the resistance of the vegetation throughout this period, it is assumed that vegetation settled in a favourable location, allowing development of the seedlings into tussocks. This is given by the governing establishment equations, see equation 3.18.

3.2.4 Stage 2: Stem density growth

The stem density growth or population growth is the process that describes the vegetation density increase within a patch of vegetation in time. It is this increase in density that enhances the influence of tussocks on the surroundings, which represents the tussock development process in section 2.2.2 ('Stage 2: Tussock development').

The population growth function adopted in both vegetation models to describe this increase in stem density is a logistic growth function, which can be given by the following formula,

$$\left(\frac{dn_b}{dt} \right)_{\text{growth}} = r \left(1 - \frac{n_b}{n_{b, \text{max}}} \right) n_b \quad (3.22)$$

Where,

$$\begin{aligned} r &= \text{Intrinsic growth rate of stem density} && [yr^{-1}] \\ n_{b, \text{max}} &= \text{Maximum carrying capacity stem density, uniform and constant} && [m^{-2}] \end{aligned}$$

This function, as can be seen in figure 3.4, is characterised by an initial and final period where the stem density increase is more gradual, and a middle period with a more rapid increase. This corresponds quite well to the stem density growth characteristic observed in salt marshes, as the initial increase in growth rate is a result of the improving growth conditions due to the biophysical feedback effect, this effect is eventually hampered as a consequence of resource limitation.

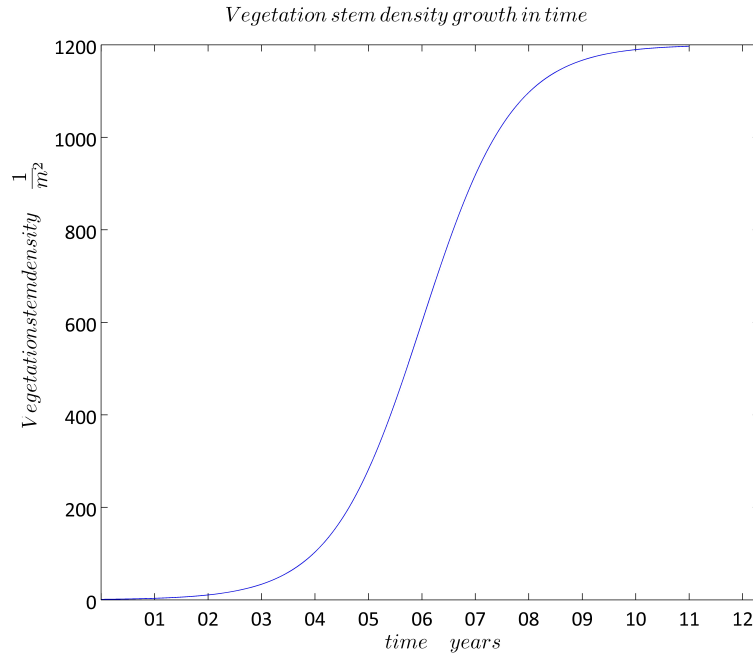


FIGURE 3.4: Stem density growth described by a logistic growth function

3.2.5 Stage 3: Marsh platform succession

The lateral expansion of vegetation represents the process that drives the marsh platform succession described in section 2.2.3 ('stage 3: Marsh platform succession'). It is this process that is responsible for the development, the expansion and finally the merging of tussocks of vegetation, which results in an overgrown marsh platform. However, this does require favourable hydrodynamic conditions in the area adjacent to the tussock's edge. Therefore, the windows of opportunity model imposes requirements in terms of favourable elevation height and low hydrodynamic stresses before expansion can occur, whereas the population dynamics model, as mentioned before, takes this into account through decay functions.

Apart from this, the lateral expansion is represented in both models by the same equation. This equation describes the radial growth of tussocks by a displacement velocity in the direction of decreasing plants density. The magnitude of this displacement or expansion is related to the radial growth rate, D and the difference between the stem densities in the tussock and the adjacent area. This formulation is given by:

$$\left(\frac{dn_b}{dt}\right)_{\text{expansion}} = K \frac{\nabla n_b}{|\nabla n_b|} \cdot \nabla n_b \quad (3.23)$$

Where:

$$\begin{aligned} \nabla n_b &= \text{Stem density gradient} && [m^{-3}] \\ K &= \text{Uniform radial growth rate} && [m \cdot yr^{-1}] \end{aligned}$$

3.2.6 Vegetation decay processes

Population dynamics model

In the theory and the previous sections there has been mention of certain requirements regarding favourable hydrodynamic conditions that must be satisfied before vegetation can establish or expand. One of these requirements, as is known from section 2.2, is the need for an inundation free period for establishment and the need for sufficient emergence time for photosynthesis. This requirement can be represented by a vegetation density decay process that considers vegetation loss due to inundation, since the inundation and the submergence duration are strongly correlated. The result is a formulation that describes vegetation mortality when the inundation height is too high and/or the inundation duration is too long, which is the case when vegetation establishes or grows in an insufficiently shallow area. This equation is given by,

$$\left(\frac{dn_b}{dt}\right)_{inundation} = \max\{(h - h_{crit}), 0\} \cdot PE_h \quad (3.24)$$

Where,

$$\begin{aligned} h_{crit} &= \text{Critical inundation water depth} && [m] \\ PE_h &= \text{Plant mortality rate for inundation stress} && [m^{-3} \cdot s] \end{aligned}$$

In addition, the theory also discussed a requirement for adequately calm flow conditions that need to be satisfied in order for vegetation to successfully establish or expand. This requirement prevents vegetation to settle in gullies with a drainage function or other areas with high flow velocities. Therefore, it considers vegetation density loss due to flow velocity induced shear stress. The formulation used to describe this process has a similar form as the formulation for mortality due to inundation stress, since it also contains a shear stress threshold value. See equation 3.25 below.

$$\left(\frac{dn_b}{dt}\right)_{flow} = \max\{(\tau_b - \tau_{b, crit}), 0\} \cdot PE_\tau \quad (3.25)$$

Where,

$$\begin{aligned} \tau_b &= \text{Measured bed shear stress} && [N \cdot m^{-2}] \\ \tau_{b, crit} &= \text{Critical bed shear stress resistance vegetation} && [N \cdot m^{-2}] \\ PE_\tau &= \text{Plant mortality rate for shear stress} && [N \cdot s^{-1}] \end{aligned}$$

Window of opportunity model

Although the window of opportunity model does not consider any decay processes, it does monitor the conditions of existence for vegetation. This is necessary since the conditions after settlement can be subjected to change as a consequence of erosion, subsidence, sea level rise or changes in the hydrodynamic conditions. Therefore, the model monitors and checks as to whether the conditions of existence for the vegetation, in terms of elevation height and hydrodynamic stresses, remain favourable.

3.3 Discussion

This chapter presents, based on the findings in chapter 2, the framework for a bio-geomorphological model, which consists of a method describing the vegetation growth processes, and an approach that couples this to the hydrodynamics.

The purpose of this chapter is to develop a bio-geomorphological model that is capable of describing the important processes and characteristics identified in the theory. To this end, two vegetation growth models are presented, one based on the method by Temmerman et al. (2007) and a new method based on the window of opportunity concept (Balke et al., 2011). The essence of these vegetation methods is to capture the temporal and spatial vegetation growth characteristics in one normative variable, the stem density. This vegetation stem density is in turn related to the morpho-hydrodynamics through the representative roughness and shear stress approach developed by Baptist (2005)

However, it is good to be aware of the fact that the models are a simplification of nature, which can hardly explain the full dynamics of the system. This applies both to the vegetation methods, and the approach taking into account the influence of vegetation on the hydrodynamics, sediment transport and morphology. For instance:

- vegetation growth also depends on ecological processes like nutrient availability
- spatial and temporal vegetation patterns are also affected by cliff erosion and waves
- the influence of vegetation on sediment transport is a more complex phenomenon than only an effect on the hydrodynamic roughness (see section 3.1.5).

Nevertheless, it is hypothesized that the processes considered in the models can be used to describe and reproduce the long-term characteristics of salt marsh formation and development. In addition, development of the window of opportunity model raises the question which vegetation method is better in reproducing the vegetation growth characteristics. To address these issues, the next step is to implement the vegetation models presented in this chapter in the numerical software FINEL2D. This will be discussed in detail in the next chapter.

Chapter 4

Numerical implementation

The aim of this chapter is to describe the implementation of the vegetation growth models in the numerical model FINEL2d. To this end, section 4.1 will start with a short description of the finite element model FINEL2d. Subsequently, the implementation of the representative roughness and shear stress that describes the interaction between vegetation and hydrodynamics will be presented in section 4.2. Next, in section 4.3 the implementation of the vegetation growth models is discussed. Finally, section 4.4 will introduce the bio-geomorphological acceleration factor and discuss the use and the implementation of this factor in the bio-geomorphological model.

Figure 4.1 shows an overview of the mathematical framework and indicates in which section the different aspects of the bio-geomorphological model are presented.

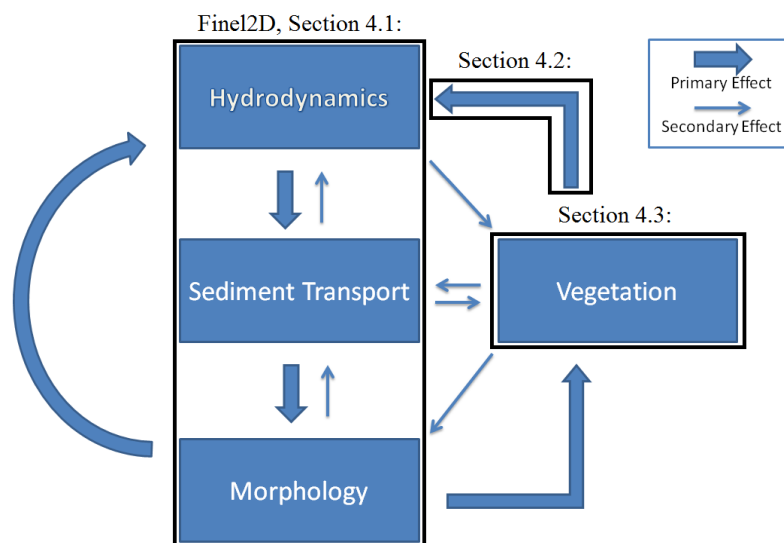


FIGURE 4.1: Interaction of vegetation with the morpho-hydrodynamics (Baptist, 2005)

4.1 Description FINEL2d

The software used in this thesis is FINEL2d, which is a morpho-hydrodynamic model developed by Svašek hydraulics. FINEL2d is a 2DH numerical model based on the finite element method that uses unstructured triangular grid cells that can vary in size and shape. This has the advantage that it allows for flexible schematisations, or in other words for high resolution modelling in the area of interest.

4.1.1 Hydrodynamics

The hydrodynamics in this model are based on the depth-integrated shallow water equations (Vreugdenhil, 1994), which are given by,

The continuity equation:

$$\frac{\partial h}{\partial t} + \frac{\partial uD}{\partial x} + \frac{\partial vD}{\partial y} = 0 \quad (4.1)$$

The momentum balance in the x direction:

$$\frac{\partial Du}{\partial t} + \frac{\partial Du^2}{\partial x} + \frac{\partial Duv}{\partial y} + f_c Dv + gD \frac{\partial h}{\partial x} - \frac{1}{\rho} \tau_{x,b} + \frac{1}{\rho} \tau_{x,w} + \frac{1}{\rho} \tau_{x,r} = 0 \quad (4.2)$$

The momentum balance in the y direction:

$$\frac{\partial Dv}{\partial t} + \frac{\partial Duv}{\partial x} + \frac{\partial Dv^2}{\partial y} - f_c Du + gD \frac{\partial h}{\partial y} - \frac{1}{\rho} \tau_{y,b} + \frac{1}{\rho} \tau_{y,w} + \frac{1}{\rho} \tau_{y,r} = 0 \quad (4.3)$$

In which,

$$D = h + z_b$$

where,

u, v	= Depth average velocity in x and y direction	$[m \cdot s^{-1}]$
D	= Water depth	$[m]$
h	= Water level	$[m]$
z_b	= Bottom level	$[m]$
f_c	= Coriolis coefficient	$[s^{-1}]$
τ_b	= Bottom shear stress	$[N \cdot m^{-2}]$
τ_w	= Wind shear stress	$[N \cdot m^{-2}]$
τ_r	= Radiation stress	$[N \cdot m^{-2}]$

These equations take into account the advection and pressure gradients, and external forces like Coriolis force, bottom shear stress, wind shear stress and radiation stress. However, it does not take into account turbulent shear stresses.

These shallow water equations are solved for every grid cell with the discontinuous Galerkin method (Hughes, 1987), which takes the water level and the two velocity components as a constant in each grid cell, see figure 4.2.

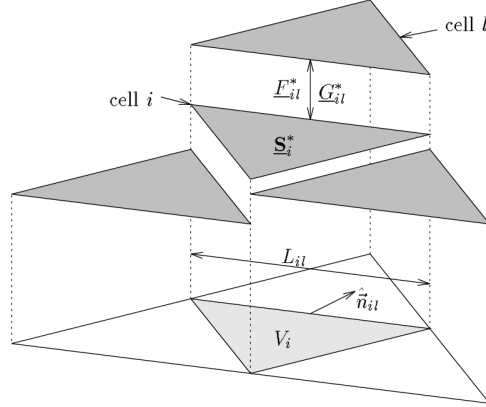


FIGURE 4.2: Discontinuous Galerkin method with constant flow and water level variables

However, since these flow and water level variables are determined at the cell centres, the fluxes at the element boundaries are not known beforehand. To compute these fluxes at all interfaces from cell averaged state variables, the model uses an approximate Riemann solver according to Roe (Glaister, 1993), which is mass and momentum conservative. These equations are in turn solved with an explicit time integration scheme for which the time step is controlled automatically. The use of this explicit time integration scheme in combination with the discontinuous discretisation allows for a relatively easy handling of flooding and drying of elements, which is useful for estuaries and thus for salt marsh modelling.

4.1.2 Morphodynamics

The starting point for the morphological changes or bed level evolution in FINEL2d follows from the sediment balance equation:

$$\frac{\partial z_b}{\partial t} + \frac{\partial q_x}{\partial x} + \frac{\partial q_y}{\partial y} = 0 \quad (4.4)$$

Where,

$$q_x, q_y = \text{Sediment flux in respectively x and y direction} \quad [m^2 \cdot s]$$

The non-cohesive part of these sediment fluxes is determined through the use of the transport formula by Engelund and Hansen for total load (Engelund et al., 1967) in combination with a time lag effect according to Gallapatti et al. (1985). Therefore, the following non-dimensional equilibrium concentration is determined,

$$c_e = \frac{S}{D\sqrt{u^2 + v^2}} \quad (4.5)$$

Where,

S	= Magnitude of the equilibrium sand transport	$[m^2 \cdot s]$
c_e	= Equilibrium sediment concentration in the water	$[kg \cdot m^{-3}]$

Subsequently, equation 4.6 compares the equilibrium concentration to the emergent concentration in a grid cell. When this concentration is lower than the equilibrium equation erosion will occur and when the concentration is higher sedimentation will occur.

$$\frac{dc}{dt} = \frac{1}{T_A} [c_e(t) - c(t)] \quad (4.6)$$

Where,

T_A	= Characteristic time scale	$[s]$
-------	-----------------------------	-------

T_A is the characteristic time scale, that represents the time needed for the flow to adjust to the equilibrium situation. For erosion this is defined by the water depth and the sediment fall velocity.

4.2 Implementation of representative roughness and shear stress

Numerical discretisation

This section describes the implementation of the representative roughness and shear stress equations, which account for the effect of the vegetation on the hydrodynamics. The discretisation of these equations is quite straight forward and identical for both vegetation growth models, although it contains one additional conditional statement that needs to be satisfied. This statement ensures that the hydrodynamics are only influenced when a vegetation patch is dense and mature enough to have an influence. This conditional statement is not only a consequence of the physical representation, but also of the applicability of the formulations for representative shear stress, see section 3.1.

This leads to the following discretisation for the representative roughness equation:

$$\begin{aligned} &\text{If } n_{b,i} > n_{b,threshold} C_{fr} \text{ Then} \\ &C_{fr,i} = \left(\frac{1}{\frac{1}{\kappa} \cdot \log\left(\frac{\max\{h_i, k\}}{k}\right) + \sqrt{\frac{1}{C_{fb,i} + \frac{1}{2} \cdot C_{Dv} \cdot n_{b,i} \cdot \phi \cdot \min\{h_i, k\}}}}} \right)^2 \\ &\text{Else} \\ &C_{fr,i} = C_{fb,i} \end{aligned} \quad (4.7)$$

And for the bed shear stress this can be discretion by,

$$\begin{aligned}
 &\text{If } n_{b,i} > n_{b,threshold} C_{fr} \quad \text{Then} \\
 \tau_{bv,i} &= \frac{1}{1 + \frac{1}{2} \cdot C_{Dv} \cdot k \cdot \phi \cdot n_{b,i} \cdot C_{fb,i}} \cdot \rho \cdot C_{fr,i} \cdot u_i^2 \\
 &\text{Else} \\
 \tau_{bv,i} &= \rho \cdot C_{fb,i} \cdot u_i^2
 \end{aligned} \tag{4.8}$$

Where,

$$n_{b,threshold} C_{fr} = \text{Threshold hydrodynamic influence stem density} \quad [m^{-2}]$$

4.3 Implementation vegetation models

This section describes the numerical discretisation and implementation of the vegetation growth equations described in chapter 3. The normative variable used in both models to describe the vegetation growth is the stem density n_b . This variable is taken as a constant in each grid cell, i . This implies that the grid cell size determines the modelled tussock size. Ideally the grid cell size should approximate the tussock size observed in reality, but more importantly the grid cell size should not affect the outcome of the models. To this end, it is important that the numerical discretisation chosen is not dependent on the grid cell size.

4.3.1 Governing equation

The temporal variation in stem density in these modelled tussocks is computed for both vegetation models through an assessment of the change in stem density, $\Delta n_{b,i}$, for every computational time step, Δt . This is given by,

$$n_{b,i}^{t+\Delta t} = \max \{n_{b,i}^t + \Delta n_{b,i}, 0\} \tag{4.9}$$

Population dynamics model

The governing equation that describes this temporal change of vegetation density for each time step and each grid cell is discretised by:

$$\Delta n_{b,i} = \Delta n_{b,establishment,i} + \Delta n_{b,growth,i} + \Delta n_{b,expansion,i} - \Delta n_{b,flow,i} - \Delta n_{b,inundation,i} \tag{4.10}$$

Window of opportunity model

A similar discretisation can be used for the window of opportunity model:

$$\Delta n_{b,i} = \Delta n_{b,establishment,i} + \Delta n_{b,growth,i} + \Delta n_{b,expansion,i} \tag{4.11}$$

4.3.2 Stage 1: Stem establishment

Population dynamics model

The establishment of patches of vegetation in bare grid cells is modelled with a stochastic function. This function can be represented in the model by two conditional statements which simulate the occurrence of establishment in a bare grid cell, when these conditions are satisfied some initial stem density is assigned. These statements are given by:

$$\left. \begin{array}{l} \text{If } n_b < n_{b, \text{threshold bare}} \\ \text{If } \chi < 1 - (1 - P_{est})^{\Delta t_{yr}} \end{array} \right\} \quad \text{Then } \Delta n_{b, \text{establishment}, i} = n_{b, \text{establishment}} \quad (4.12)$$

Where,

$$\begin{array}{ll} n_{b, \text{threshold bare}} & = \text{Threshold bare grid cell} & [m^{-2}] \\ \chi & = \text{Number from pseudo-random number generator between 0 and 1} & [-] \\ P_{est} & = \text{Establishment chance per grid cell} & [yr^{-1}] \\ \Delta t_{yr} & = \text{Time step converted to years} & [yr] \\ n_{b, \text{establishment}, i} & = \text{Initial establishment density of vegetation stems} & [m^{-2}] \end{array}$$

Window of opportunity model

The establishment process in the window of opportunity model consists of three phases. After surviving these three phases, it is assumed that the established seedlings, $n_{b, \text{seedlings}, i}$, indeed settled in a favourable location which allows development into permanent tussocks, $n_{b, \text{establishment}, i}$. This final step into permanent vegetation, after surviving the three stages, is discretised by the following equation:

$$\begin{array}{ll} \text{If } T_{rec:3, i} > T_{ph:3} & \text{Then} \\ \Delta n_{b, \text{establishment}, i} = n_{b, \text{seedlings}, i} & \end{array} \quad (4.13)$$

Where,

$$\begin{array}{ll} T_{Rec:3, i} & = \text{Recorded duration in phase 3} & [s] \\ T_{Ph:3} & = \text{Duration of phase 3} & [s] \\ \Delta n_{b, \text{establishment}, i} & = \text{Stem density increase due to establishment} & [m^{-2}] \\ n_{b, \text{seedling}, i} & = \text{Initial establishment density of seedlings} & [m^{-2}] \end{array}$$

Prior to this permanent establishment are the three phases, which are discussed below.

Phase 1: Establishment of seedlings

The first phase in the establishment process represents the establishment of seedlings, $n_{b, \text{seedlings}, i}$. The establishment of these seedlings in a bare grid cell is described, similarly to the establishment in the population dynamics model, by a stochastic function, although it contains an additional condition. This condition is an inundation free window of opportunity, $T_{Ph:1}$, which is recorded for each grid cell separately with the variable $T_{Rec:1, i}$.

This is discretised by:

$$\left. \begin{array}{l} \text{If } n_b < n_{b, \text{threshold bare}} \\ \text{If } T_{Rec:1, i} > T_{Ph:1} \\ \text{If } \chi < 1 - (1 - P_{est})^{\Delta t_{yr}} \end{array} \right\} \text{Then } n_{b, \text{seedlings}, i} = n_{b, \text{establishment}} \quad (4.14)$$

With,

$$\begin{array}{ll} \text{If } h_i \leq 0 & \text{Then } T_{Rec:1, i} = T_{Rec:1, i} + \Delta t \\ \text{Else} & T_{Rec:1, i} = 0 \end{array}$$

Where,

$$\begin{array}{ll} T_{Rec:1, i} & = \text{Recorded inundation free period} & [s] \\ T_{Ph:1} & = \text{Inundation free period required} & [s] \\ n_{b, \text{establishment}} & = \text{Input establishment density seedling} & [m^{-2}] \\ h_i & = \text{Computed water depth} & [m] \\ \Delta t & = \text{Time step} & [s] \end{array}$$

Phase 2: *Development of the root system*

Phase 2 starts after initial establishment of the seedlings. During this phase the development of the roots system and the associated increase in shear stress resistance is modelled and compared to the occurring hydrodynamic shear stresses. This development is represented by a linear function that describes the increasing resistance of the stems to shear stress in time, which is implemented as:

$$\tau_{b, \text{crit}, \text{phase } 2, i} = a_\tau \cdot T_{rec:2, i} + b_\tau \quad (4.15)$$

In which,

$$a_\tau = \left[\frac{\tau_{b, \text{ph}:3} - \tau_{b, \text{ph}:1}}{T_{ph\ 2, i}} \right]$$

$$b_\tau = \tau_{b, \text{ph}:1}$$

Where,

$$\begin{array}{ll} T_{Rec:2, i} & = \text{Recorded duration in phase 2} & [s] \\ \tau_{b, \text{ph}:3} & = \text{Maximum shear stress resistance of mature vegetation} & [N \cdot m^{-2}] \\ \tau_{b, \text{ph}:1} & = \text{Shear stress resistance of seedlings after phase 1} & [N \cdot m^{-2}] \\ T_{Ph:2} & = \text{Duration of phase 2} & [s] \end{array}$$

The resistance, $\tau_{b, \text{crit}, \text{phase } 2, i}$ is subsequently compared to the occurring hydrodynamic shear stresses. In the situation that the threshold resistance is exceeded, then the initial established seedlings are dislodged and disappears.

This is discretised by:

$$\left. \begin{array}{l} \text{If } T_{Rec:2, i} < T_{Ph:2} \\ \text{If } \tau_{bv, i} > \tau_{b, crit, phase 2, i} \end{array} \right\} \quad \text{Then } n_{b, seedlings, i} = 0 \quad (4.16)$$

With,

$$\begin{array}{ll} \text{If } n_{b, seedlings, i} > 0 & \text{Then } T_{Rec:2, i} = T_{Rec:2, i} + \Delta t \\ \text{Else} & T_{Rec:2, i} = 0 \end{array}$$

Phase 3: Perseverance throughout high energy events

The last phase of the stem establishment process begins when the established seedlings survived phase 2. This third and final phase is similar to the previous in a sense that the occurring shear stresses are compared to the shear resistance as well. However, the aim in this phase is to test whether the settled seedlings can survive the high energy events and thereby to check if the vegetation has settled in the right location. As a result, the discretisation of this phase is quite similar to equation 4.16 in phase 2, as can be denoted:

$$\left. \begin{array}{l} \text{If } T_{Rec:3, i} < T_{Ph:3} \\ \text{If } \tau_{bv, i} > \tau_{b, ph:3} \end{array} \right\} \quad \text{Then } n_{b, seedlings, i} = 0 \quad (4.17)$$

With,

$$\begin{array}{ll} \text{If } T_{Rec:2, i} > T_{Ph:2} & \text{Then } T_{Rec:3, i} = T_{Rec:3, i} + \Delta t \\ \text{Else} & T_{Rec:3, i} = 0 \end{array}$$

4.3.3 Stage 2: Stem density growth

The stem density growth, representing the development of the vegetation patches by a logistic growth function, is identical for both models. The implementation of this logistic growth function is quite straight forward, as it is a simple ordinary differential equation. Therefore, the equation can be discretised by:

$$\Delta n_{b, growth, i} = \max \left\{ r \left(1 - \frac{n_{b, i}}{n_{b, max}} \right) n_{b, i} \cdot \Delta t_{yr}, 0 \right\} \quad (4.18)$$

Where,

$$\begin{array}{ll} r & = \text{Intrinsic growth rate of stem density} & [yr^{-1}] \\ n_{b, max} & = \text{Maximum carrying capacity stem density} & [m^{-2}] \\ \Delta t_{yr} & = \text{Time step converted to years} & [yr] \\ \Delta n_{b, growth, i} & = \text{Stem density growth} & [m^{-2}] \end{array}$$

4.3.4 Stage 3: Marsh platform succession

Population dynamics model

The lateral expansion of the vegetation through the rhizome system is represented by an equation that describes the stem density flux-difference from one cell to the other. This process is schematised for the triangular grid cell structure used in FINEL2d in figure 4.3 and is discretised by the equation below:

$$\Delta n_{b, \text{expansion}, i} = \frac{\sum_{j=1}^{j=3} K \cdot \max \{n_{b,j} - n_{b,i}, 0\} \cdot \Gamma_j}{A_i} \cdot \Delta t_{yr} \quad (4.19)$$

Where,

K	= Uniform radial growth rate	$[m \cdot yr^{-1}]$
$n_{b,j}$	= Stem density in neighbouring grid cell	$[m^{-2}]$
$n_{b,i}$	= Stem density in grid cell under consideration	$[m^{-2}]$
Γ_j	= Interface length between the two cells under consideration	$[m]$
$\Delta n_{b, \text{expansion}, i}$	= Stem density increase due to lateral expansion	$[m^{-2}]$

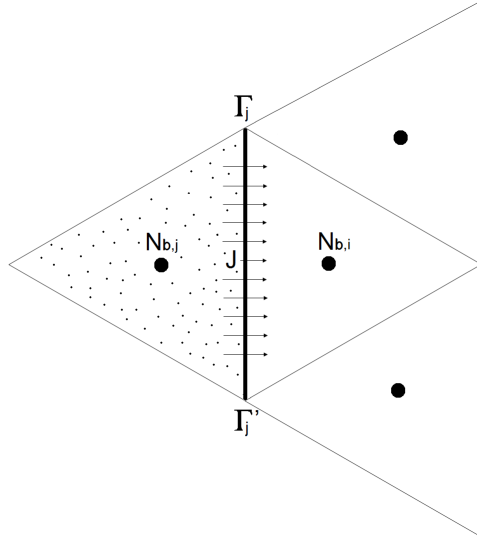


FIGURE 4.3: Schematisation of the stem density flux for triangular grid discretisation

In this equation the stem density flux-difference is represented by the stem density difference between two neighbouring grid cells multiplied by the radial growth rate or lateral expansion rate, K . Subsequently, the total flux over the cells edge can be determined by multiplying this flux by the interface length, Γ . Ultimately, the total increase in stem density within one cell is the result of the summation of these fluxes divided by the grid cell surface area.

Window of opportunity model

The lateral expansion of the rhizomes system is discretised with the same equation as is used for the population dynamics model. However, the difference is that this model considers additional conditions that need to be satisfied before expansion can occur.

As a result, the model evaluates two conditional statements concerning the submergence conditions and the shear stress conditions in the grid cell under consideration and an additional statement concerning the maturity of vegetation in the cell from which the flux originates. This can be discretised as follows:

$$\left. \begin{array}{l} \text{If } I_{\%,i} < I_{\%,crit} \\ \text{If } \tau_{bv,i} < \tau_{b,crit} \\ \text{If } n_{b,j} > n_{b,crit\ diff} \end{array} \right\} \text{ Then } \Delta n_{b,expansion,i} = \frac{\sum_{j=1}^{j=3} K \cdot \max\{n_{b,j} - n_{b,i}, 0\} \cdot \Gamma_j}{A_i} \Delta t_{yr} \quad (4.20)$$

Where,

$$\begin{array}{ll} I_{\%,i} & = \text{Average submergence percentage} & [-] \\ I_{\%,crit} & = \text{Critical submergence percentage} & [-] \\ n_{b,crit\ diff} & = \text{Threshold hydrodynamic influence stem density} & [m^{-2}] \end{array}$$

This does, however, require an additional expression to determine the averaged submergence percentage, $I_{\%}$, which can be recorded for each grid cell separately. To this purpose a running or moving average is computed as follows:

$$I_{\%,i} = \frac{1}{m} \sum_{j=i}^{i+m-1} a_j \quad (4.21)$$

Where,

$$\begin{array}{ll} a_i & = 100 \text{ when vegetation is submerged} & [-] \\ a_i & = 0 \text{ when vegetation is unsubmerged} & [-] \\ m & = \text{Number of measurements} & [-] \end{array}$$

An efficient way to implement this equation, without needing to store an array of numbers for each grid cell, is given by:

$$\begin{array}{l} \text{If } h_i > k \\ I_{\%,i}^{t+\Delta t} = I_{\%,i}^t \cdot (1 - \varphi) + \varphi \\ \text{Else} \\ I_{\%,i}^{t+\Delta t} = I_{\%,i}^t \cdot (1 - \varphi) \end{array} \quad (4.22)$$

In which,

$$\varphi = \frac{\Delta t}{T_{I\%, avg}}$$

Where,

$$T_{I\%, avg} = \text{Inundation relaxation time} \quad [s]$$

4.3.5 Vegetation decay processes

Population dynamics model

The requirement for favourable growth conditions is represented by the vegetation decay processes. So, if vegetation settles in a location with less favourable conditions, then the stem density experiences a decay. This decay rate is computed by comparing the hydrodynamic output to the critical threshold. The coupling of these vegetation decay rates with the hydrodynamic output is carried out in an online fashion, meaning that the hydrodynamic output is used as input for the decay functions at every computational time step.

This is discretised for the inundation decay rate as:

$$\Delta n_{b, inundation, i} = \max\{(h_i - h_{crit}), 0\} \cdot PE_h \cdot \Delta t \quad (4.23)$$

Where,

$$\begin{aligned} h_i &= \text{Computed water depth} & [m] \\ h_{crit} &= \text{Critical inundation water depth} & [m] \\ PE_h &= \text{Plant mortality coefficient for inundation stress} & [m^{-3} \cdot s^{-1}] \\ \Delta n_{b, inundation, i} &= \text{Reduction in stem density due to inundation stress} & [m^{-2}] \end{aligned}$$

And for the shear stress this is implemented as:

$$\Delta n_{b, flow, i} = \max\{(\tau_{bv, i} - \tau_{b, crit}), 0\} \cdot PE_\tau \cdot \Delta t \quad (4.24)$$

Where,

$$\begin{aligned} \tau_{bv, i} &= \text{Computed instantaneous bed shear stress} & [N \cdot m^{-2}] \\ \tau_{b, crit} &= \text{Critical bed shear stress} & [N \cdot m^{-2}] \\ PE_\tau &= \text{Plant mortality coefficient for shear stress} & [N \cdot s^{-1}] \\ \Delta n_{b, flow, i} &= \text{Reduction in stem density due to shear stress} & [m^{-2}] \end{aligned}$$

Window of opportunity model

As mentioned, the window of opportunity model does not consider any decay processes, instead it does monitor the conditions of existence for vegetation. This monitoring of these conditions

consists of determining whether the hydrodynamic conditions, in terms of emergence times and shear stresses, remain favourable. In the situation that one of these conditions is not met, then vegetation disappears and the grid cell become bare again. For the submergence condition, this is discretised by,

$$\begin{aligned} \text{If } I_{\%, i} &> I_{\%, crit} \\ \text{Then } n_{b, i} &= 0 \end{aligned} \quad (4.25)$$

And for the shear stress condition, this is implemented by:

$$\begin{aligned} \text{If } \tau_{bv, i} &> \tau_{b, ph:3} \\ \text{Then } n_{b, i} &= 0 \end{aligned} \quad (4.26)$$

4.4 Bio-geomorphological acceleration factor

The bio-geomorphological acceleration factor has a similar function as the well-known morphological factor. This function is to accelerate, not only the morphological processes, but also the biological processes, with the purpose to save computation time. In fact, the bio-geomorphological acceleration factor replaces the morphological acceleration factor, as the biological and morphological processes interact with each other on the same time scale and thus should remain on this same scale. It is, however, important that the numerical implementation and use of this acceleration factor should not affect the interaction between processes and outcome of the models.

4.4.1 Governing equations

The implementation of the morphological acceleration factor is quite straight forward for most growth and decay processes, as the biological processes can be multiplied by the acceleration factor for each computation. However, this approach cannot be applied for the stem establishment process, but this will be discussed in more detail in the next section.

This leads to the following implementation for the population dynamics model:

$$\Delta n_{b, i} = \Delta n_{b, establishment, i} + \lambda \cdot \Delta n_{b, growth, i} + \lambda \cdot \Delta n_{bi, exp} - \lambda \cdot \Delta n_{b, flow, i} - \lambda \cdot \Delta n_{b, inundation, i} \quad (4.27)$$

And for the window of opportunity model as:

$$\Delta n_{b, i} = \Delta n_{b, establishment, i} + \lambda \cdot \Delta n_{b, growth, i} + \lambda \cdot \Delta n_{bi, exp} \quad (4.28)$$

Where,

$$\lambda = \text{Bio-geomorphological acceleration factor} \quad [-]$$

The use of this acceleration factor, in general, is justified for relatively small changes in the bio-geomorphodynamics during each time step, so that these changes do not affect or alter the hydrodynamics too significantly. In other words, this approach is only applicable when the bio-geomorphological time scales are significantly larger than the hydrodynamic time scales. This is the case for the growth and decay processes under consideration, as the changes in stem density are small for the relatively small computational time steps with respect to the hydrodynamic changes.

4.4.2 Establishment

The implementation of the acceleration factor for the establishment process needs to be applied in a different manner, as multiplying the establishment, $\Delta n_{b,i}$, with the acceleration factor, λ , does not represent its purpose. Instead, the acceleration factor should affect the number of establishments. This can be achieved by multiplying the establishment chance with the acceleration factor.

$$\left. \begin{array}{l} \text{If } n_b < n_{b, \text{threshold bare}} \\ \text{If } \chi < [1 - (1 - P_{est})^\lambda \Delta t_{yr}] \end{array} \right\} \quad \text{Then } \Delta n_{b, \text{establishment}, i} = n_{b, \text{establishment}} \quad (4.29)$$

And for the window of opportunity model as:

$$\left. \begin{array}{l} \text{If } n_b < n_{b, \text{threshold bare}} \\ \text{If } T_{Rec:1, i} > T_{Ph:1} \\ \text{If } \chi < 1 - (1 - P_{est})^\lambda \Delta t_{yr} \end{array} \right\} \quad \text{Then } n_{b, \text{seedlings}, i} = n_{b, \text{establishment}} \quad (4.30)$$

4.5 Discussion

This chapter presents the implementation of the vegetation models in the numerical modelling software FINEL2d. In addition it also discussed the implementation of a bio-geomorphological acceleration factor to reduce the computational time. However, the numerical discretisations also introduce additional numerical difficulties, since the grid cell size and the use of a bio-geomorphological acceleration factor should not affect the outcome of the models. Therefore, it is important to assess whether the use of different grid cell sizes and bio-geomorphological acceleration factors lead to different vegetation patterns.

The numerical issues raised in this section will be discussed and assessed in the next chapter, where to this end a sensitivity analysis will be carried out.

Chapter 5

Sensitivity analysis

The aim of this chapter is to assess the effect of bio-geomorphological modelling on the morphodynamic development in small test case simulations. The simulations will also be used to evaluate the functioning, performance and sensitivity of the two vegetation models.

To this end, a sensitivity analysis will be conducted to identify:

- the similarities and differences between the vegetation models.
- the relative importance of input parameters on the models outcome.
- the influence of the numerical implementation and applicability of certain theoretical concepts on the model performance.

The sensitivity analysis is split into three parts. In the first part, section 5.1, simple numerical simulations are utilized to highlight and assess the functioning of the crucial interaction between vegetation and the hydrodynamics. These simple numerical simulations will also be used to demonstrate the influence of the grid cell size on the different growth processes. Subsequently in section 5.2, the functioning and performance of the two vegetation models are evaluated in small test case simulation with the full FINEL2d bio-geomorphological model. In addition, it discusses the influence of a selection of input parameters on the test case results, since assessing the influence of all the vegetation input parameters individually is outside the scope of this research project. This selection is partly based on theoretical concepts and/or numerical issues of the model implementation, and for the other part based on findings and questions raised in the previous chapters.

The parameters that have been selected are:

- Bio-geomorphological acceleration factor
 - In order to assess whether the acceleration parameter required to save computational time affects the model results (Numerical issue, see section 4.5)
- Grid cell size
 - In order to assess whether the discretisation of the growth and mortality processes affects the model results (Numerical issue, see section 4.5)
- Sediment grain size (D_{50})
 - In order to assess the sensitivity of the model results to variations in the grain size, as this is generally considered as an influential parameter (D_{50} input parameter sensitivity)

- $n_{b,threshold} C_r$
 - In order to examine the influence of this parameter on the model results, as this parameter determines the practical applicability range of the representative roughness and shear stress equations. In other words, it determines the stem density threshold above which vegetation influences the hydrodynamics (Theoretical concept, described in section 3.1.2)
- Establishment process representation
 - In order to assess whether the establishment process representation leads to significant differences in the vegetation patterns, as this is the main difference between the two models (Theoretical concept, described in section 3.2.2).

5.1 Simple numerical simulations

In this section simple numerical simulations will be carried out in order to examine the numerical implementation and applicability of certain theoretical concepts. To this end, section 5.1.1 evaluates the performance of the representative roughness and shear stress formulae that describe the influence of the vegetation on the hydrodynamics. Subsequently, section 5.1.2 examines the influence of the grid cell size on the different growth processes.

5.1.1 Influence of vegetation on the hydrodynamics

The influence of the vegetation on the hydrodynamics is an essential process for salt-marsh development and succession, as mentioned in the theory. This influence as described by the representative roughness and shear stress formulae is demonstrated with simple numerical tests.

Model setup

The starting point for these simple tests is a situation with steady uniform flow under a constant surface slope, i , where only the stem density n_b and the water depth are varied, see figure 5.1. For this situation, the depth averaged velocity and the representative roughness can be computed with, respectively, equation 3.8, the forces balance and equation 3.13.

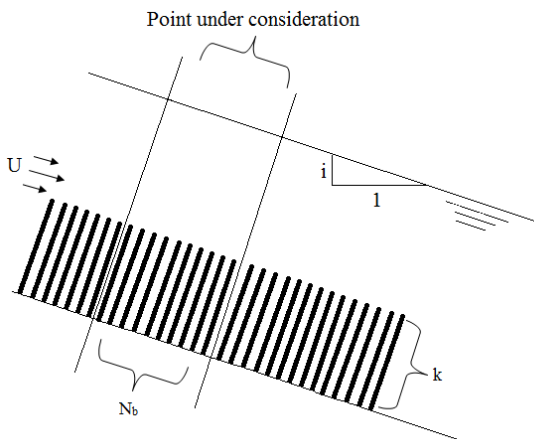


FIGURE 5.1: The 1D model setup

Parameter	Value	Unit
i	$5 \cdot 10^{-3}$	$[m^1 \cdot m^{-1}]$
C_{fb}	$3.9 \cdot 10^3$	$[-]$
C_{Dv}	1	$[-]$
ϕ	$43 \cdot 10^{-4}$	$[m]$
k	0.4	$[m]$

TABLE 5.1: The input parameters

Subsequently, various input parameters necessary for these computations are obtained from literature, i.e. similar to the values used by Temmerman et al. (2007) and Ye (2012). The values for the vegetation drag coefficient C_{Dv} , the stem diameter ϕ and the vegetation height k are characteristic for *Spartina Anglica*, the dominant salt marsh vegetation in Europe. These are given in table 5.1.

Influence of the representative roughness

The purpose of this first simulation is to demonstrate the influence of the vegetation characteristics on the velocity and the hydrodynamic roughness. The results of this simulation are presented in figure 5.2, where the depth averaged flow velocity (top figure, vertical axis) and the hydrodynamic roughness (bottom figure, vertical axis) are plotted against the inundation height (horizontal axis) for different stem densities.

The graphs reveal a notable effect of the vegetation on the depth averaged velocity both for submerged and unsubmerged situations, which finds its origin in the significant increased hydrodynamic roughness. This is due to the fact that the friction coefficient captures the force exerted on vegetation by the flow in a bed shear stress. Furthermore, it also shows a more or less constant depth average flow velocity in the unsubmerged range, and the expected increase in flow velocities and decrease in hydrodynamic roughness when the vegetation is fully submerged. This shows that the representative roughness equation is capable of describing the correct tendency when it comes to the influence of vegetation on the flow. For more information regarding the performance of this representative roughness equation see Baptist (2005).

Applicability of the representative roughness and shear stress

In this second simulation the purpose is to evaluate the applicability of the representative roughness and bed shear stress formulae for sparsely vegetated situations. The reason for this simulation is that the derivation of these formulae is based on the assumption of uniform flow velocity through the vegetation, which might not be valid in these sparsely vegetated situations, see also section 3.1. The result of this simulation is presented in figure 5.3, where the depth averaged flow velocity (top figure, vertical axis) and the shear stress (bottom figure, vertical axis) are plotted against the inundation heights (horizontal axis) for different stem densities.

These results indicate that for sparse vegetated situations the depth averaged velocity is dependent on the water depth, as the velocity increases in the unsubmerged range for increasing inundation depths. However, from a stem density of approximately 50 stems per square meter this assumption is justifiable. This implies that the representative roughness and shear stress formulae are applicable, for these particular parameter settings, above this stem density threshold. To this end, the stem density threshold input parameter $n_{b,threshold} C_{fr}$ is introduced in the numerical implementation of these formulae, see equations 4.7 and 4.8.

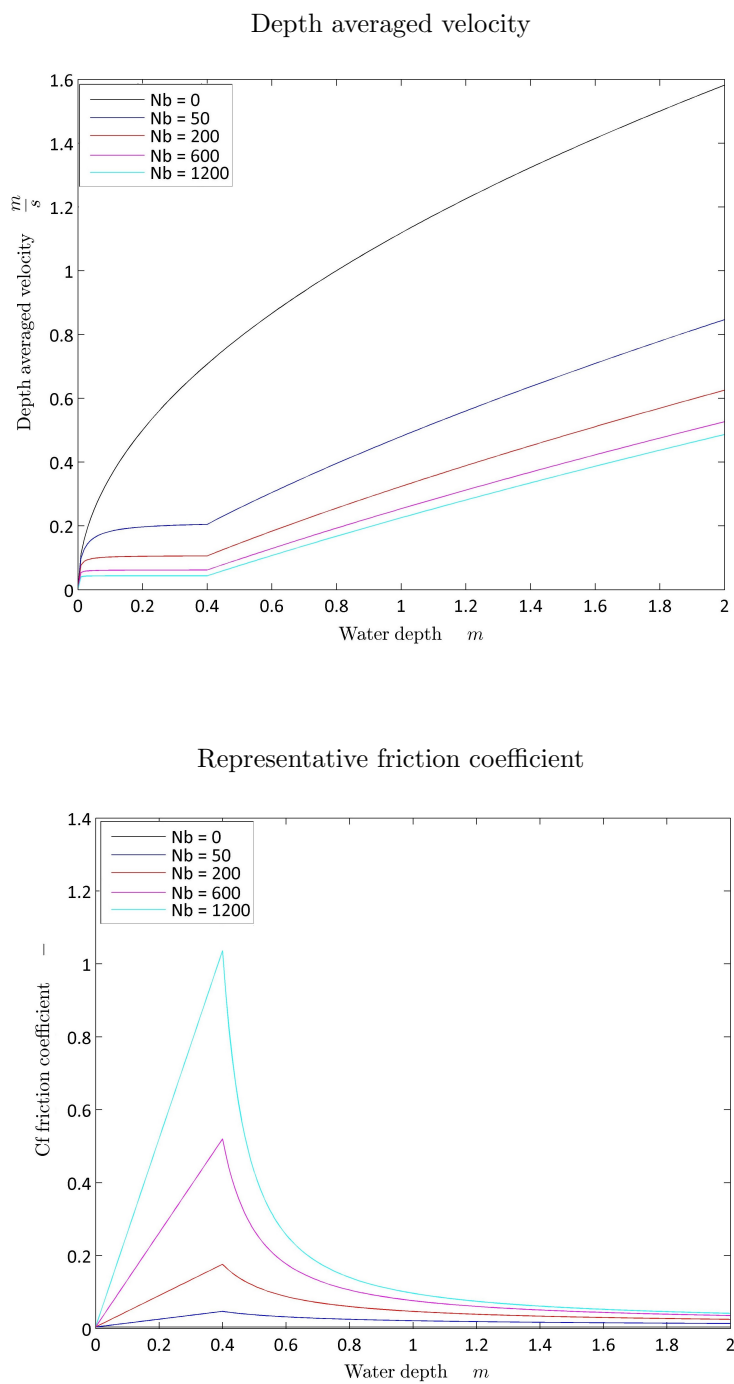


FIGURE 5.2: Depth averaged velocity and representative friction coefficient for different stem densities, where the water depth is varied

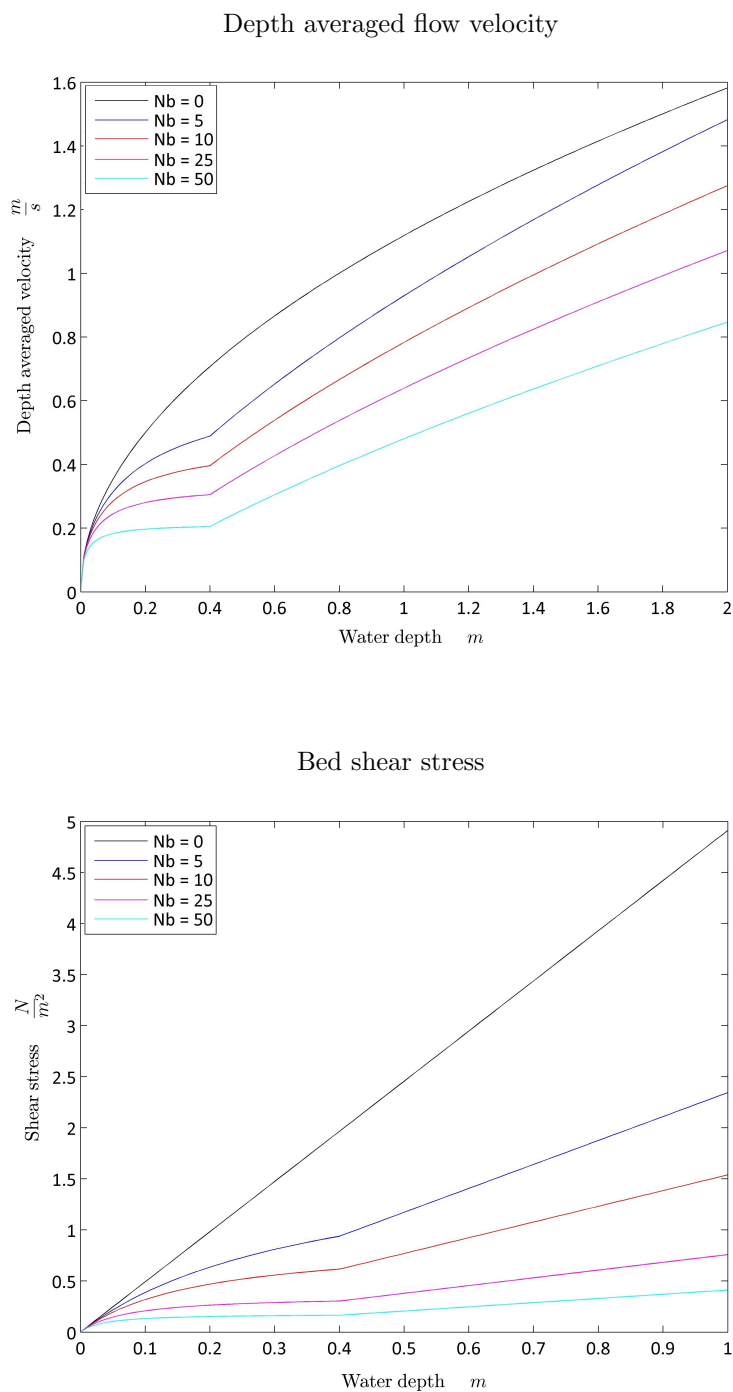


FIGURE 5.3: Depth averaged velocity and bed shear stress for different stem densities, where the water depth is varied

5.1.2 Grid cell size dependency

Ideally the grid cell size should not influence the magnitude of individual processes. This means that for different grid cell sizes, the growth and decay processes should give the same outcome. This is the case for most processes in the vegetation models as the normative variable is the stem density, which is already independent of the grid cell size. For instance the vegetation establishment discretisation is independent of the grid cell size since the expected amount of established area remains the same. However, there is one exception, namely the discretisation of the lateral expansion. This discretisation contains grid cell dimensions, i.e. the surface area and the grid cell interface length. This potential effect of the grid cell size on the lateral expansion process will be assessed in more detail in the test and simulation below.

Lateral expansion for different sizes of isolated tussocks

The purpose of this first simple test is to identify the effect of different grid cell sizes on the lateral expansion amounts of isolated tussocks. To determine this effect, a simple calculation is done with the lateral expansion discretisation given by equation 4.19. Although this is not the standard grid cell dependency test, it is representative for the situation in which new isolated tussocks settle. The results of this calculation are presented in table 5.2. These results indicate that the lateral expansion amounts of isolated cells are influenced by the cell size. This finds its origin in the fact that the ratio of interface length, Γ , and surface area, A , increases more for smaller grid cells, which means that lateral expansion of isolated tussocks becomes more important for smaller grid cell schematisations. In addition, this implies that the contribution of lateral expansion in a 2D full bio-geomorphological simulation is different for variations in the grid cell size, since isolate tussocks will be presented due to establishment.

TABLE 5.2: Numerical example, lateral expansion isolated tussock

A	Γ	K	J	$\sum \Delta n_b$
5 [m^2]	3.4 [m]	0.2 [$m \cdot yr^{-1}$]	1200 [m^{-2}]	489.6 [m^{-2}]
10 [m^2]	4.8 [m]	0.2 [$m \cdot yr^{-1}$]	1200 [m^{-2}]	345.6 [m^{-2}]

However, this does not mean that the lateral expansion discretisation itself is grid cell dependent, since this difference is in fact a consequence of the assumption that the grid cell represents the tussock size, in combination with the fact that an initial stem density, $n_{b, establishment}$, is applied to newly established tussocks.

Lateral expansion for different refinements of vegetation platforms

The purpose of this second simulation is to identify the effect of a different grid refinement on the lateral expansion amounts of the same vegetation platform. To assess this effect, a simple 2D numerical simulation is carried out with the lateral expansion discretisation presented in equation 4.19. In this simulation, the spatial lateral expansion is computed for a square vegetated platform discretised by grid cells with a surface area of 5 m^2 and 10 m^2 , see figure 5.4 and table 5.3. These results indicate that lateral expansion in this simulation is similar for different refinements. This suggests that the lateral expansion discretisation itself is independent of the grid cell size.

TABLE 5.3: Numerical example, refinement of vegetation platform

Dimension	Time	A	Γ	K	J	$\sum \Delta n_b \cdot A$
100x100 [m]	7 [yrs]	5 [m ²]	3.4 [m]	4 [m · yr ⁻¹]	1200 [m ⁻²]	7.11 · 10 ⁶ [stems]
100x100 [m]	7 [yrs]	10 [m ²]	4.8 [m]	4 [m · yr ⁻¹]	1200 [m ⁻²]	7.06 · 10 ⁶ [stems]

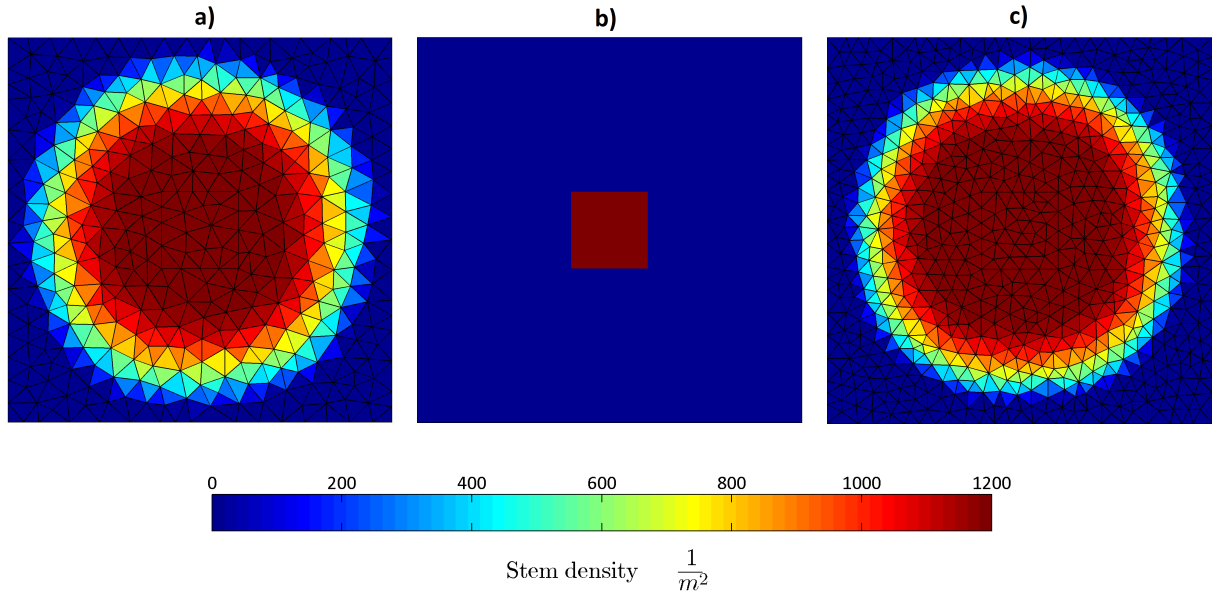


FIGURE 5.4: Comparison of lateral expansion for different grid refinements of a vegetation platform

5.1.3 Conclusion

The simple numerical simulations reveal that:

- the representative roughness approach is capable of describing the correct tendency for approximating the depth average velocity on a vegetated bottom.
- the representative roughness approach is only valid for a stem density of 50 stems or more, which is a consequence of the underlying assumptions.
- the grid cell size does influence the lateral expansion for isolated tussocks, which is a consequence of the model assumptions rather than the lateral expansion discretisation.

In addition, these simulations raise some questions, namely:

- Whether the influence of the vegetation on the hydrodynamics is also capable of capturing the 2D flow and sediment phenomenon.
- Whether the influence of the grid cell size on the contribution of the lateral expansion affects the overall vegetation patterns.

These questions will be discussed in the 2D numerical sensitivity simulations in the next section.

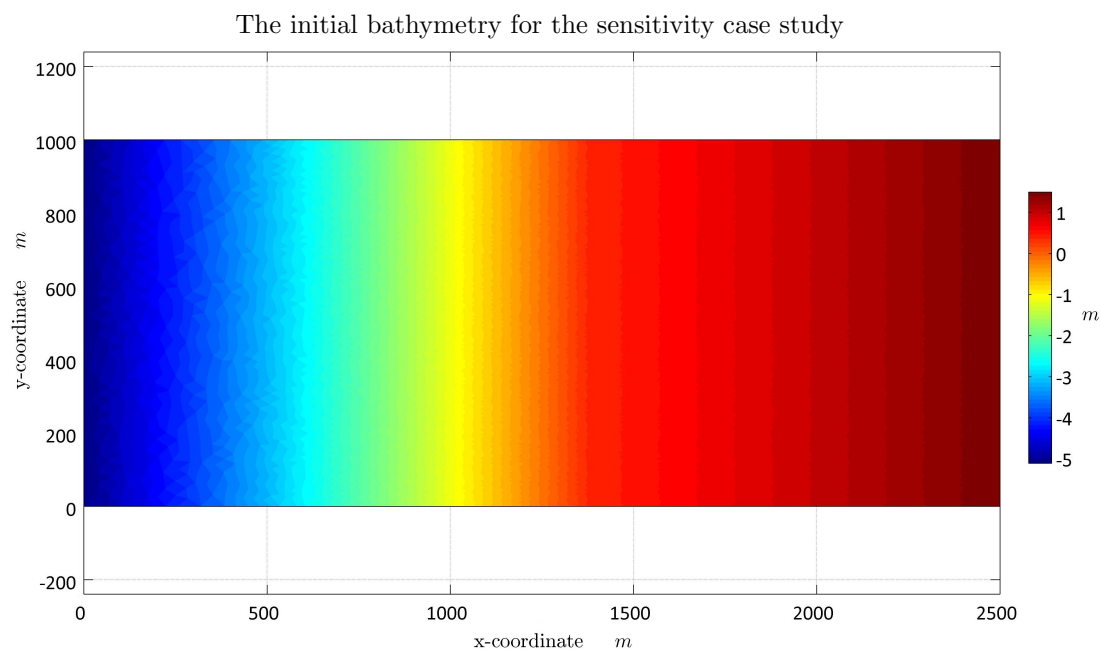
5.2 2D Sensitivity analysis

The aim of the 2D sensitivity simulations is, as mentioned before, to assess the functioning, performance and sensitivity of the bio-geomorphological model in small test simulations. To this end, section 5.2.1 will start with a description of the sensitivity test case, i.e. grid and bathymetry, model settings, and input parameter selection. Subsequently, section 5.2.2 will assess the results of the sensitivity test case for the baseline simulations, where the two vegetation models and a purely morpho-hydrodynamic simulation are compared. Finally, in section 5.2.3 the influence of the selected sensitivity parameters on the model outcome will be evaluated.

5.2.1 Model setup

Grid and bathymetry

The purpose of the sensitivity case study is to give an insight into the functioning, performance and sensitivity of the bio-geomorphological model with respect to the representation of the salt marsh formation and development characteristics. This requires a sensitivity test case that is capable of reproducing representative conditions in a realistic, but simplified situation, where the processes that drive the formation and development are highlighted. This resulted in the sensitivity test case shown in figure 5.5, where the tide enters the modelling domain from the deeper part and where the more elevated bare tidal flat is ideal for salt marsh development.



The idea behind this relatively simple test case is that it resembles a characteristic cross-section that can result in the development of a realistic young salt marsh. In this simple test case the effect of the establishment and growth of vegetation on the morphological development can be singled out and highlighted. It must be noted that generally the development of a characteristic salt marsh cross-section occurs in stages. Initially accumulation of sediments is required prior to any establishment of vegetation. Subsequently, this vegetation is required for

further accumulation and bed level elevation. However this sediment accumulation phase is not emphasized in this sensitivity test case, instead an ideal cross-section is selected for the establishment and growth of vegetation to save computation time. The characteristics of the sensitivity test case are given below:

TABLE 5.4: Sensitivity case grid properties

Simulation time	30 [yr]
Domain dimensions	1x2.5 [km]
Cell size	8.5x8.5 [m]
Highest bed level	1.5 [m]
Lowest bed level	-5.5 [m]
Slope < $x = 1375$ [m]	1/250 [$m \cdot m^{-1}$]
Slope < $x = 1375$ [m]	1/1000 [$m \cdot m^{-1}$]

Parameter selection

In this section the parameter selection is discussed for the sensitivity baseline simulations, where most parameters for the vegetation are adopted from Temmerman et al. (2007) and Hulzen et al. (2007). The vegetation considered in these simulations is *Spartina Anglica*, which is the dominant vegetation on salt marshes in Europe.

Table 5.5 presents the morpho-hydrodynamics and vegetation characteristic input parameters that apply to both vegetation models. This selection of parameters partly follows from the literature, i.e. observed characteristics for *Spartina Anglica*, and partly follows from the assumption for a sandy system. The exception is the parameter $n_{b,threshold} C_r$, as this is a numerical parameter, the density threshold after which the vegetation affects the hydrodynamics. The value selected for this parameter follows from the findings regarding the applicability of the representative roughness and shear stress formulae in section 5.1.1, and on the assumption that a patch should be dense and mature enough before it can affect the hydrodynamics.

TABLE 5.5: Morpho-hydrodynamic parameters

Parameter	Value	Unit	Reference
C_{Dv}	1	[-]	Temmerman et al., 2007
ϕ	$43 \cdot 10^{-4}$	[m]	Hulzen et al., 2007
k	0.4	[m]	Hulzen et al., 2007
$n_{b,threshold} C_{fr}$	200	[m^{-2}]	Section 5.1.1
k_n	0.02	[m]	-
D_{50}	$150 \cdot 10^{-6}$	[m]	-
$M2 - amp$	1.75	[m]	-
$Morfac$	100	[-]	-

The next table, table 5.6, presents the input parameters for the population dynamics model, which are adopted from Temmerman et al. (2007) and Hulzen et al. (2007) as well. The exception being the numerically based parameter $n_{b, threshold\ bare}$. This parameter is required due to the unbounded lateral expansion which leads to negligible, but non-zero stem densities in the grid cells. These non-zero stem densities in turn prevent establishment, see also equation 4.12. In addition, the value for the inundation threshold water level, H_{crit} , and the inundation mortality rate, PE_H , adopted from Temmerman et al. (2007) have been adjusted. The reason for this adjustment is that an online coupling method is used in this vegetation model, whereas Temmerman et al. (2007) applied a tidally averaged approach, for more details see appendix B.

TABLE 5.6: Vegetation input parameters: Population dynamics model

	Parameter	Value	Unit	Reference
Stage 1: Stem establishment	P_{est}	0.01	$[yr^{-1}]$	Temmerman et al., 2007
	$n_{b, establishment}$	200	$[m^{-2}]$	Hulzen et al., 2007
	$n_{b, threshold\ bare}$	1	$[m^{-2}]$	-
Stage 2: Stem density growth	r	1	$[yr^{-1}]$	Temmerman et al., 2007
	$n_{b, max}$	1200	$[m^{-2}]$	Temmerman et al., 2007
Stage 3: Platform succession	K	0.2	$[m \cdot yr^{-1}]$	Hulzen et al., 2007
Decay processes	$\tau_{b, crit}$	0.26	$[N \cdot m^{-2}]$	Temmerman et al., 2007
	PE_{τ}	30	$[N^{-1} \cdot s^{-1}]$	Temmerman et al., 2007
	H_{crit}	1	$[m]$	Temmerman et al., 2007 ¹
	PE_H	12000	$[m^{-3} \cdot yr^{-1}]$	Temmerman et al., 2007 ¹

¹ adjusted from Temmerman et al. (2007), see appendix B

Finally, table 5.7 presents the input parameters for the window of opportunity model, where part of the parameter settings can be adopted from the population dynamics model. However, the other part are new/additional parameters that mainly represent time scales of growth processes. The values that represent the time scale of the different stages, $T_{Ph:1, 2, 3}$, are partly based on the literature (Balke et al., 2011), but have been adjusted to the M2-tide. Generally the total duration of the three phases is in the order of a spring neap cycle, where stage 1 represents the duration of an inundation free window of opportunity during a neap tide, and the second and third phase represents the occurrence of an extreme event during a spring tide. In addition, there are the related, numerical parameters $n_{b, threshold\ bare}$ and $n_{b, crit\ diff}$, where the later represents the requirement that lateral expansion can only occur when a tussock reaches a certain maturity. Due to this requirement, the lateral expansion is no longer unbound which means that $n_{b, threshold\ bare}$ is no longer required. Finally, there are the parameters $T_{I_{\%}, avg}$ and $I_{\%, crit}$ that represent the submergence conditions. The averaging time, $T_{I_{\%}, avg}$ is linked to the tidal period in order to find the submergence percentage of a grid cell over one tidal period. The value for $I_{\%, crit}$, on the other hand, has been calibrated on forehand, just like the value for the establishment chance. This has been carried out using numerical simulations test simulation with FINEL2d, where the submergence requirements and establishment numbers were calibrated so that they show similar establishment amounts and salt marsh dimensions.

TABLE 5.7: Vegetation input parameters: Window of opportunity model

	Parameter	Value	Unit	Reference
Stage 1: Stem establishment	$T_{Ph:1}$	6	[hrs]	-
	P_{est}	0.05	[yr ⁻¹]	Calibrated
	$n_{b, establishment}$	200	[m ⁻²]	Hulzen et al., 2007
	$n_{b, threshold bare}$	0	[m ⁻²]	-
	$T_{Ph:2}$	3	[hrs]	-
	$\tau_{b, ph:1}$	0.2	[N · m ⁻²]	Balke et al., 2011
	$\tau_{b, ph:3}$	0.26	[N · m ⁻²]	Temmerman et al., 2007
Stage 2: Stem density growth	$T_{Ph:3}$	4	[hrs]	-
	r	1	[yr ⁻¹]	Temmerman et al., 2007
	$n_{b,max}$	1200	[m ⁻²]	Temmerman et al., 2007
Stage 3: Platform succession	K	0.2	[m · yr ⁻¹]	Hulzen et al., 2007
	$n_{b, crit diff}$	200	[m ⁻²]	-
	$I_{\%, crit}$	0.41	[-]	Calibrated
	$T_{I_{\%}, avg}$	13	[hrs]	-

5.2.2 Baseline simulations

In the previous section the parameter settings have been presented for the baseline simulations of the two vegetation models. In this section the results of these simulations will be presented, analysed and compared. This will be carried out for the different aspects of the bio-geomorphological model, i.e. the growth and decay/mortality processes, the hydrodynamic characteristic and the morphodynamic characteristic. However, this section will start with a comparison between the simulation with and without vegetation to demonstrated the effect of vegetation on the morphodynamic development.

The results of the comparison between the bio-geomorphological simulations and the morphological simulations are shown in figure 5.6. These figures clearly indicates that vegetation models have an effect on the morphological development, since both bio-geomorphological models show the development of a creek system, whereas there is barely any morphological change visible in the purely morphodynamic simulation. This effect on the morphodynamic development and the differences between the two vegetation models will be assessed in more detail in the coming sections, starting with the vegetation growth characteristics that triggered this.

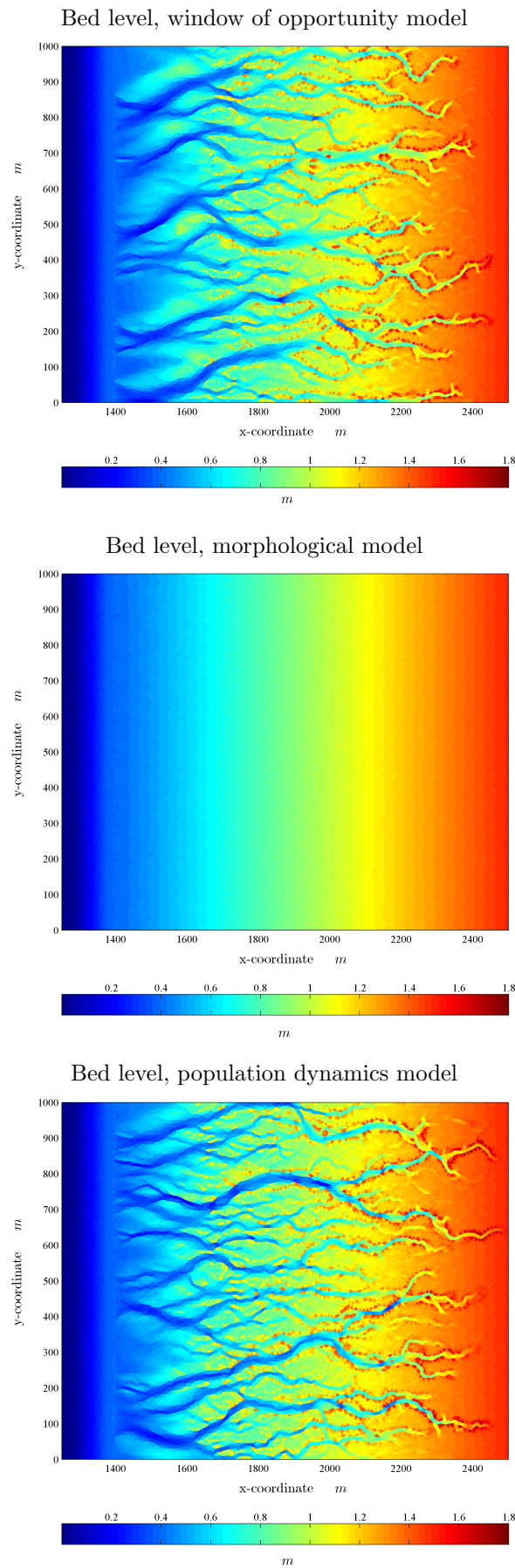
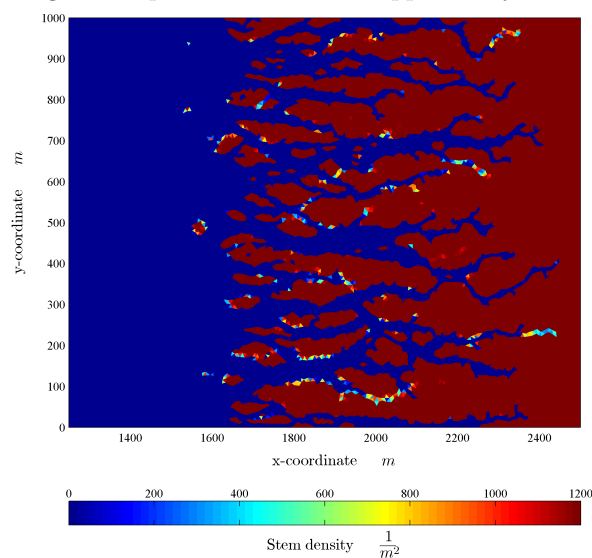


FIGURE 5.6: Comparison of the bed level after 30 years for the two bio-geomorphological models and the morphological model

Vegetation growth characteristics

Figure 5.7 presents the vegetation patterns for the window of opportunity model and the population dynamics model, which corresponds to the morphological development shown in figure 5.6. An assessment of the similarities between the vegetation patterns shows that both models are capable of representing the characteristic overgrown marsh platform dissected by non-vegetated tidal creeks. Moreover, it reveals that the final equilibrium situation for both models almost exclusively consists of mature salt marsh vegetation. However, also differences between the patterns can be observed, as the vegetation pattern of the population dynamics model is dissected by smaller tidal creeks that run further to the back of the salt marsh. In addition, the pattern of the population dynamics model shows more smaller patches at the marsh edge. In order to determine the cause for these agreements and differences between the patterns of the two models, the growth and mortality processes will be assessed in more detail.

Vegetation pattern, window of opportunity model



Vegetation pattern, population dynamics model

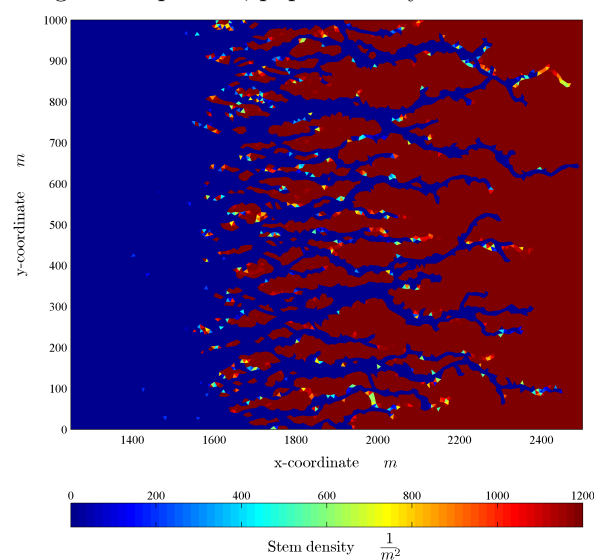


FIGURE 5.7: Vegetation patterns after 30 years for the bio-geomorphological models

Therefore, figures 5.8 and 5.9 show the growth and mortality characteristics for the two models throughout the 30 simulated years. These graphs give a good insight in the growth and mortality characteristic of the vegetation models and indicate that growth and mortality occur according to a similar trend. Moreover, figure 5.8 with growth characteristics suggests that:

- The main contributor to the vegetation growth is the stem density growth
- The establishment is the initiator for vegetation growth (see figure 5.12).
- The lateral expansion is mostly responsible for the spreading after which stem density growth can occur.

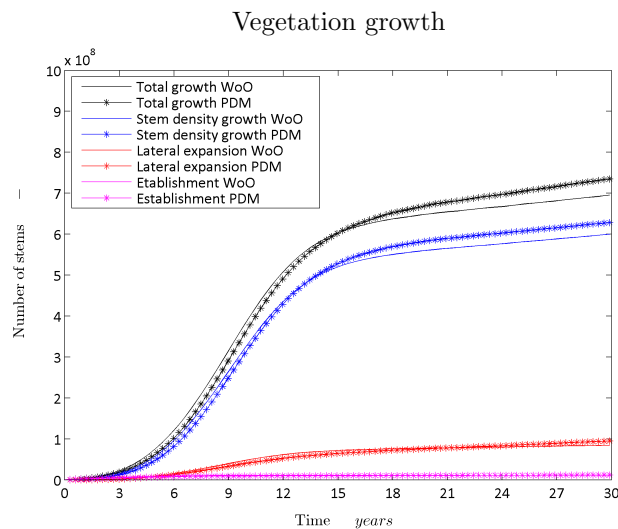


FIGURE 5.8: Vegetation growth characteristics for the baseline simulations throughout 30 years, in total and broken down for each of the growth processes. The contributions of the different growth processes are corrected for vegetation mortality and thus depict the effective contribution of the vegetation growth processes.

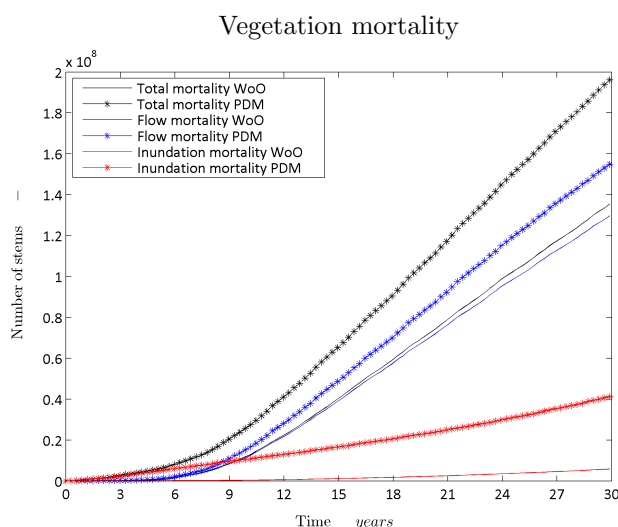


FIGURE 5.9: Vegetation mortality characteristics for the baseline simulations throughout 30 years, in total and broken down for each of the mortality processes

In addition, the graphs also reveal that the magnitudes of the growth processes are larger for the population dynamics model. This observation, together with the fact that the location of the marsh edge is similar for the two models, is reflected in the amount of vegetated area in table 5.8, and in the earlier observed smaller tidal creeks. However, it is not clear whether the gain in vegetated area is caused by the increased growth processes, the adjustments to decay processes or by a combination of both.

TABLE 5.8: Vegetated area

Model	$x > 1500 \text{ m}$	$x > 1700 \text{ m}$	$x > 1900 \text{ m}$	$x > 2100 \text{ m}$	$x > 2300 \text{ m}$
WoO Model	$58.5 \cdot 10^5 \text{ m}^2$	$56.1 \cdot 10^5 \text{ m}^2$	$46.5 \cdot 10^5 \text{ m}^2$	$34.5 \cdot 10^5 \text{ m}^2$	$18.8 \cdot 10^5 \text{ m}^2$
PD Model	$62.0 \cdot 10^5 \text{ m}^2$	$59.2 \cdot 10^5 \text{ m}^2$	$49.2 \cdot 10^5 \text{ m}^2$	$35.3 \cdot 10^5 \text{ m}^2$	$18.7 \cdot 10^5 \text{ m}^2$

The larger magnitude of the vegetation mortality observed in the population dynamics model can partly be contributed to the unfavourable and unbound establishment. This is illustrated in figures 5.10 and 5.11, where significant amounts of stem mortality are observed for the population dynamics model beyond the eventual marsh edge (i.e. $x < 1600\text{m}$).

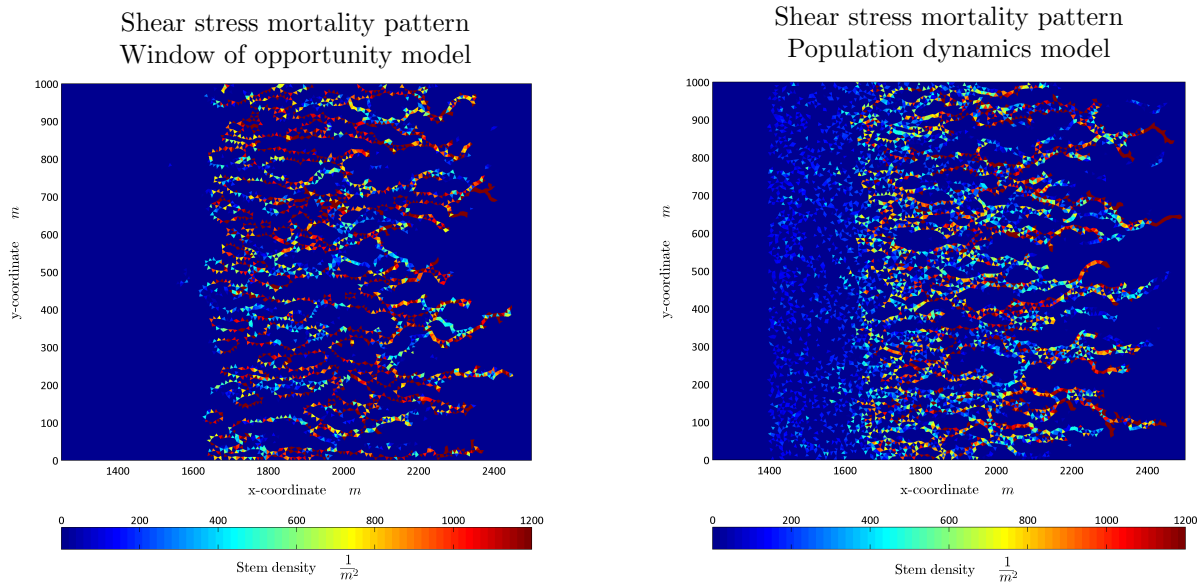


FIGURE 5.10: Shear stress mortality patterns after 30 years for the bio-geomorphological models

Furthermore, these figures reveal that the mortality due to shear stress, which shows similar patterns for both models, is crucial for keeping the tidal creeks from overgrowing with vegetation. The patterns for the inundation mortality, on the other hand, show significant differences. In the window of opportunity model the inundation mortality is minimal, whereas the inundation decay in the population model does seem to affect the vegetation growth, although to a lesser extent than the shears stress mortality. This additional vegetation mortality near the marsh edge partly explains the more patchy tussock structure observed in the population dynamics model.

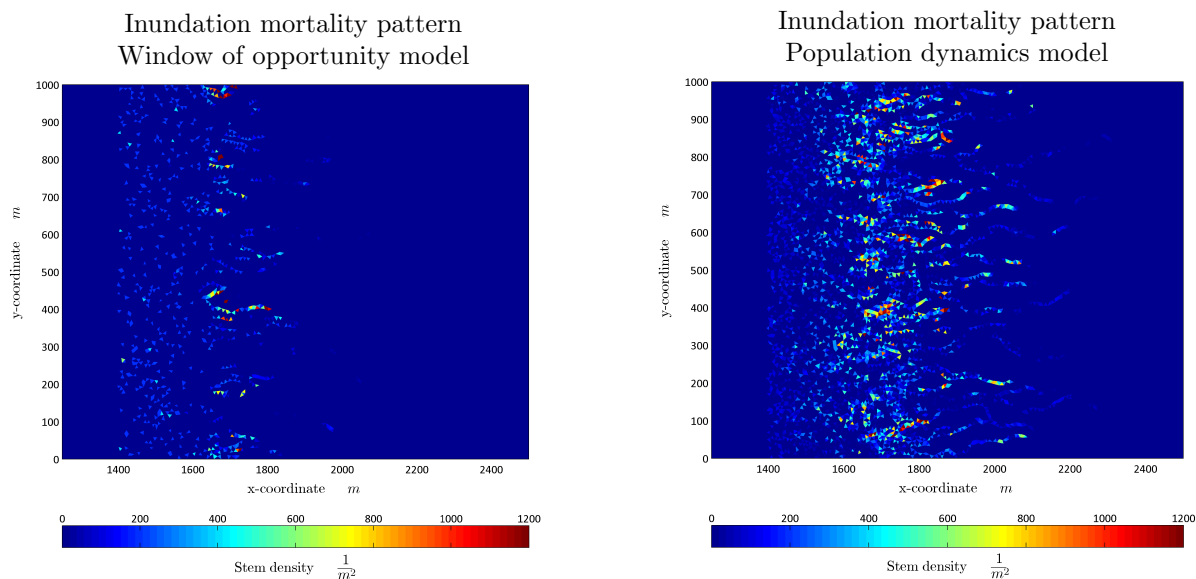


FIGURE 5.11: Inundation mortality patterns after 30 years for the bio-geomorphological models

Finally, the difference in the establishment is highlighted, as the representation of this process characterizes the difference between the models, and might explain the observed difference between the model. Therefore, figure 5.12 presents the detailed establishment characteristics throughout the 30 year simulation for both model. The graph in fact shows a similar trend in establishment attempts and successful establishments for both models, where the establishment mainly takes place in the first six to nine years.

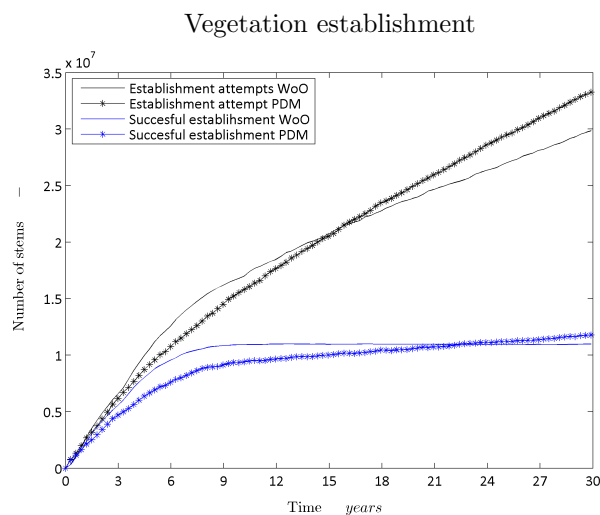


FIGURE 5.12: Establishment process highlighted for the two bio-geomorphological models throughout 30 years

The establishment characteristics of the two model would suggest that there is actually little difference between the establishment processes, however an additional assessment of the establishment height demonstrates that there actually are differences to observe. This is presented in figures 5.13 and 5.14.

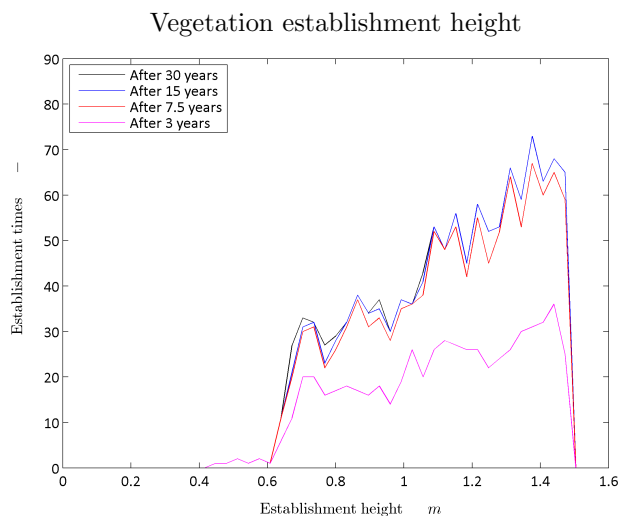


FIGURE 5.13: Establishment height graph for the window of opportunity model (Histogram with 50 bins).

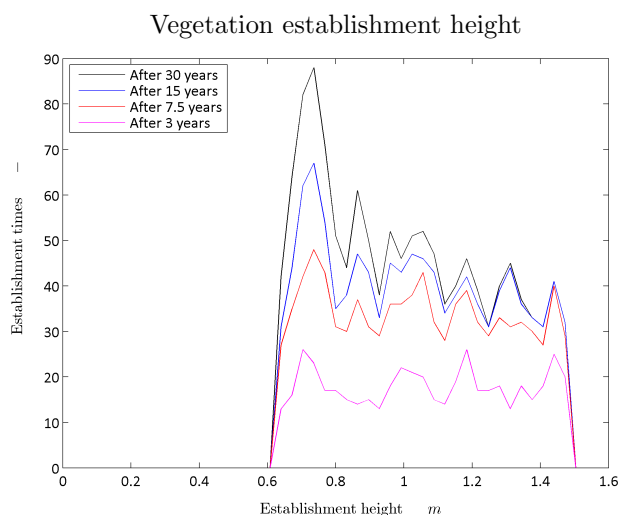


FIGURE 5.14: Establishment height graph for the population dynamics model (Histogram with 50 bins)

These additional graphs show the true character of the establishment processes quite well, in particular for the first 7.5 years. Since, the population dynamics models reveals its random establishment character, whereas the window of opportunity model shows more establishments at more elevated bare tidal flats, which is also observed in nature (Wang et al., 2013). Moreover, the window of opportunity model shows barely any additional establishment after the 7.5 years, while there are still establishments observed in the population dynamics model, especially at the lower elevations. These insights explain the longer extension of the tidal creeks to the back of the salt marsh and the other part of the observed more patchy structure at the marsh edge in the population model. Furthermore, the on-going establishment after the first 7.5 years suggests that unbound establishment in the population model is part of the reason for the smaller tidal creeks.

These findings are also substantiated by the vegetation pattern after 9 years, where the influence of the establishment is clearly visible, see figures 5.15 and 5.16. The window of opportunity model indeed shows a greater tussock density at the higher elevations and a sparser tussock density closer to the marsh edge. In fact, the figures already show the outlines for the eventual vegetation pattern at the end of the simulation for both models, which suggest that the location of establishment determines the global vegetation pattern.

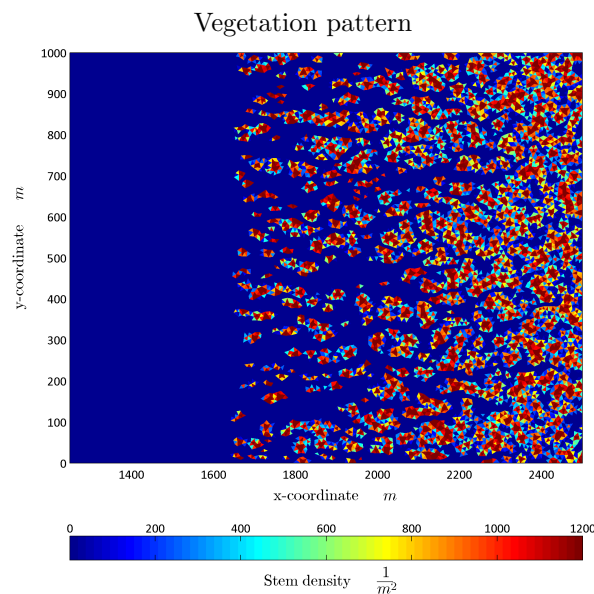


FIGURE 5.15: Vegetation pattern after 9 years for the window of opportunity model

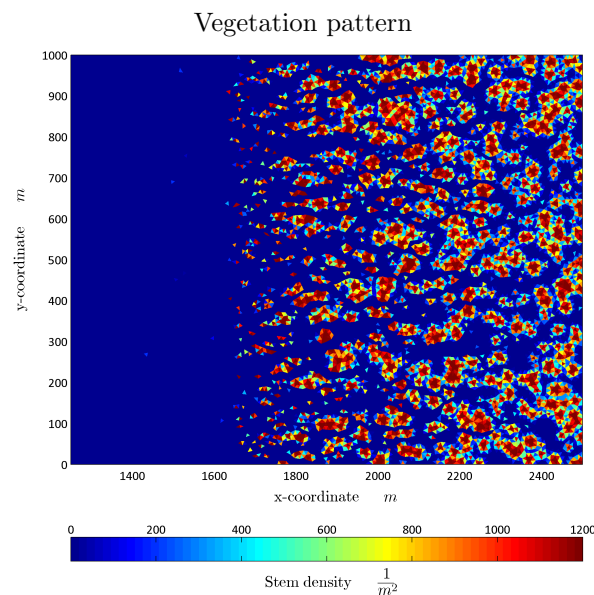


FIGURE 5.16: Vegetation pattern after 9 years for the population dynamics model

Sedimentation and erosion characteristics

In this section the erosion and sedimentation patterns are discussed in more detail. Therefore, the figures 5.17, 5.18, 5.19 and 5.20 present the bed level and vegetation pattern, and the erosion/sedimentation pattern for both models after 30 years. These figures again show the earlier observed smaller tidal creeks and larger proportion of vegetated area in the population dynamics model. This difference is, in turn, also reflected in the erosion sedimentation patterns, since the population dynamics plot shows smaller, but deeper gullies.

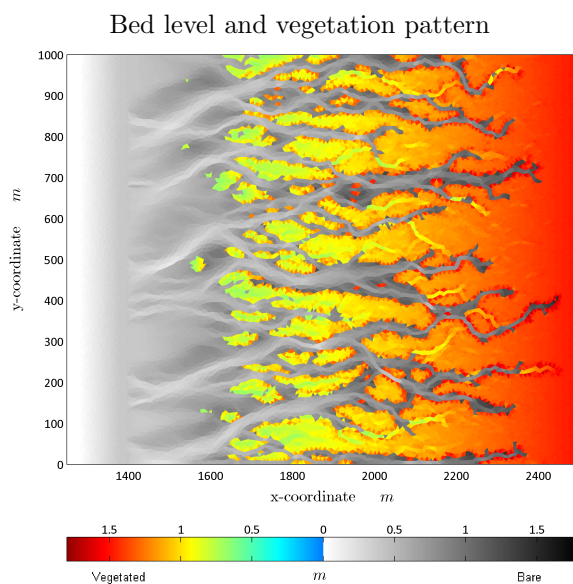


FIGURE 5.17: Bed level and vegetation pattern after 30 years for the window of opportunity model

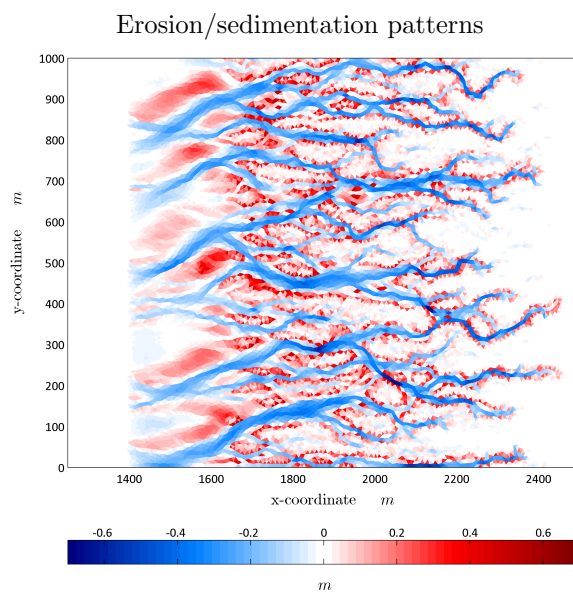


FIGURE 5.18: Erosion/sedimentation pattern after 30 years for the window of opportunity model

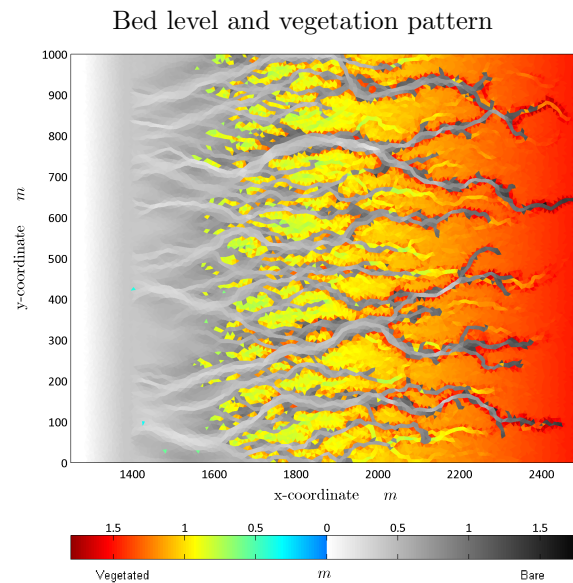


FIGURE 5.19: Bed level and vegetation pattern after 30 years for the population dynamics model

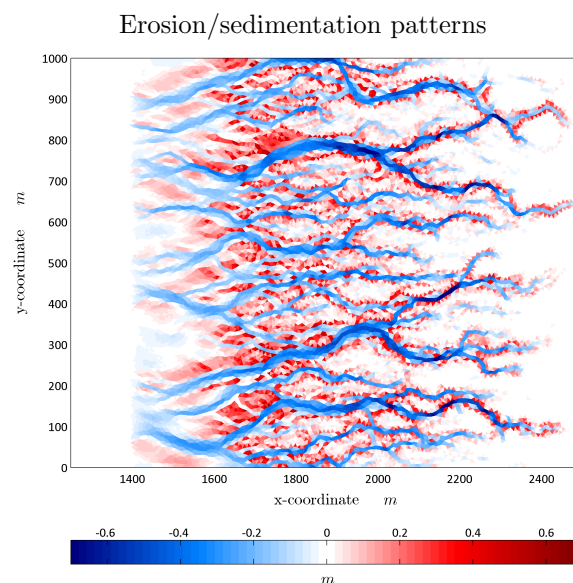


FIGURE 5.20: Erosion/sedimentation pattern after 30 years for the population dynamics model

Moreover, the erosion and sedimentation characteristics in figure 5.21 reveal that these smaller channels and more densely overgrown marsh platforms lead to more sedimentation and erosion, although cumulatively more erosion is observed. These findings can be contributed to the fact that more vegetation leads to more flow concentration, higher velocities and more erosion. On the other hand, more vegetation also leads to more sediment capture due to the flow reduction.

In addition the bed level plots reveal the occurrence of levees alongside the tidal creeks, which can be identified by the higher elevations. This suggests that both models are capable of representing the tidal creek levees observed in nature (Beefink, 1965, Temmerman et al., 2005b).

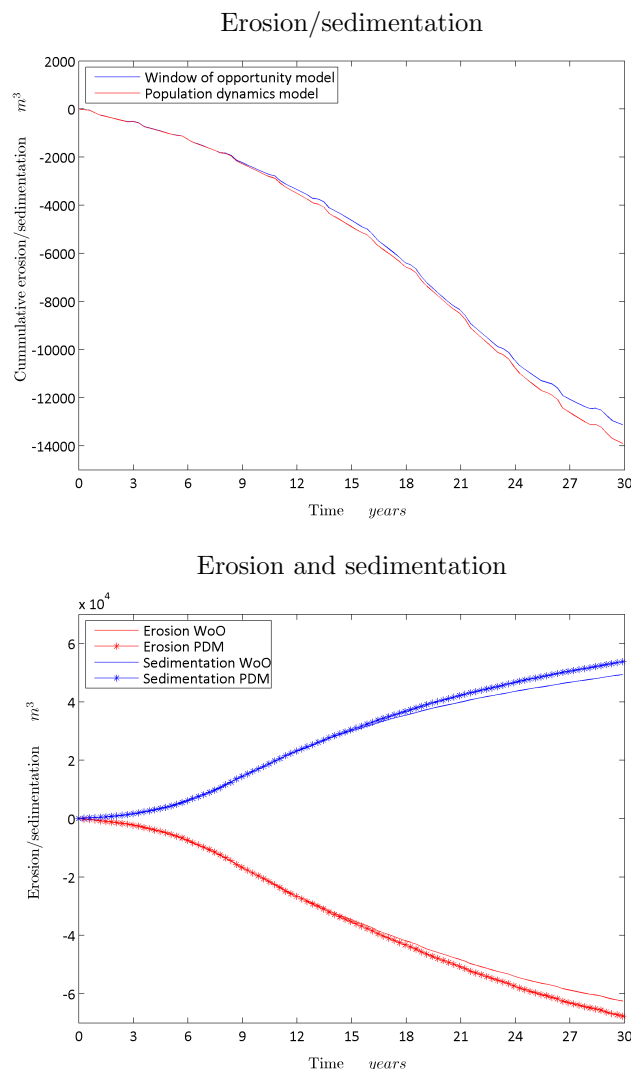


FIGURE 5.21: Erosion and sedimentation characteristics after 30 years for the two biogeomorphological models

Hydrodynamic characteristics

Finally in this section the flow characteristics are examined after the 30 years of salt marsh development. The purpose is to assess the computed flow velocities and pattern in the tidal creeks and in the vegetation. Additionally, the occurrence of the characteristic velocity pulse is investigated, which should occur around bank full discharge in the creeks due to the sudden flooding of the levees and/or vegetated flats (see section 2.3.1). The reason for assessing these characteristics is that the hydrodynamics are the driving force behind the morphodynamic development. Therefore, a good representation of these characteristics contributes to the morphological modelling capabilities of the model.

Figures 5.22 and 5.23 show two identical flow patterns, the only difference is that a different colour range has been applied to show the occurring maximum flow velocities and patterns during falling tide. In addition, figures 5.24 and 5.25 show the characteristic flow velocities throughout one M2 tidal cycle.

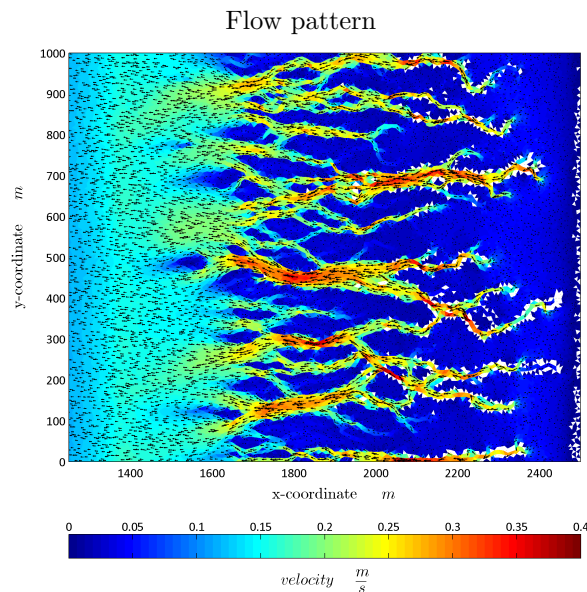


FIGURE 5.22: Maximum flow velocity and patterns during falling tide for window of opportunity model

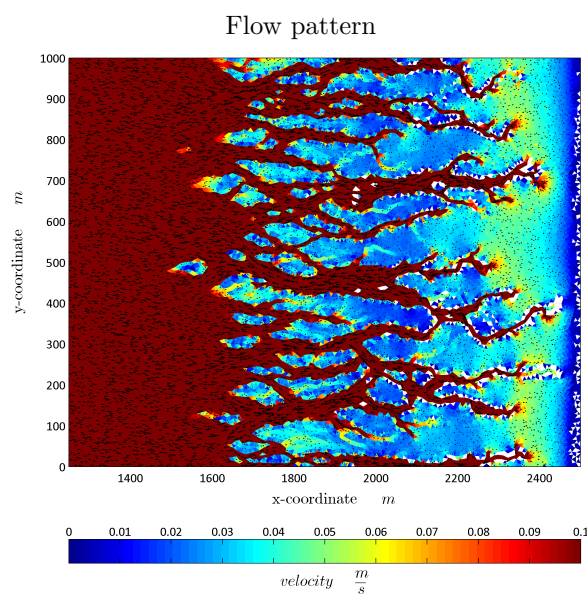


FIGURE 5.23: Maximum flow velocity and patterns during falling tide for window of opportunity model

These figures reveal that the flow velocities are an order of magnitude smaller within salt marsh vegetation, since the maximum velocities in the tidal creeks are approximately around $0.3 \text{ m} \cdot \text{s}^{-1}$ and within the vegetation around $0.04 \text{ m} \cdot \text{s}^{-1}$. Similar velocity values have been observed in salt marshes (Temmerman et al., 2005a), suggesting that the representation of the vegetation influence on the hydrodynamics is reasonable.

However, the characteristic perpendicular flow patterns of the tidal creeks and the velocity pulse have not been identified, see also figures 5.24 and 5.25. A simple explanation is that these phenomena only occur in mature marshes with a relatively flat topography and well developed

levees alongside the tidal creeks, which requires more sediment accumulation in the model simulations. This might in turn require different input parameter settings and/or a different sensitivity test case.

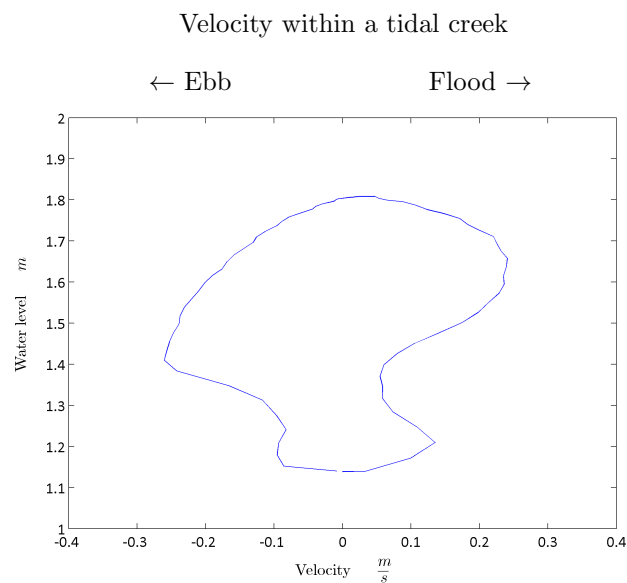


FIGURE 5.24: Computed flow velocity during a M2 Tidal cycle for the window of opportunity model

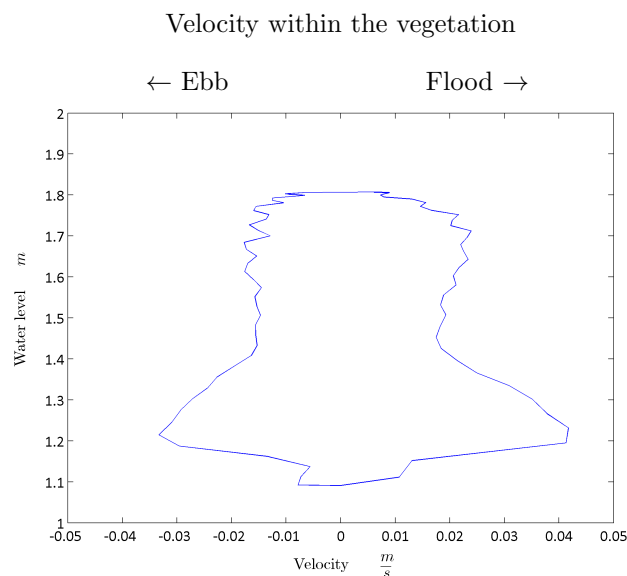


FIGURE 5.25: Computed flow velocity during a M2 Tidal cycle for the window of opportunity model

Conclusion:

The model results of the baseline simulation clearly demonstrate that the vegetation models have an effect on the morphological development. Moreover, an analysis on the functioning and the performance of these two models reveal the potential of bio-geomorphological modelling with regard to reproduction of salt marsh characteristic phenomena. As the models are capable of reproducing:

- The characteristic overgrown marsh platform dissected by tidal creeks.
- Realistic flow velocities both within the vegetation and the tidal creeks.
- The characteristic sedimentation/erosion patterns and the emergence of levees alongside the tidal creeks.

However, other salt marsh characteristics, such as perpendicular flow patterns near the tidal creeks and the velocity pulse within the creeks, have not been identified. This can be related to the absence of mature marshes with a flat topography and a well-developed levee system.

Furthermore, the purpose of the baseline results analysis is also to identify the similarities and differences between the two vegetation models. This analysis reveals that the two models show similar vegetation growth and mortality trends. However, the vegetation patterns do exhibit some differences between the models. The population dynamics model results show a more patchy vegetation structure at the marsh edge, and smaller tidal creeks that run further to the back of the marsh. A more detailed analysis of the growth and mortality characteristics suggest that these differences can be contributed to the representation of the establishment processes. In turn, this difference in vegetation pattern is reflected in the sedimentation patterns, as the smaller tidal creeks together with the larger proportion vegetated area in the population dynamics simulation lead to more erosion and sedimentation.

This raises the following questions,

- Whether a model that does have a well-developed mature marsh is capable of representing the characteristic flow patterns and velocity pulse.
- Whether it is indeed the establishment process that causes the differences between the vegetation patterns.

These questions will be discussed in the parameter sensitivity simulations in the next section.

5.2.3 Parameter sensitivity simulation

In this section the influence of a selection of input parameters on the model results will be discussed in order to assess the importance of certain processes, parameters or numerical/theoretical assumptions. The selection of parameters for this assessment is partly based on theoretical concepts and/or numerical issues of the model implementation, and for the other part based on findings and questions raised in the previous section.

The parameters that have been selected are:

- The bio-geomorphological acceleration factor
- The grid cell size
- Sediment grain size
- $n_{b,threshold} C_{fr}$
- The establishment process

A more detail overview is given in the introduction of this chapter.

Bio-geomorphological acceleration factor

In this section, the influence of the bio-geomorphological acceleration factor on the model results is assessed. To this end, two additional simulations are carried out for each vegetation model, where the bio-geomorphological acceleration factor is set to 25 and 50 instead of the factor 100 used in the baseline simulation, see also table 5.9.

TABLE 5.9: Bio-geomorphological acceleration factor sensitivity simulations

Model	Morfac	Erosion/sedimentation	Sedimentation	Sedimentated area	Vegetated area
WoO	100	$-1.31 \cdot 10^4 m^3$	$4.93 \cdot 10^4 m^3$	$62.0 \cdot 10^4 m^2$	$58.6 \cdot 10^4 m^2$
WoO	50	$-1.22 \cdot 10^4 m^3$	$4.63 \cdot 10^4 m^3$	$62.2 \cdot 10^4 m^2$	$57.7 \cdot 10^4 m^2$
WoO	25	$-1.31 \cdot 10^4 m^3$	$4.70 \cdot 10^4 m^3$	$61.5 \cdot 10^4 m^2$	$57.4 \cdot 10^4 m^2$
PDM	100	$-1.39 \cdot 10^4 m^3$	$5.45 \cdot 10^4 m^3$	$63.0 \cdot 10^4 m^2$	$62.1 \cdot 10^4 m^2$
PDM	50	$-1.39 \cdot 10^4 m^3$	$5.10 \cdot 10^4 m^3$	$62.9 \cdot 10^4 m^2$	$61.8 \cdot 10^4 m^2$
PDM	25	$-1.40 \cdot 10^4 m^3$	$5.38 \cdot 10^4 m^3$	$63.6 \cdot 10^4 m^2$	$62.7 \cdot 10^4 m^2$

The bed level and vegetation patterns in figure 5.27 reveal that the tidal creek patterns differ significantly for the two window of opportunity sensitivity simulations, as the tidal creeks are located at different places in the model domain. This was to be expected, as the random establishment of vegetation determines the location of the tidal creeks. However, the vegetation pattern and tidal creek characteristics, i.e. width and length of the channels, appear to be similar. This is also substantiated by the growth characteristics in figure 5.26, despite of some minor differences.

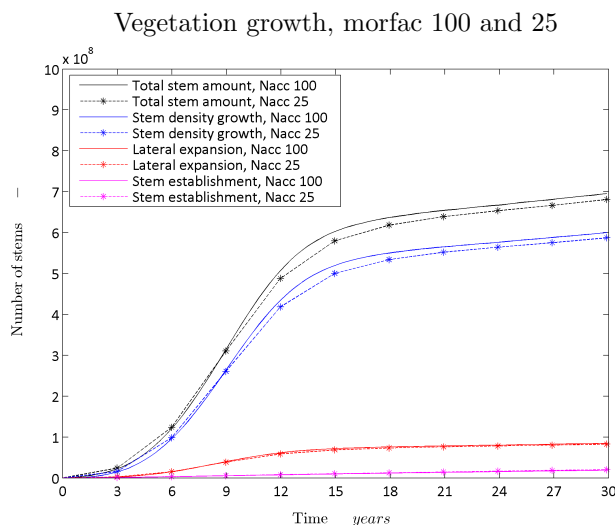
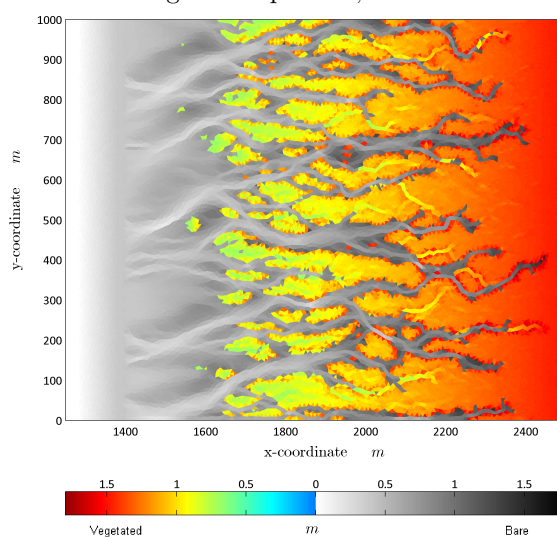


FIGURE 5.26: Vegetation growth characteristics for different acceleration factors throughout 30 years, window of opportunity model

Bed level and vegetation pattern, baseline: morfac 100



Bed level and vegetation pattern, morfac 25

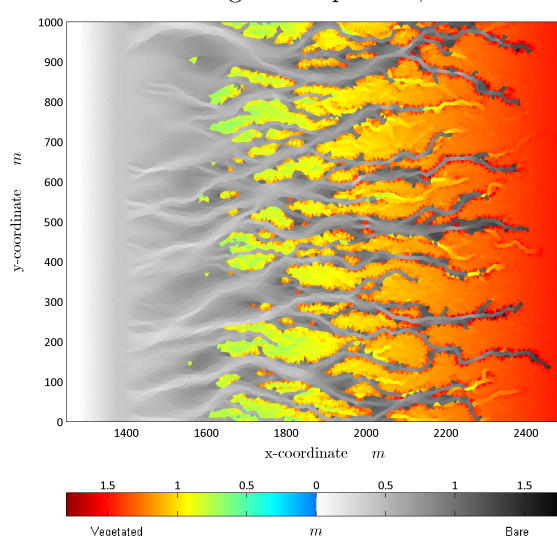
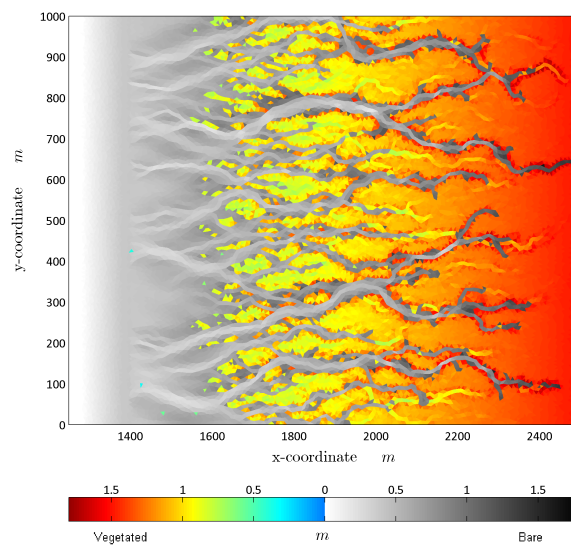


FIGURE 5.27: Bed level and vegetation patterns after 30 years, window of opportunity model

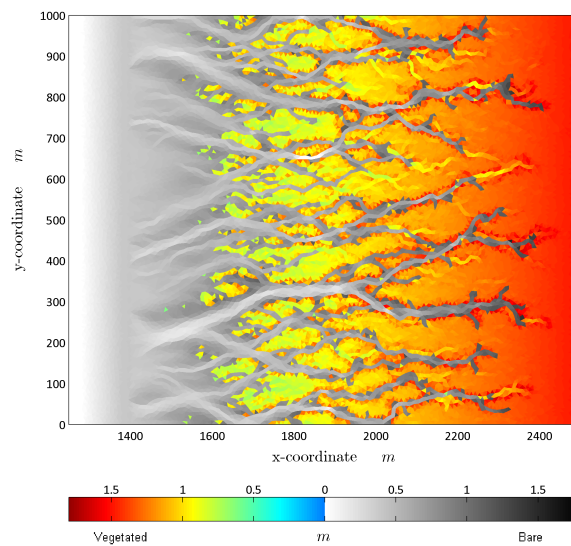
The results of the population dynamics simulations show a similar tendency, different tidal creek locations, but similar quantitative characteristics for the simulations. This is shown in figure 5.28.

These results suggest that the location of the tidal creeks is sensitive to different acceleration factors due to the random nature of the establishment process. More important is that the large scale vegetation and morphological characteristics (see table 5.9) and the global patterns are not sensitive. Therefore justifying the choice made for the acceleration factor in the baseline simulation. A remark to this conclusion is that the sensitivity to the acceleration factor is only tested for a simple harmonic M2 tide, the results might be more sensitive under a more complex tidal signal including spring-neap effects.

Bed level and vegetation pattern, baseline: morfac 100



Bed level and vegetation pattern, morfac 25



Vegetation growth, morfac 100 and 25

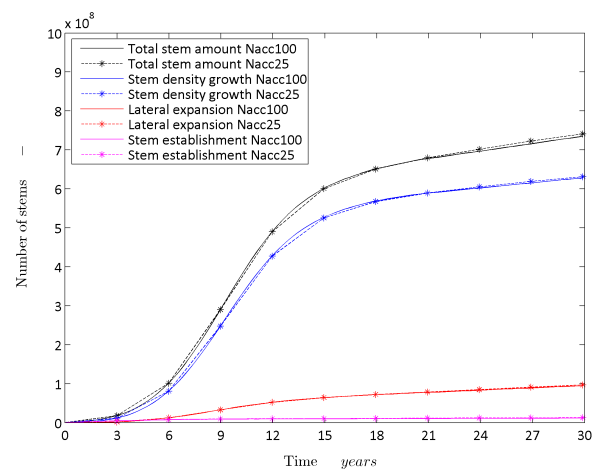


FIGURE 5.28: Bed level and vegetation patterns and the vegetation growth characteristics for different acceleration factors after/throughout 30 years, population dynamics model

Grid cell size

In this section the influence of the grid cell size is evaluated. The reason for analysing the influence of this parameter stems from the findings of the simple simulation in section 5.1.3. These simulations revealed that the grid cell size influences the lateral expansion for isolated tussocks. Moreover, there is an interest in the effects of the grid cell size on the tidal creek pattern. Therefore, one simulation is conducted with a larger grid cell size and one with a smaller grid cell size. The selection of grid cell dimensions for these two simulation is chosen such that the surface area is a factor 2 larger or smaller, see table 5.10.

TABLE 5.10: Grid cell size sensitivity simulation

Model	Element dimensions	Relative surface area	Vegetated area
WoO baseline	8.5 x 8.5 m	1	$58.6 \cdot 10^4 m^2$
WoO coarse grid	12.5 x 12.5 m	2	$56.3 \cdot 10^4 m^2$
WoO fine grid	6 x 6 m	0.5	$59.8 \cdot 10^4 m^2$

A comparison of the bed level patterns presented in figure 5.29 shows the effect of a smaller grid cell size, as loss of resolution is reflected in the number of tidal creeks running to the back. This suggests that for coarser grid cells less tidal creeks suffice to drain the marsh platform, which is due to the larger minimum width of the creeks.

The simulation with the finer grid discretisation also shows some differences compared to the baseline simulation. This manifests itself in a more patchy vegetation pattern with more and smaller tidal creeks, especially closer to the marsh edge. The total vegetated area, on the other hand, is comparable, see table 5.10.

In addition, an assessment of the growth characteristics in figure 5.30 reveals that there is an effect of the grid cell size on the contribution of the growth processes. Firstly, the graphs show the expected smaller lateral expansion amounts for larger grid cells and vice versa, see section 5.1.2. Secondly, it reveals a difference in the establishment characteristics, which start to become apparent after the first 6 years. These findings are in fact related, since the combination of smaller grid cell sizes and larger lateral expansion amounts lead to faster spreading and thus to less establishment possibilities. This also explains the patchy vegetation structure for the finer grid schematisation, as the lateral expansion process is more pronounced. On the other hand, the total growth rate appears to be less sensitive, i.e. the differences between lateral expansion and establishment even out.

These simulations indicate that the model is affected by variations in the grid cell size, since the contribution of the growth processes and the global vegetation patterns reveal some differences. On the other hand, the overall growth characteristics in terms of vegetated area and total growth rate are fairly similar and do lead to a realistic looking tidal creek pattern for the various grid cell sizes. Furthermore, a higher grid cell resolution also inherently results in a more detailed vegetation and creek pattern. In conclusion, the results are affected by variations in the grid cell size, but that spatial discretisation approach is numerically justifiable.

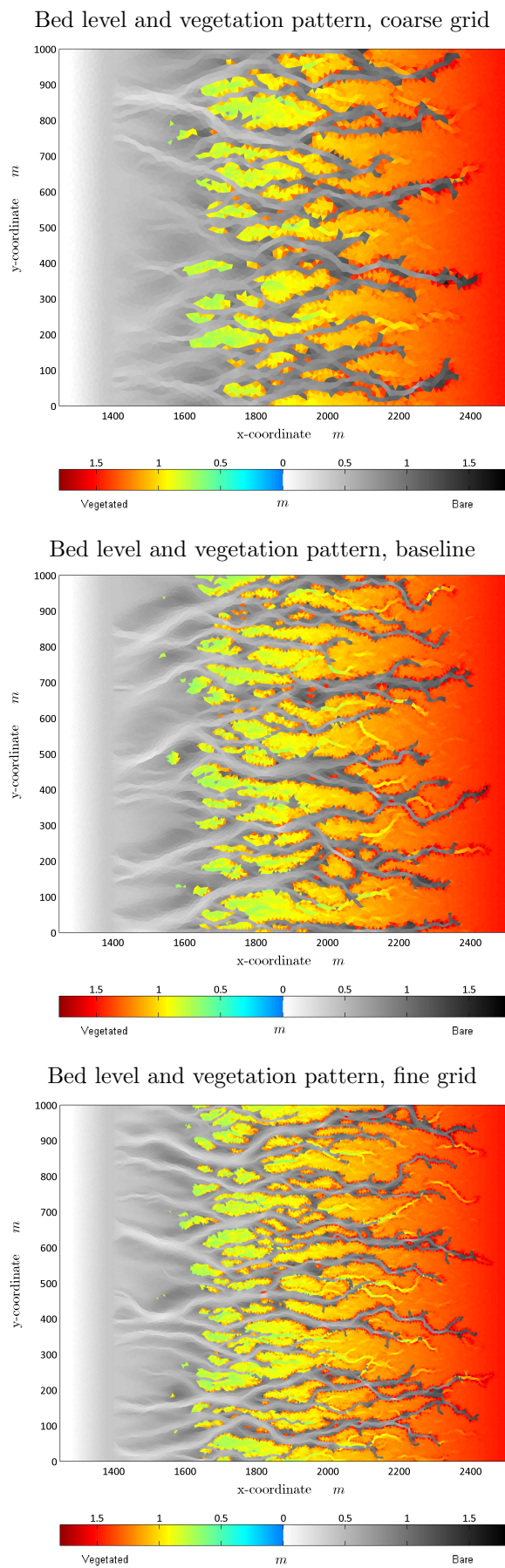


FIGURE 5.29: Bed level and vegetation patterns for different grid cell sizes after 30 years, window of opportunity model

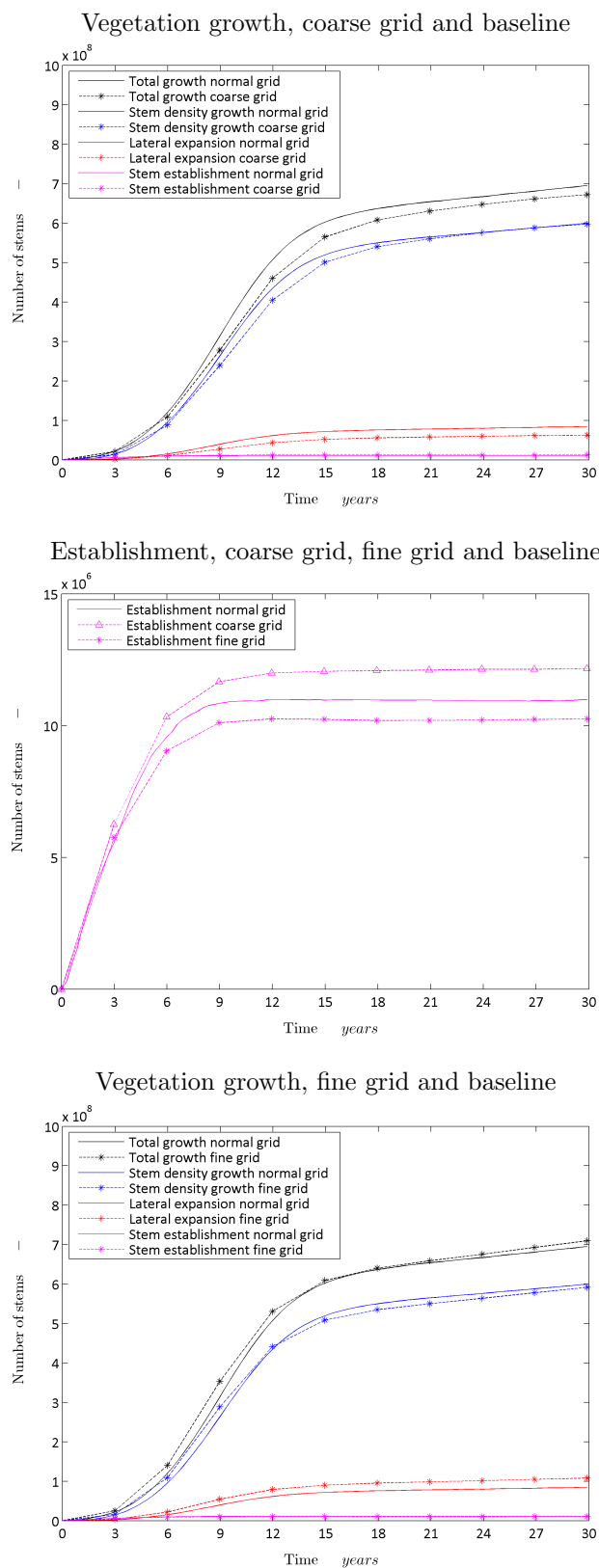


FIGURE 5.30: Growth characteristics for different grid cell sizes after 30 years, window of opportunity model

Sediment grain size

In this section the sediment grain size is varied to assess the influence on the simulation results and in particular on the morphodynamic development. The reason for varying the sediment grain size originates from the fact that the sediment grain size selected in the baseline simulations leads to a negative net sediment influx. Whereas salt marshes are in fact sedimentation dominated systems. Secondly, the grain size used in the baseline simulation resembles a purely sandy system, while salt marshes generally consists of a mix of sand and silt. Therefore, the grain size is reduced to resemble a silt dominated system, i.e. a sediment grain size of $30 \mu m$ is chosen instead of the sandy grain size of $150 \mu m$ that is used in the baseline simulation, see table 5.11. The results of these simulations are presented in the figures 5.31 and 5.32.

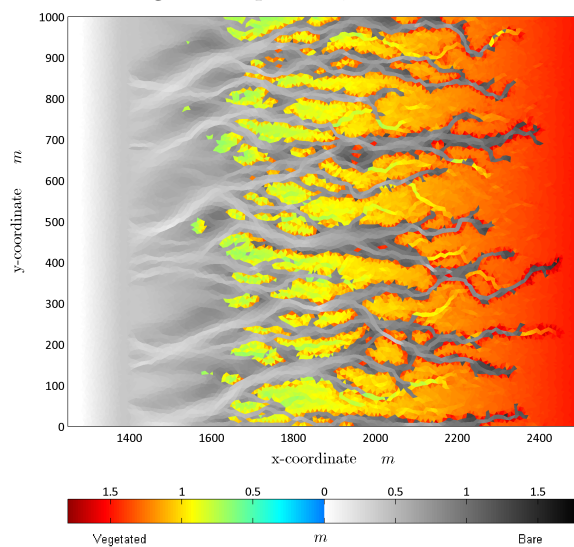
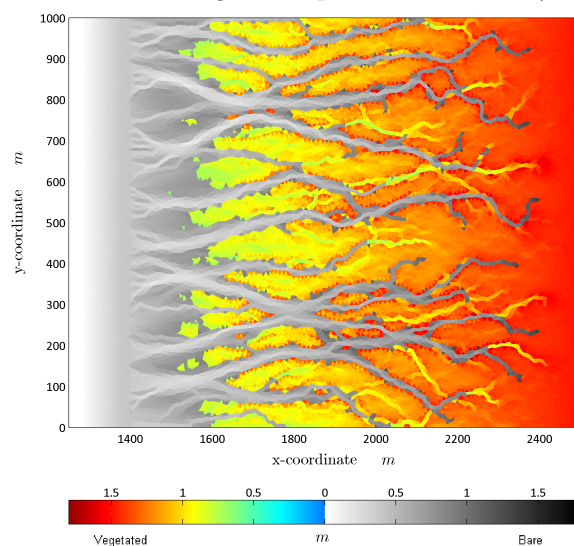
TABLE 5.11: Sediment grain size sensitivity simulation

Model	D_{50}
WoO baseline	$150 \mu m$
WoO fine sediment	$30 \mu m$

The bed level and vegetation pattern of the simulation with a smaller sediment grain size reveals significant differences compared to the baseline simulation. This is reflected in smaller tidal creeks, a less patchy vegetation pattern and a more seaward shifted salt marsh edge. The reason for these differences is found in the erosion/sedimentation characteristics in figure 5.32, as the results show a change from an erosion dominated system into a sedimentation dominated system. This increase in sedimentation in turn favours the growth processes.

The increase in the net sediment influx can be contributed to the fact that smaller sediment grain size require lower flow velocities to settle. Therefore it can reach further into the vegetated marsh area. Despite this change into a sediment dominated system, the salt marsh still does not meet the characteristics of a mature marsh, i.e. relatively flat bed level and well developed levees alongside the tidal creeks. Therefore, phenomena such as the velocity pulse and the flow patterns perpendicular to the tidal creeks are not observed. However, figure 5.32 suggests that the development of the salt marsh is still an ongoing process, as the influx of sediment has not reached equilibrium after the 30 simulated years. This is substantiated by the fact that the time scale overview in the theory indicated that this transition takes, generally, 50 years or more.

The analysis of the influence of the grain size on the model results suggests that the model is sensitive to changes in the sediment grain size. This applies both to the tidal creek locations, the large scale vegetation and morphological development characteristics and the global patterns. However, it must be noted that the difference in sediment grain size is significant.

Bed level and vegetation pattern, baseline: $D50 = 150 \mu m$ Bed level and vegetation pattern, $D50 = 30 \mu m$ 

Bed level difference pattern

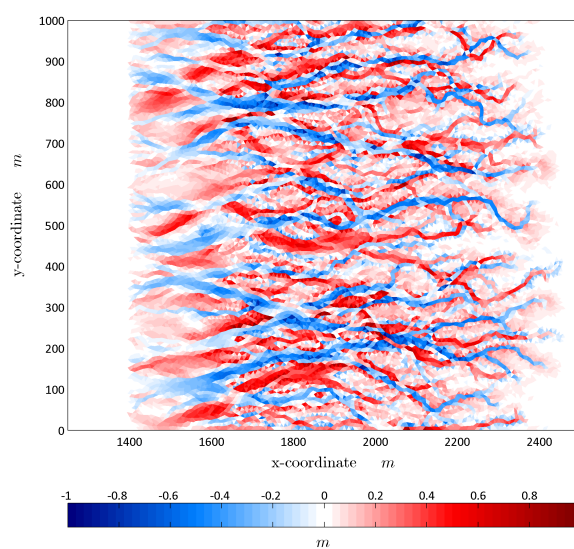


FIGURE 5.31: Bed level and vegetation patterns, and the bed level difference pattern for different sediment diameters after 30 years, window of opportunity model. In the bed level difference plot, the red colour indicates a higher bed level elevation for the $D50 = 30 \mu m$ simulation.

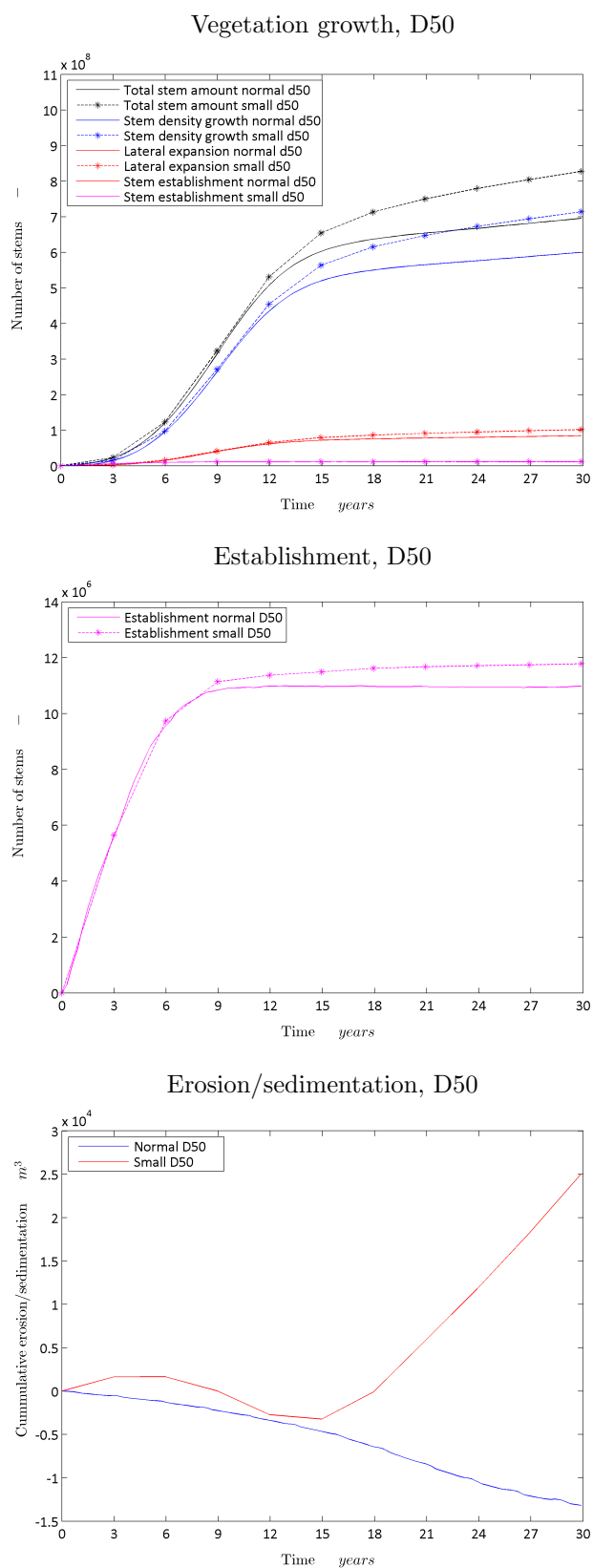
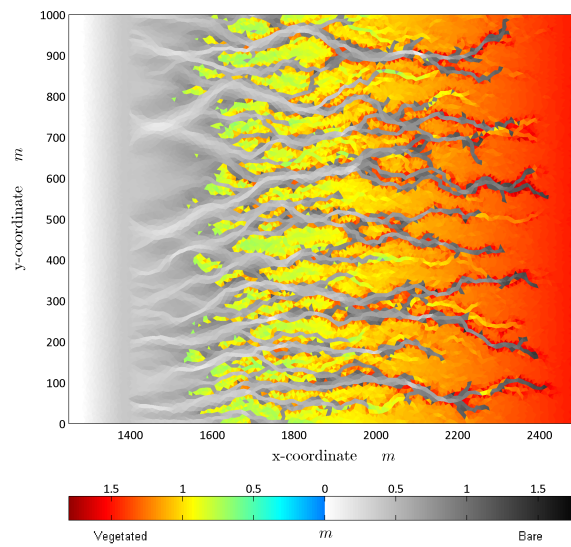
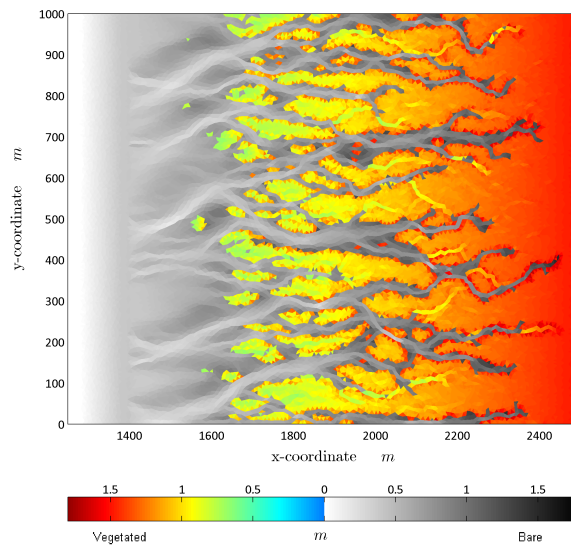


FIGURE 5.32: Growth and erosion/sedimentation characteristics for different sediment diameters throughout 30 years, window of opportunity model

Bed level and vegetation pattern, $n_{b,threshold} C_{fr} = 0 \text{ m}^{-2}$



Bed level and vegetation pattern, baseline



Bed level and vegetation pattern, random establishment concept

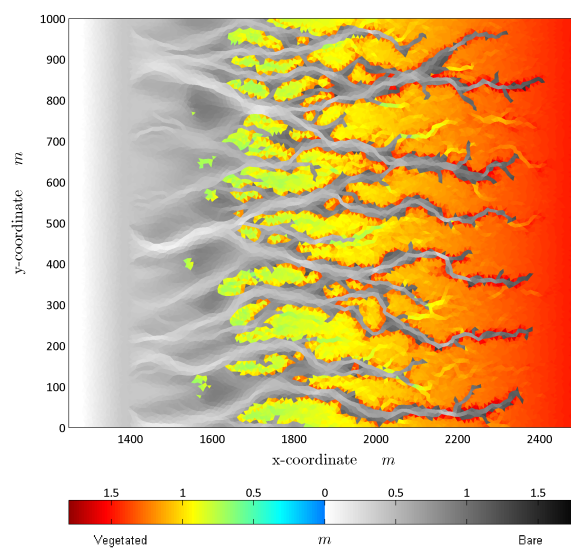


FIGURE 5.33: Vegetated and bare bed level pattern for different value for $n_{b,threshold} C_{fr}$ and for different establishment approaches after 30 years, window of opportunity model

Density threshold for influence of the vegetation on the hydrodynamics

In this sensitivity simulation, the influence and necessity of the threshold density parameter $n_{b,threshold} C_{fr}$ is examined regarding the model's performance. This parameter determines the threshold stem density above which the vegetation influences the hydrodynamics, which is in turn described by the representative roughness and shear stress formulae, see section 4.2. From a theoretical point of view, this parameter is necessary due to the applicability range of the representative formulae, see the simple simulations in section 5.1.1. The purpose of this particular simulation is to assess the more practical necessity of this parameter. Therefore, a simulation is carried out where the threshold value $n_{b,threshold} C_{fr}$ is set to 0 stems per surface area, which implies that vegetation affects the hydrodynamics as soon as stems are present.

TABLE 5.12: $n_{b,threshold} C_{fr}$ sensitivity simulation

Model	$n_{b,threshold} C_{fr}$
WoO baseline	200 m^{-2}
WoO sensitivity simulation	0 m^{-2}

The results of this sensitivity simulation for the window of opportunity model are presented in figure 5.33 (see previous page). The bed level and vegetation pattern shows a less patchy vegetation pattern with smaller tidal creeks. This finding is logical, as the lateral expansion to bare grid cells starts to have an effect on the hydrodynamics in an earlier stage, resulting in lower hydrodynamic stresses and thus better growth conditions. In other words, this density threshold fulfils a function similar to the window of opportunity concept that is applied for the establishment process. The window of opportunity in this case is that the vegetation settled due to lateral expansion needs to survive the hydrodynamic conditions until the threshold density is reached. Only then can the vegetation alter the hydrodynamic stresses which leads to more favourable growth conditions for itself.

The sensitivity simulations indicates that the model results are affected due to the presence/absence of a density threshold value. This is reflected in the tidal creek locations and the global vegetation patterns, although the differences in global vegetation patterns are not that significant. Moreover, the necessity of this threshold density is substantiated from a practical point of view due to the fact that it ensures lateral expansion of vegetation to locations with favourable conditions.

Establishment process

In this section the influence of the establishment process is assessed. It was hypothesised that the change in establishment representation in the window of opportunity model was the reason for the less patchy vegetation pattern with wider and longer tidal creeks when compared to the population dynamics model. Therefore, the durations of the different stages in the window of opportunity establishment phase, i.e. $T_{Ph:1, 2, 3}$, are set to zero. This results in the same establishment representation as used in the population dynamics model, see table 5.13

The sensitivity simulation results are shown in figure 5.33 (see previous page) and substantiate the hypothesis, as the sensitivity run indeed shows a more patchy pattern with wider tidal

TABLE 5.13: Establishment representation sensitivity simulation

Model	$T_{Ph:1}$	$T_{Ph:2}$	$T_{Ph:3}$	P_{est}
WoO baseline	6 hrs	3 hrs	4 hrs	0.05 yr ⁻¹
WoO sensitivity simulation	0 s	0 s	0 s	0.01 yr ⁻¹

creeks. These differences can be contributed to the effect that the vegetation has on the hydrodynamics directly after establishment, i.e. lower hydrodynamic stresses and thus better growth conditions. This can lead to successful establishment of vegetation in unfavourable locations, which explains the observed more patchy pattern and smaller tidal creeks.

The results of the sensitivity simulation substantiate the hypothesis that unbound establishment explains the observed differences in vegetation patterns between the window of opportunity model and population dynamics model. This demonstrates that the tidal creek locations, the large scale vegetation characteristics and the global vegetation patterns are sensitive to the representation of the establishment process. Moreover, the findings suggest that the unbound establishment applied in the population dynamics model can result in vegetation growth in unfavourable locations.

Conclusion

In the sensitivity analysis that has been conducted, the influence of a selection of input parameters on the model results has been assessed to identify the importance of certain processes, parameters or numerical/theoretical assumptions.

The findings of this sensitivity analysis indicate that the vegetation patterns in terms of tidal creek locations are inherently sensitive to changes in the input parameters. This is due to the random character of the establishment representation in the vegetation models. Furthermore, the findings suggest that the vegetation models are sensitive to:

- The sediment grain size
 - As it affects the sediment influx and accumulation, which in turn influences large scale vegetation characteristics and the global patterns.
- Establishment process
 - As it affects the effectiveness of the vegetation establishment, which affects the large scale vegetation characteristics and the global vegetation patterns.

In addition, the simulations indicate that the vegetation models are less sensitive, but are affected by the following parameters:

- The grid cell size
 - As it affects the contribution of the different growth processes and influences the global vegetation patterns.
- $n_{b,threshold} C_{fr}$
 - As it affects the effectiveness of the lateral expansion, which influences the large scale vegetation characteristics and the global vegetation patterns.

On the other hand, the analysis reveals that the vegetation models are insensitive to variation in the bio-geomorphological acceleration factor, when considering the large scale vegetation and

morphological characteristics and the global patterns. Moreover, the simulation demonstrated that, despite the effect of the grid cell size on the growth characteristics, the spatial discretisation approach applied in the vegetation models is numerically justifiable. However, there is room for improvement of the spatial discretisation of the lateral expansion.

5.3 Discussion

The simulations carried out in this chapter clearly demonstrate the effect of vegetation modelling on the morphodynamics, as the increase in hydrodynamic roughness caused by the vegetation leads to flow concentration and tidal creek formation. This underlines the findings by Temmerman et al. (2007), who stated that '*the feedbacks between vegetation, flow, and landforms have an important control on landscape evolution*'. The assessment on the functioning and the performance of the models reveals the capabilities for reproducing the salt marsh characteristic phenomena. This substantiates the potential of bio-geomorphological models to add value to formation and succession modelling of salt marshes.

The similarities and differences between the vegetation models have been assessed as well. This analysis reveals that the main differences in the vegetation patterns can be related to the representation of the vegetation establishment. Moreover, it reveals that the window of opportunity model shows the more realistic establishment characteristics and assures establishment and growth of vegetation at favourable locations. This suggests that the window of opportunity model performs better, however the difference observed in the simulations are not that significant and might not affect the equilibrium situation of the system. Meaning that the differences observed might be purely time scale dependent and diminish when the model reaches the equilibrium situation.

Finally, the sensitivity analysis reveals that the model results are influenced by a number of variations in the input parameters, particularly if this affects the vegetation establishment and the sediment accumulation. In the simulations, this is reflected in the fact that the establishment process influences the development of the global tidal creek pattern and the sediment accumulation can lead to additional vegetation establishment and growth.

However, this sensitivity analysis only considers a situation where there would have been little to none morphological activity without the influence of vegetation. In reality salt marshes generally occur in morphologically active regions. In fact, the formation of a salt marsh often depends on initial accumulation of sediments prior to any vegetation establishment.

Therefore, the questions that remain are:

- To which extent can bio-geomorphological modelling contribute to the long-term morphodynamic prediction of salt marsh development in a morphologically active region?
- How do the bio-geomorphological models perform in case study in a morphologically active region?

To this end, the next chapter will employ the vegetation models to hindcast the formation and succession of 'The drowned land of Saeftinghe'.

Chapter 6

Case study

'The drowned land of Saeftinghe'

6.1 Introduction

In this chapter the vegetation models will be applied and tested in a case study to assess the performance and the practical applicability, but more importantly to find an answer to the main research question:

"To which extent can vegetation modelling contribute to the long-term morphodynamic prediction of salt marsh formation and succession?"

To this end, the two bio-geomorphological models and an additional purely morphological model will be employed to hindcast the formation and succession of 'The drowned land of Saeftinghe', hereinafter referred to as 'Saeftinghe'. Subsequently, the models performance on these test cases will be analysed and compared to field data. The first step in this process is the model setup for this case study, where the insights gained from the sensitivity analysis into the relative importance of the different parameters and processes can be utilized.

6.2 Case study setup

Study area

The Western Scheldt estuary is, with a length of approximately 160 km, one of the major estuaries of North-West Europe. It is located in the South-West of the Netherlands and the North-West of Belgium, indicated by the 'A' in figure 6.1. This estuary is characterised by a macro-tidal semi-diurnal tide with a mean tidal range of around 3.8 meter at the mouth, to 5.0 meters 100 kilometer inland. The morphological development is dominated by this tidal motion.

The salt marsh under consideration in this case study is Saeftinghe, an area of approximately 3000 hectares. This marsh is located in the Scheldt estuary at approximately 70 kilometers from the mouth, indicated by the 'B' in figure 6.1. At this location the tidal range is around 4.9 meters, where the water is brackish with a salinity of around 5 to 18 PSU (Wang et al., 2013) and has a mean suspended sediment concentration of on average 60 micrograms per litre

(Dam, 2013). The vegetation that dominates the lower marshes in this area are the pioneer plant species *Spartina anglica* and *Salicornia europaea*, which start establishing on bare tidal flat from around -1.1 meters to around 0.8 meters relative to mean high water level (Wang et al., 2013).

The reason for selecting this case study area is that Saeftinghe has experienced a rapid expansion of marshes in the last 80 years, where the development of vegetation growth and morphodynamics development is relatively well registered. Moreover, the salt marsh satisfies the conditions for which the vegetation models are applicable, i.e. tide dominated morpho-hydrodynamic conditions at a sheltered low-energy shoreline.

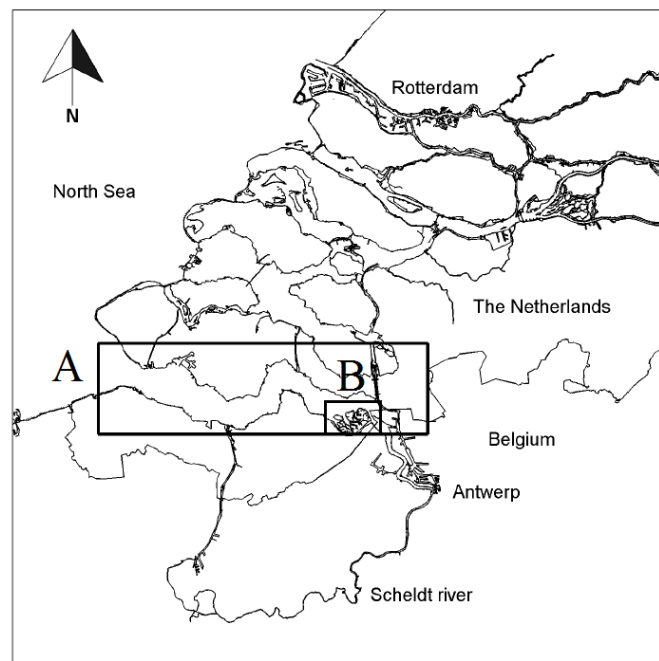


FIGURE 6.1: Location of 'Saeftinghe'

6.2.1 Model setup

The starting point is the calibrated morpho-hydrodynamic FINEL2d Western Scheldt model, which has been developed by Svašek Hydraulics (Dam et al., 2006; Dam et al., 2007; LVT, 2013). This model is characterized by a grid consisting of triangular elements to describe the complete Western Scheldt. The computational grid with a 1500x1500 meters grid resolution at the sea side and a higher resolution of 24x24 meters at Saeftinghe. The model has a water level boundary at the sea side to impose the tidal forcing and a discharge boundary at the upstream river boundary. This results in the spring-neap water level fluctuations shown in the right graph in figure 6.2 at Saeftinghe. In addition, the left figure shows the initial bathymetry for Saeftinghe in 1905, which has been interpolated from historical bathymetry data. This model will be utilized to hindcast the formation and development until 2004.

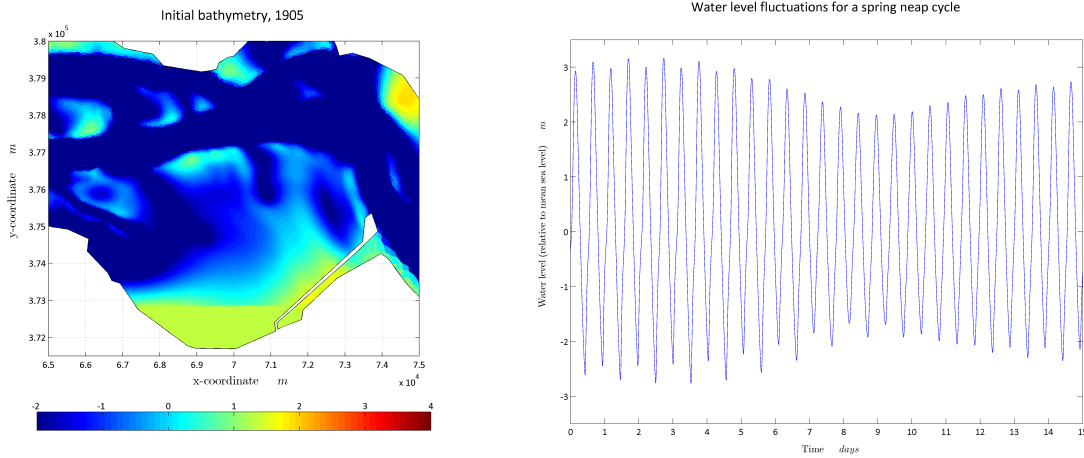


FIGURE 6.2: Model setup

6.2.2 Input parameters

In this section the parameter selection is presented for the bio-geomorphological FINEL2d model, where the majority of the parameters are adopted from the sensitivity analysis. The vegetation parameters utilized to determine the influence of the vegetation on the hydrodynamics are in fact identical to the values used in the sensitivity case study. For the morphodynamic parameters some different values are used, for instance the hydrodynamic roughness that is chosen for this calibrated model is smaller. More importantly the sediment grain size, D_{50} has been set to $50 \mu m$ in order to resemble a sediment mixture of sand and silt characteristic for this area. This is necessary in order for sedimentation to occur in Saeftinghe and in particular for sediment accumulation at the back of this area.

TABLE 6.1: Morpho-hydrodynamic parameters

Parameter	Value	Unit	Reference
C_{Dv}	1	[-]	Temmerman et al., 2007
ϕ	$43 \cdot 10^{-4}$	[m]	Hulzen et al., 2007
k	0.4	[m]	Hulzen et al., 2007
$n_{b,threshold} C_{fr}$	200	[m^{-2}]	Section 5.1.1
k_n	0.01	[m]	-
D_{50}	$50 \cdot 10^{-6}$	[m]	-
$Morfac$	100	[-]	-

Table 6.2 presents the input parameters of the population dynamics model, where only one parameter has been changed. This is the parameter for the critical shear stress, $\tau_{b,crit}$. The reason for increasing this parameter in comparison to the runs in the previous chapter is because of the high shear stresses observed in the case study simulations. Therefore, the critical shear stress has been changed to $0.55 N \cdot m^{-2}$ which is based on the findings of Balke et al. (2011).

TABLE 6.2: Vegetation input parameters: Population dynamics model

	Parameter	Value	Unit	Reference
Stage 1	P_{est}	0.01	$[yr^{-1}]$	Temmerman et al., 2007
	$n_{b, establishment}$	200	$[m^{-2}]$	Hulzen et al., 2007
	$n_{b, threshold bare}$	1	$[m^{-2}]$	-
Stage 2	r	1	$[yr^{-1}]$	Temmerman et al., 2007
	$n_{b,max}$	1200	$[m^{-2}]$	Temmerman et al., 2007
Stage 3	K	0.2	$[m \cdot yr^{-1}]$	Hulzen et al., 2007
Decay processes	$\tau_{b, crit}$	0.55	$[N \cdot m^{-2}]$	Balke et al., 2011
	PE_{τ}	30	$[N^{-1} \cdot s^{-1}]$	Temmerman et al., 2007
	H_{crit}	1	$[m]$	Temmerman et al., 2007
	PE_H	12000	$[m^{-3} \cdot yr^{-1}]$	Temmerman et al., 2007 ¹

Finally, the parameters of the window of opportunity model are presented in table 6.3, where the input variables that represent the time scales of the window of opportunity process have been adjusted to the spring-neap cycle, i.e. $T_{Ph:1, 2, 3}$ and $T_{I\%, avg}$. Furthermore, the establishment chance and the critical shear stress are now equal to the values used in the population dynamics model, which are also based on the findings in literature.

TABLE 6.3: Vegetation input parameters: Window of opportunity model

	Parameter	Value	Unit	Reference
Stage 1	$T_{Ph:1}$	6	$[hrs]$	-
	P_{est}	0.01	$[yr^{-1}]$	Temmerman et al., 2007
	$n_{b, establishment}$	200	$[m^{-2}]$	Hulzen et al., 2007
	$n_{b, threshold bare}$	0	$[m^{-2}]$	-
	$T_{Ph:2}$	72	$[hrs]$	-
	$\tau_{b, ph:1}$	0.2	$[N \cdot m^{-2}]$	Balke et al., 2011
	$\tau_{b, ph:3}$	0.55	$[N \cdot m^{-2}]$	Balke et al., 2011
Stage 2	$T_{Ph:3}$	72	$[hrs]$	-
	r	1	$[yr^{-1}]$	Temmerman et al., 2007
Stage 3	$n_{b,max}$	1200	$[m^{-2}]$	Temmerman et al., 2007
	K	0.2	$[m \cdot yr^{-1}]$	Hulzen et al., 2007
	$n_{b, crit diff}$	200	$[m^{-2}]$	-
	$I\%, crit$	0.26	$[-]$	Calibrated
	$T_{I\%, avg}$	168	$[hrs]$	-

6.3 Model results

In the previous section the model setup and the parameter settings of the two bio-geomorphological models and the morphological model have been presented for the 100 year hindcast of Saeftinghe. In this section the results of these three simulations are presented, analysed and compared for the different aspects of bio-geomorphological modelling. The purpose is to identify the additional value of the bio-geomorphological models compared to the purely morphological simulations. In addition, the simulation results will be compared to the measurements to assess the performance and practical applicability.

6.3.1 Vegetation

Vegetation patterns and bed level elevation

The measured and computed vegetation patterns and bed level elevations after 100 years, thus for 2004, are presented in the figures 6.3 and 6.4. The measured pattern depicted in this figure is a combination of vegetation outlines acquired from Wang et al. (2013) and the RWS *Vaklodring* 20x20m resolution bed level elevation data interpolated to the computational grid.

The figures indicate that accumulation and vegetation growth have occurred in the correct area, since the bio-geomorphological model results clearly show that a salt marsh has formed at the location of Saeftinghe. This suggests that the two vegetation models are capable of representing the characteristic overgrown vegetated marsh platform dissected by a tidal creek system in a case study as well. Moreover, the figures reveal that both the model results and the measurements show approximately three main channels. Although the number of main channels in the models appears to be sensitive to the sediment grain size, see appendix C.4. On the other hand, the measured vegetated tidal flats are larger, more elevated and less elongated, where the latter appears to be sensitive to the sediment grain size in the simulations as well. What is striking in this case study is that the location of the global channels, the wider gullies and tidal flats are fairly similar for all three simulations. This contrasts with the situations observed in the sensitivity analysis, where the tidal creek locations were completely random. This suggests that this case study has a more deterministic character where the global morphodynamics determine the location of the channels, wider creeks and tidal flats.

Vegetation growth characteristics

The growth characteristics shown in figure 6.5 reveal that the vegetation growth is initially faster in the population dynamics model, which is the result of the significantly larger establishment numbers, see figure 6.7. However, the growth curve flattens out in time and eventually the window of opportunity model approximates the same growth amounts. This flattening of the growth curve suggests that there is a restriction on the amount of intertidal flat available with sufficient elevation for the growth and establishment of vegetation. The fluctuations observed in the growth curve of the population dynamics model indicate mortality of vegetation or in other words, the vegetation grows and establishes on unfavourable locations. The absence of these fluctuations in the window of opportunity model in turn implies vegetation settlement on favourable locations.

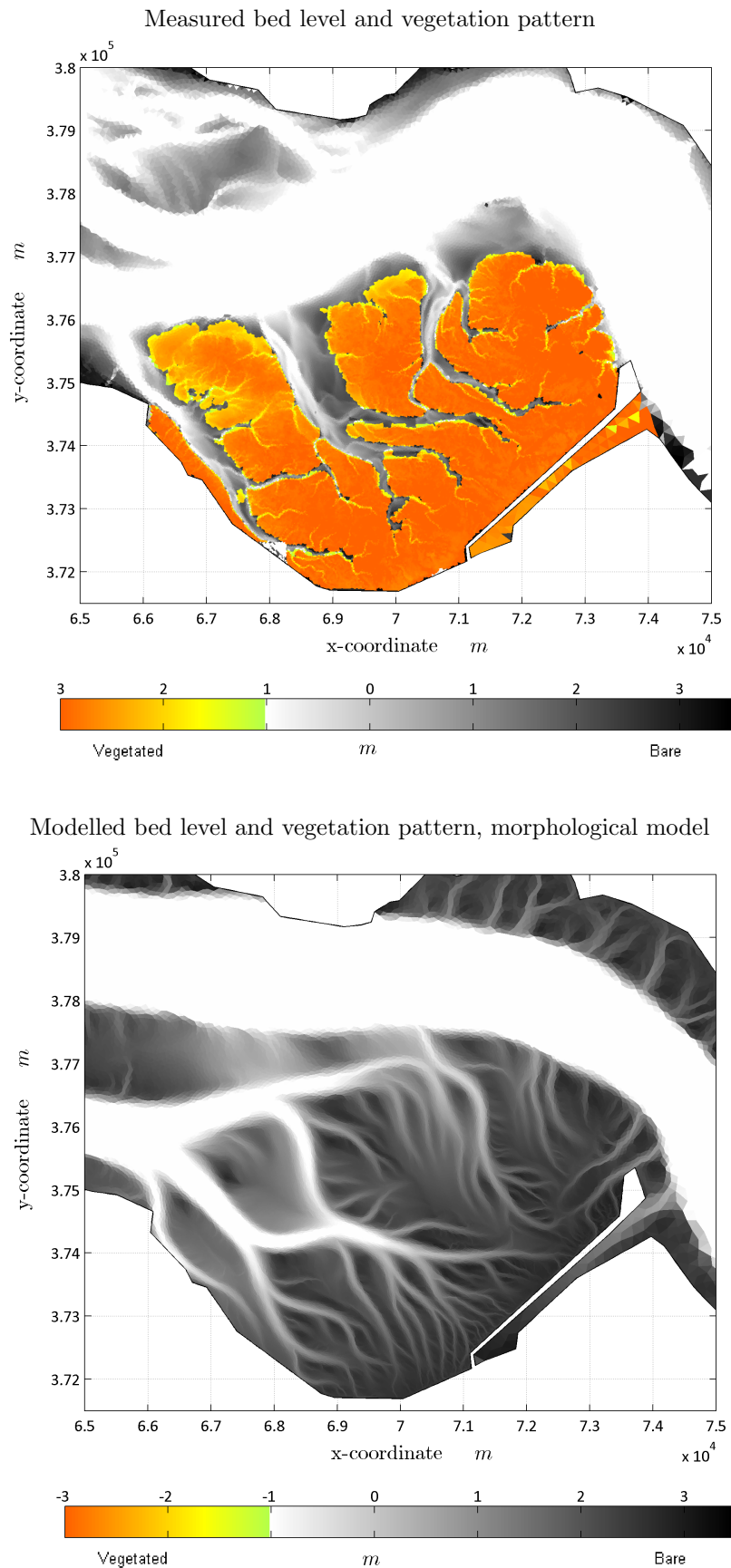
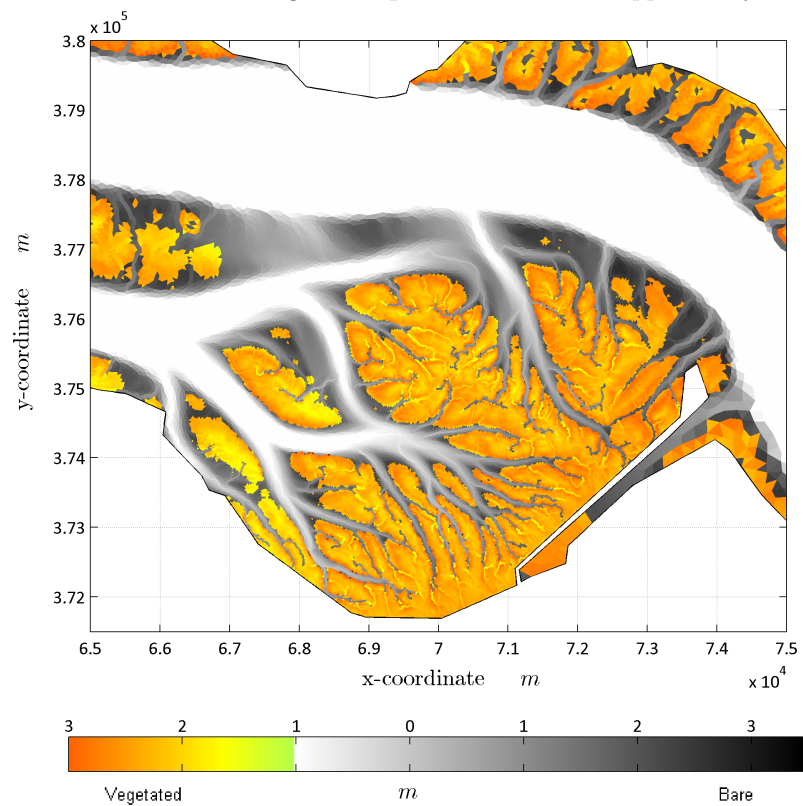


FIGURE 6.3: Measured and modelled bed level and vegetation pattern for Saeftinghe after 100 years (in 2004)

Modelled bed level and vegetation pattern, window of opportunity model



Modelled bed level and vegetation pattern, population dynamics model

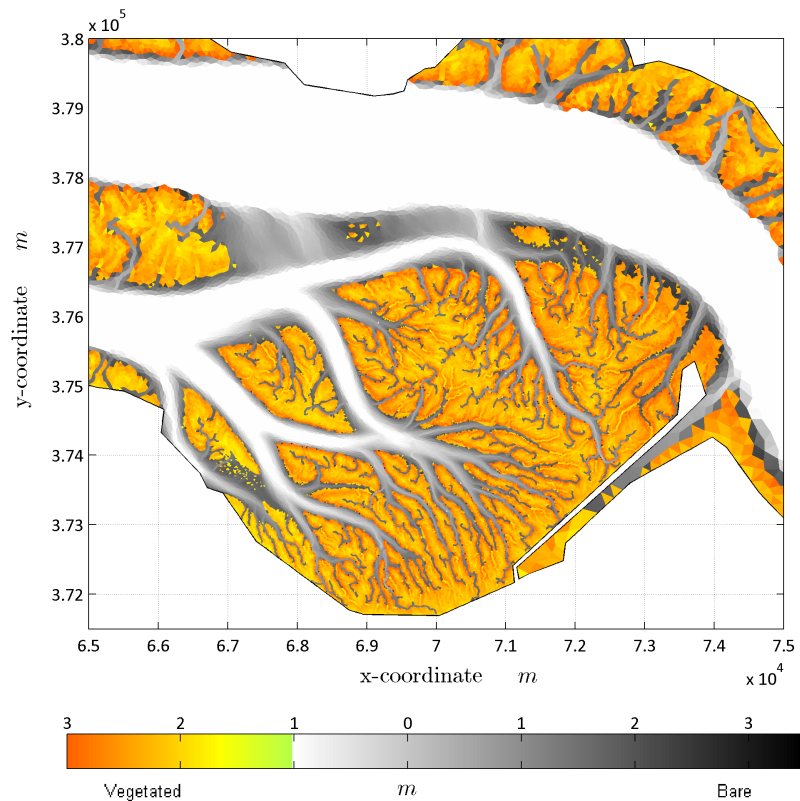


FIGURE 6.4: Modelled bed level and vegetation pattern for Saeftinghe after 100 years (in 2004)

Subsequently, figure 6.6 compares the modelled growth characteristics to the measured vegetated area. The difference between the models and the measurements are significant, particularly between 1905 and 1931. The vegetated area in the window of opportunity model is almost negligible. This again suggests an insufficiently elevated bed level in the simulations for vegetation establishment and growth. After 1931, however, vegetation establishment and growth start to occur and the difference in vegetated area stays approximately the same. In fact, the results after 1931 indicate that the growth curve of the window of opportunity model shows a similar tendency as the measured growth curve.

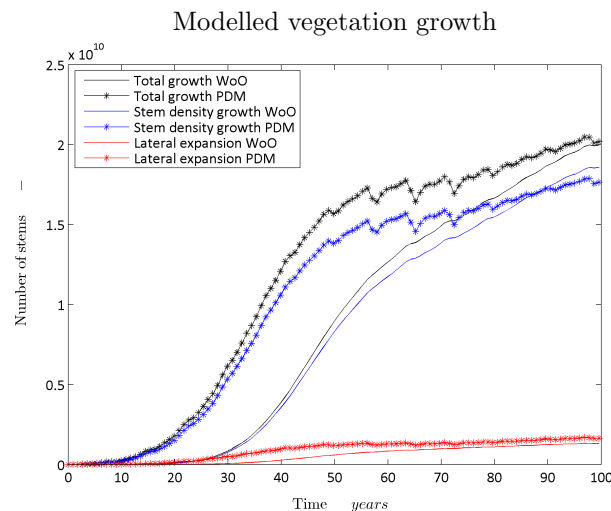


FIGURE 6.5: Vegetation growth characteristics for Saeftinghe throughout 100 years (1905-2004)

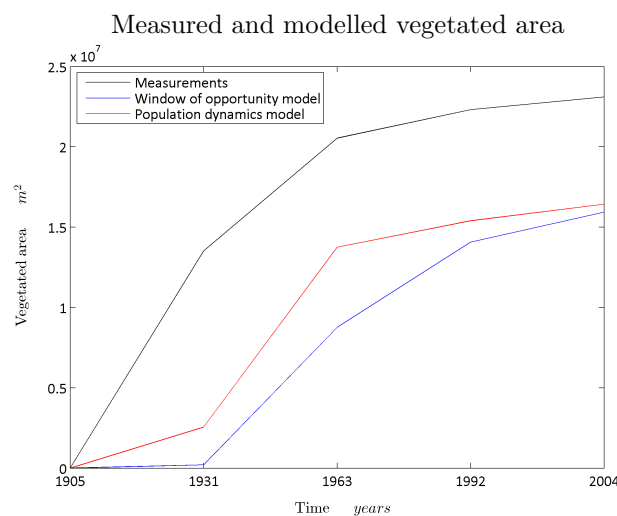


FIGURE 6.6: Comparison of the modelled and measured vegetated area for Saeftinghe throughout 100 years (1905-2004)

Finally, the establishment height graph in figure 6.8 highlights the difference in establishment characteristics of the bio-geomorphological models. Wang et al. (2013) suggested that the elevation height that corresponds to the peak's location is a measure for the threshold elevation height for landscape shifts from bare to vegetated. This means that the threshold elevation

height in the population dynamics model occurs at 1.7 m relative to mean sea level (i.e. approximately -0.8 m relative to MHWL), whereas this threshold occurs around 2.1 meters, (i.e. approximately -0.4 m (MHWL)) for the window of opportunity model. This threshold value for the window of opportunity model is in accordance with the observed peak in the establishment height graph presented by Wang et al. (2013), and the slightly skewed shape of the establishment height graph is as well. This suggests that the establishment settings and approach of the window of opportunity model is performing well in terms of establishment height.

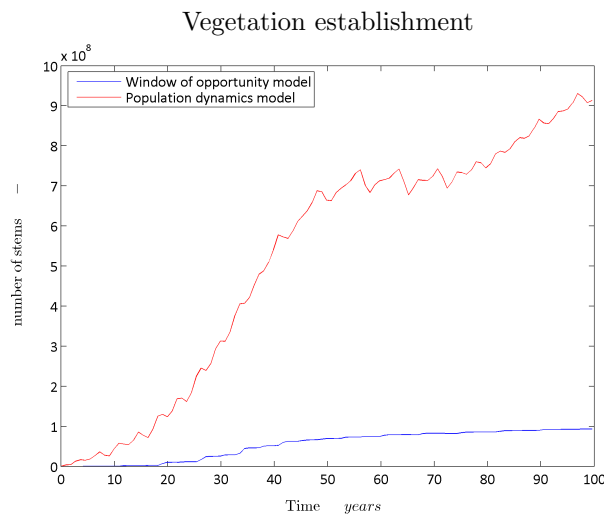


FIGURE 6.7: Establishment characteristics for Saeftinghe throughout 100 years (1905-2004)

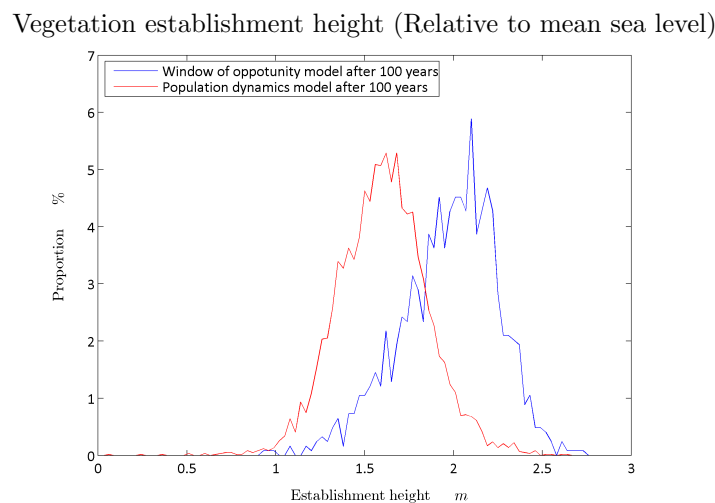
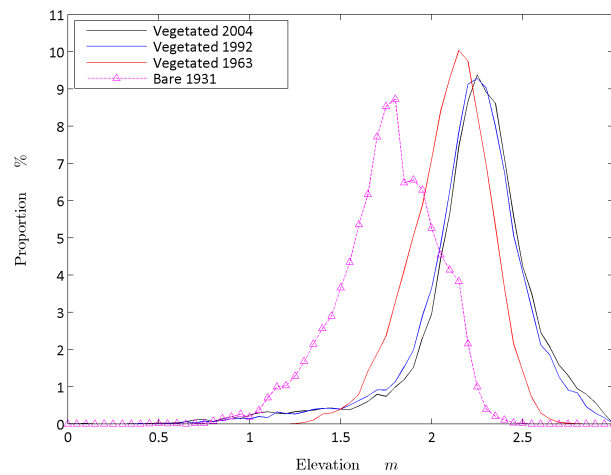


FIGURE 6.8: Establishment characteristics for Saeftinghe throughout 100 years (1905-2004)

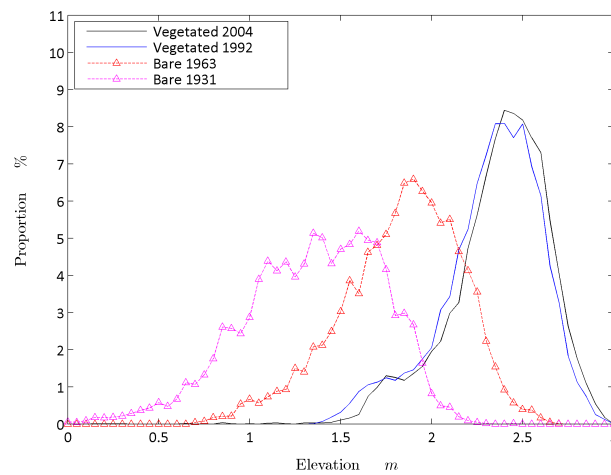
Shift from bare to vegetated tidal flats

This section compares the observed changes in landscape state, i.e. shifts from bare intertidal flats to vegetated marsh, to the modelled changes. Figure 6.9 presents the modelled elevation changes in the areas that shift from bare intertidal flats to vegetated marsh. In other words, the elevation distribution is calculated for the areas that have shifted from bare to vegetated between 1931-1963 (top graph), 1963-1992 (middle graph) and 1992-2004 (bottom graph).

Elevation changes in the areas that shifted from bare flats to vegetated marshes in 1931-1963



Elevation changes in the areas that shifted from bare flats to vegetated marshes in 1964-1992



Elevation changes in the areas that shifted from bare flats to vegetated marshes in 1992-2004

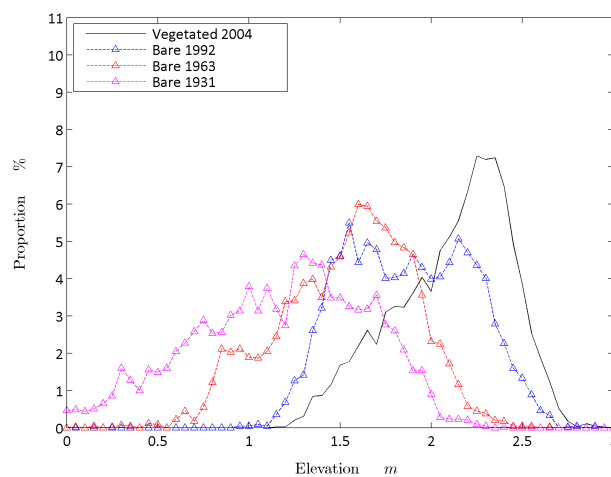


FIGURE 6.9: Elevation changes in the areas that shifted from bare to vegetated tidal flat at Saeftinghe, window of opportunity model

This type of graph is also presented by Wang et al. (2013), who used this graph to substantiate the existence of a threshold elevation height for landscape shifts in Saeftinghe. Additionally they utilized these graphs to illustrate the rapid accretion rates that are associated with these shifts. This can be identified by the shift in the peak of the elevation height graph between the different landscape states.

The results of the modelled elevation changes of the window of opportunity model in figure 6.9 do underline the existence of the threshold elevation height of 2.1 m (-0.4 m MHSL), as the peaks of the bare intertidal areas are located on the left side and the peaks of the vegetated areas are located on the right side of this threshold value. However, the existence of the rapid shift is only observed for the transition from bare to vegetated inter tidal area in the period 1931-1963, which suggests that this observed rapid shift in landscape state and thus the sediment accumulation is not represented well in this simulation.

6.3.2 Morphology

In this section the erosion/sedimentation patterns are discussed in more detail. Figures 6.10 and 6.11 present the measured and modelled sedimentation/erosion patterns after 100 years. These figures show that Saeftinghe is indeed a sedimentation dominated system, as the figures reveal a significant bed level increase. Furthermore, the patterns indicate that the modelled results show a less elevated system with more tidal creeks compared to the measurements. However, the fewer tidal creeks observed in the measurements are in fact an artefact of the resolution and the smoothing of the data. In reality, Saeftinghe is characterized by a more refined tidal creek pattern. Outside the marsh boundaries the erosion/sedimentation plot shows a completely different pattern. This can be contributed to the fact that the area just north of the marsh is a navigation channel in reality and thus subject to dredging activities which are not included in the models.

The patterns also demonstrate that the vegetation does have an effect on the morphological development, as the bio-geomorphological models show a more pronounced tidal creeks system, particularly at the high elevated tidal flats. In addition the patterns reveal that the number of tidal creeks found depends on the vegetation model. The population dynamics model shows more tidal creeks compared to the window of opportunity model, especially stretching all the way to the back of the salt marsh.

The differences between the bio-geomorphological simulations and the purely morphological simulations are compared in figure 6.12. This figure shows the bed level elevation difference, where the red colours indicate a higher bed level elevation in the bio-geomorphological models. These patterns underline the earlier findings regarding the more pronounced tidal creek system and reveal the existence of levees alongside the tidal creeks in the bio-geomorphological models. More striking are the differences in sediment accumulation on the tidal flats. The bio-geomorphological models clearly show more sediment accumulated on the tidal flats situated closer to the marsh edge, while the purely morphological model shows more accumulation at the back of the marsh. This suggests that in the bio-geomorphological models the influx of sediment is trapped by the vegetation, which leads to less accumulation at the back.

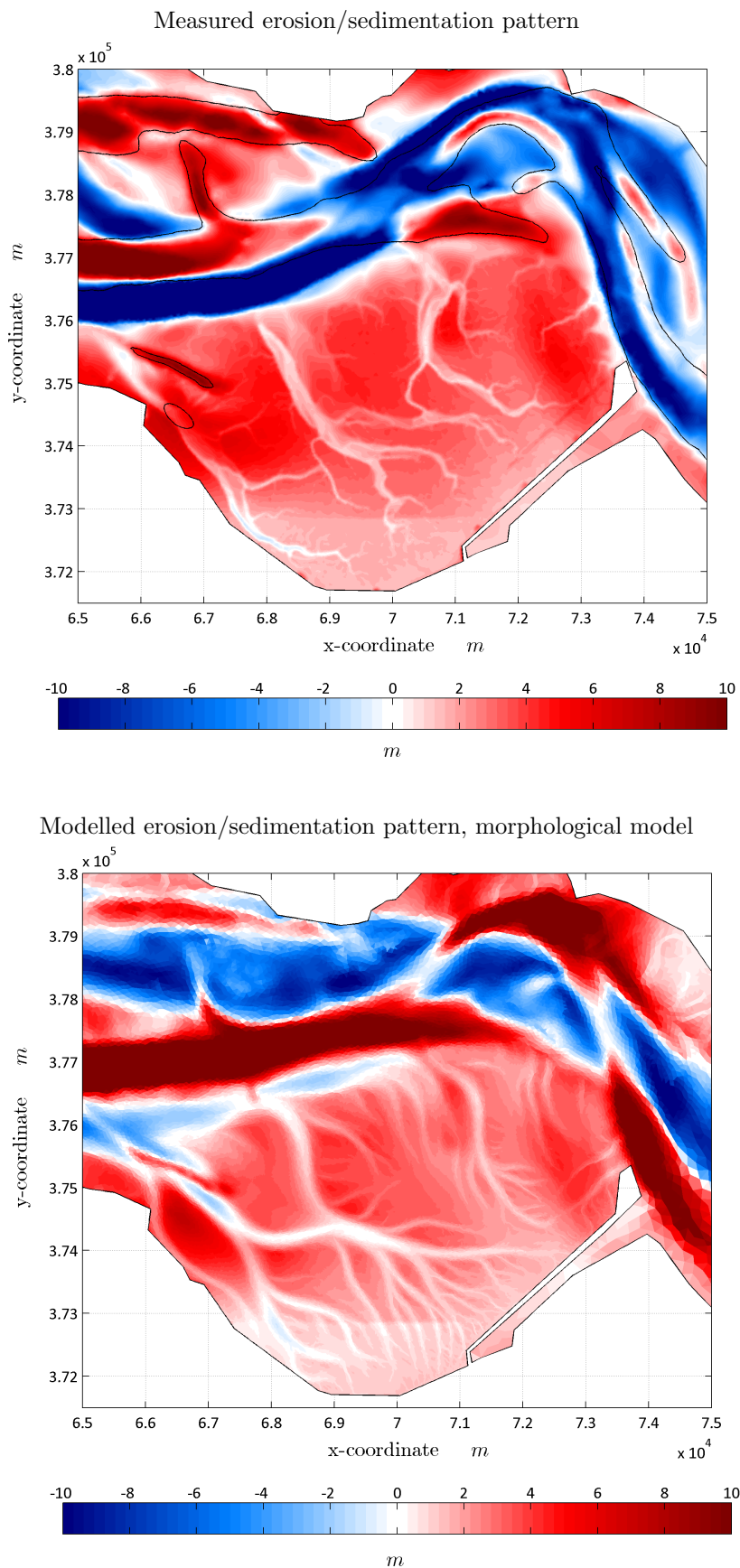
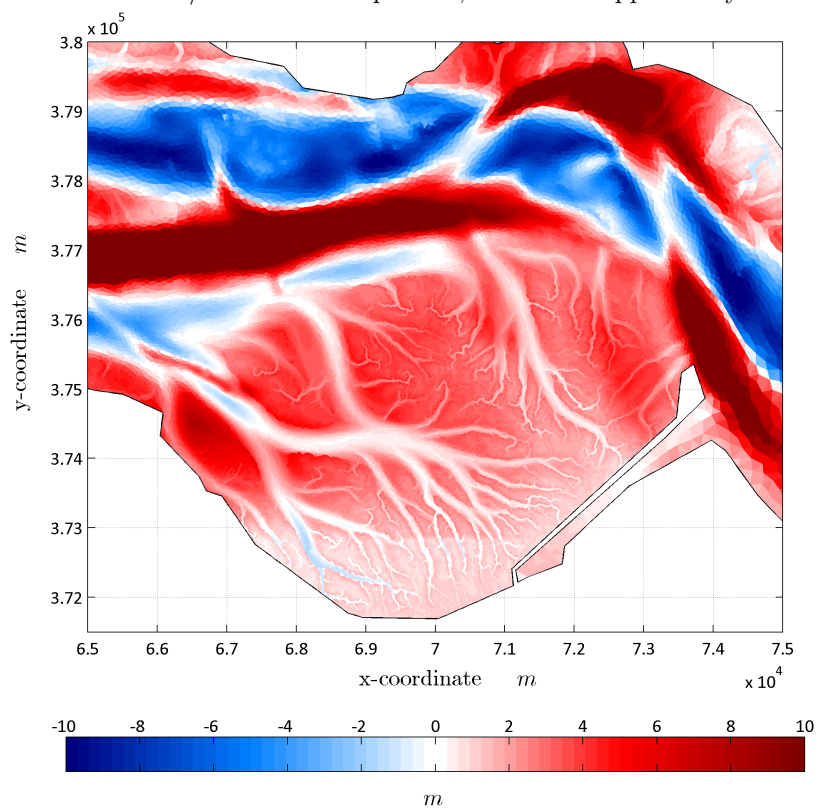


FIGURE 6.10: Measured and modelled Erosion/sedimentation patterns for Saeftinghe after 100 years (in 2004)

Modelled erosion/sedimentation pattern, window of opportunity model



Modelled erosion/sedimentation pattern, population dynamics model

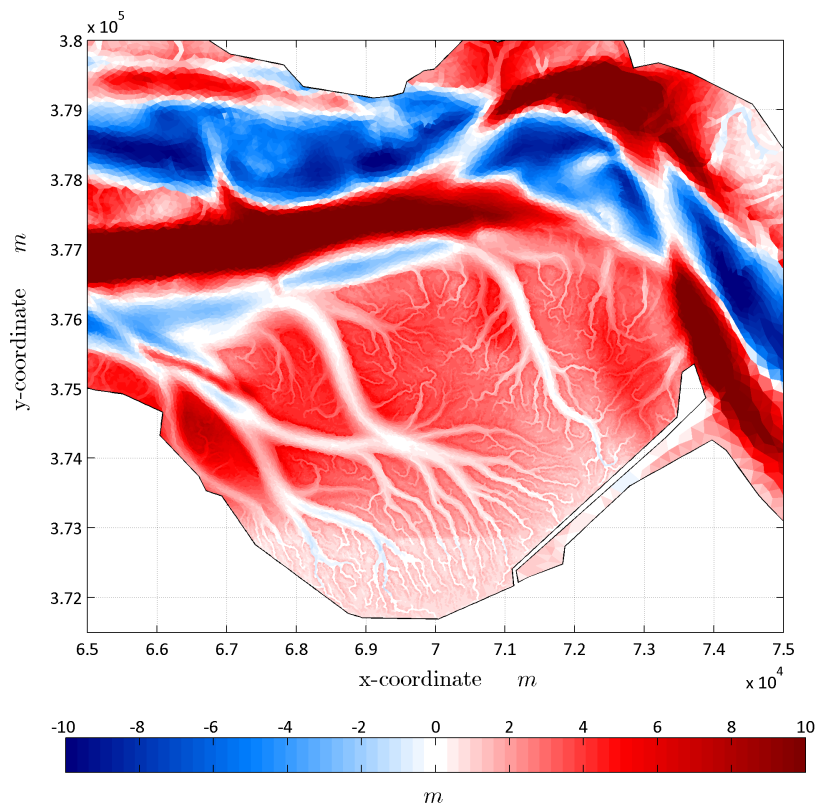
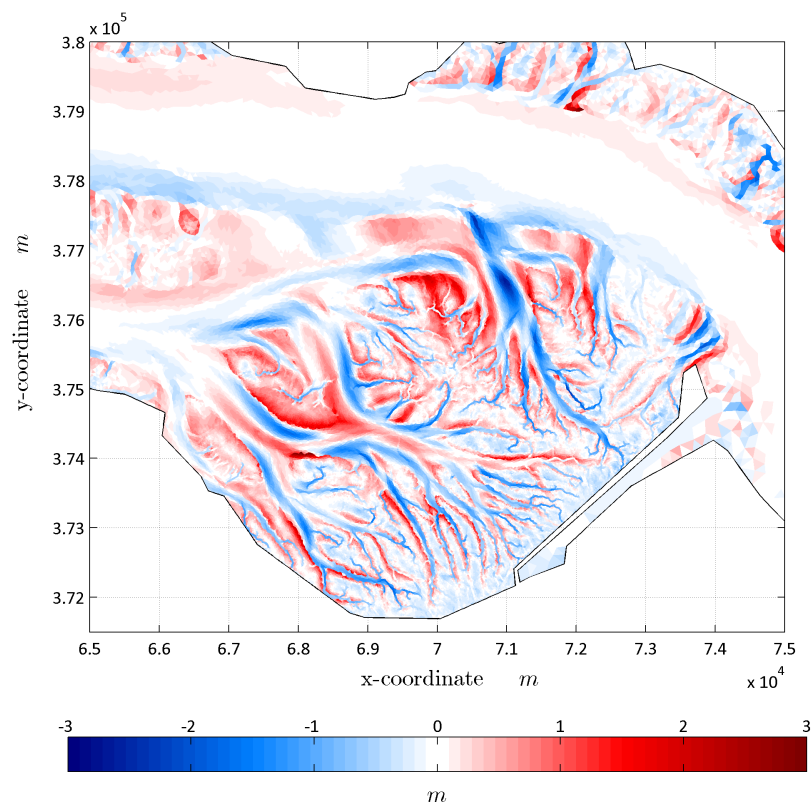


FIGURE 6.11: Modelled Erosion/sedimentation patterns for Saeftinghe in after 100 years (in 2004)

Elevation difference between window of opportunity model and morphological model



Elevation difference between population dynamics model and morphological model

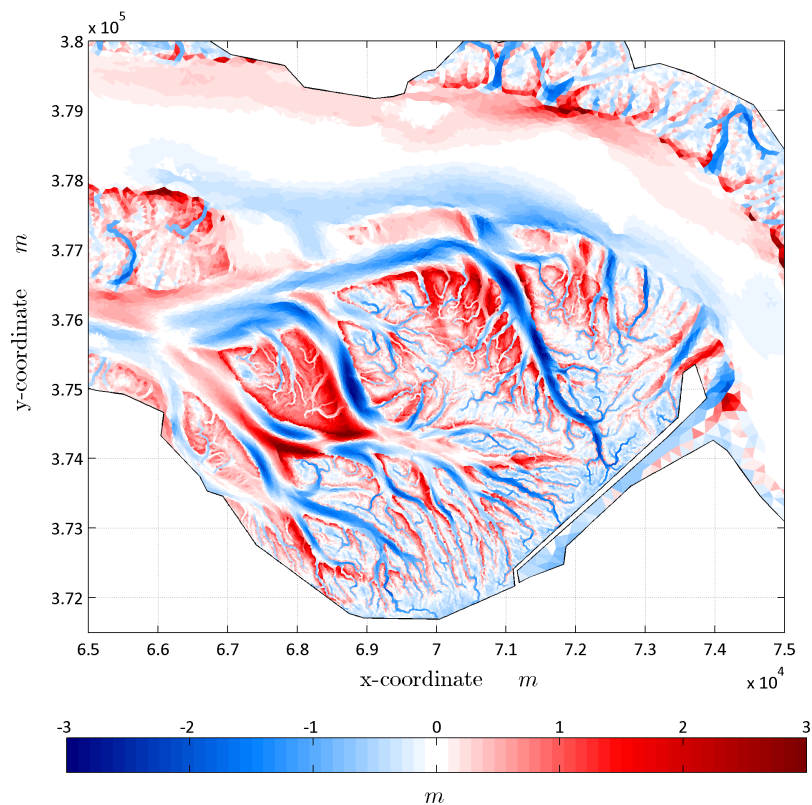


FIGURE 6.12: Elevation difference between the bio-geomorphological models and the morphological model for Saeftinghe after 100 years (in 2004). The red colours indicate a higher bed level elevation in the bio-geomorphological models.

Finally, the results of sedimentation/erosion characteristics have also been quantified, where only the actual salt marsh area is taken into account. The results of these cumulative sedimentation/erosion characteristics are presented in the top graph in figure 6.13. This graph indeed confirms the earlier suggested difference in sediment accumulation between the measurements and model results. More striking, on the other hand, is that the difference between the simulations are minimal. This suggests that the increased erosion and sedimentation observed in figure 6.12 balances each other out and that the vegetation has no significant effect on the cumulative erosion/sedimentation in Saeftinghe.

In order to quantify the performance of the model simulations the Brier-skill score or BSS is used. In this case the BSS is used to compare the erosion/sedimentation pattern of the simulations to the measured pattern. The equation used to calculate the Brier skill score is given by:

$$BSS = 1 - \frac{\langle (Y - X)^2 \rangle}{\langle (B - X)^2 \rangle} \quad (6.1)$$

Where,

X	=	computed bed level	[m]
Y	=	measured bed level	[m]
B	=	initial bed level	[m]

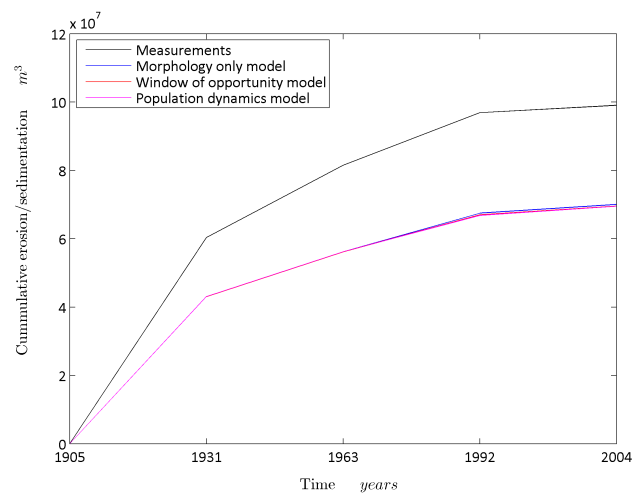
The output value of the BSS is a value between 1 and -infinity, where a score of 1 resembles a perfect match. The performance of the models according to this skill score are presented in the bottom graph in figure 6.13. The graph shows a Brier skill score values for the models between 0.7-0.8, which indicate that the model performs good according to the classifications, see table 6.4. However, the additional value of the bio-geomorphological model simulations is not reflected in this model performance score.

TABLE 6.4: BSS classification

BSS score	Rating
< 0	Bad
0 - 0.3	Poor
0.3 - 0.6	Reasonable/fair
0.6 - 0.8	Good
0.8 - 1.0	Excellent

Although this BSS value is in fact a very good score, it must be noted that this high number is partly due to the fact that the area under consideration is purely sedimentation dominated. In addition, the difference between the model results and the measurement are relatively small compared to the absolute bed level change, see figures 6.10 and 6.11. This also explains the small differences observed between the BSS scores of the model. Furthermore, this positive BSS score might benefit from the lower data and grid resolution and the data smoothing due to interpolation, so that the observed differences between the model and measurements in terms of tidal creek patterns are less pronounced.

Measured and modelled cumulative erosion/sedimentation



Brier Skill score

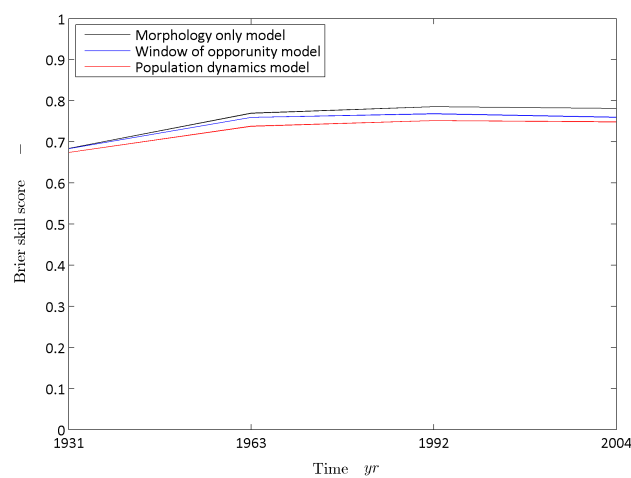


FIGURE 6.13: Measured and modelled cumulative erosion/sedimentation and the performance of the models regarding the erosion/sedimentation patterns expressed in terms of the BSS

6.4 Hydrodynamics

In this section the flow characteristics are examined after the 100 years of salt marsh development. The purpose is to assess the occurring flow velocities and patterns in the tidal creeks and in the vegetation. Additionally, the occurrence of the characteristic velocity pulse is investigated, which should occur around bank full discharge in the creeks due to the sudden flooding of the levees and/or vegetated flats (see section 2.3.1).

Figure 6.14 presents flow velocity fields during falling tide and graph 6.14 shows the flow velocities during a high tide-low tidal cycle for the indicated location. The flow field reveals that the maximum flow velocities within:

- the main channels are around $1 \text{ m} \cdot \text{s}^{-1}$
- the tidal creeks range from 0.5 to $0.8 \text{ m} \cdot \text{s}^{-1}$
- the vegetation range are an order of magnitude smaller, around 0.01 to $0.1 \text{ m} \cdot \text{s}^{-1}$

Furthermore, figure 6.15 reveals the occurrence of a velocity pulse at a water level of approximately 2.25 m during falling tide and at 2.65 m at rising tide. These water levels correspond, respectively, to the bed level of the tidal flat and the bed level plus vegetation top that surrounds the tidal creek. This suggests that a velocity pulse occurs when the vegetation is submerged and when the marsh platform is drained.

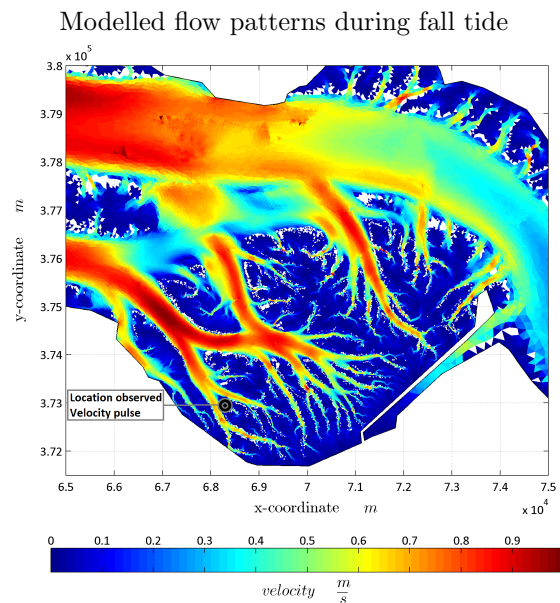


FIGURE 6.14: Flow characteristics for Saeftinghe after 100 years (in 2004), window of opportunity model

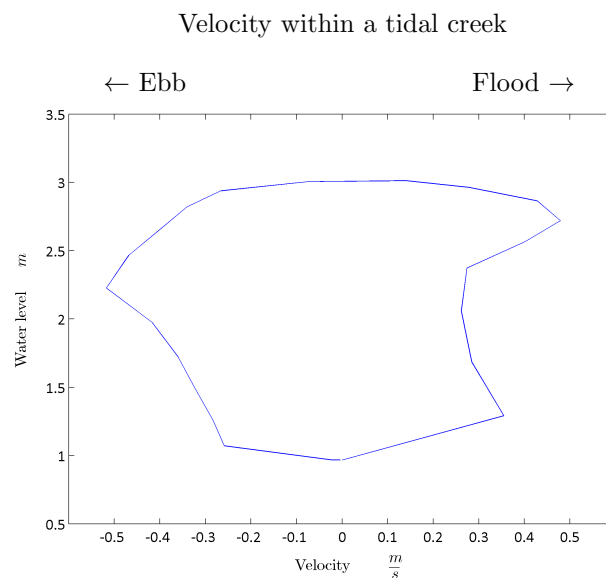


FIGURE 6.15: Flow characteristics for Saeftinghe after 100 years (in 2004), window of opportunity model

6.5 Conclusions

The results of the case study simulations demonstrate that the models are capable of predicting sediment accumulations and salt marshes formation in the 'Drowned land of Saeftinghe'. In this simulation, the additional effect of vegetation modelling on the geomorphological development is mainly visible on the higher elevated tidal flats. The vegetation on these tidal flats leads to a more pronounced tidal creek system with additional creeks. On a more global scale, vegetation is not dominating the morphological development such as the location of the main channels and the larger tidal creeks. However, the vegetation does lead to additional erosion in these channels and creeks due to flow concentration.

Additionally, the performance and practical applicability of the bio-geomorphological models has been assessed. This assessment revealed that:

- The bio-geomorphological models are able to represent a characteristic overgrown marsh platform dissected by tidal creeks.
- The representation and parameter settings of the establishment process in the window of opportunity is capable of reproducing the observed vegetation establishment characteristics in terms of establishment height.
- The windows of opportunity model presents a similar growth trend after 1931 to the one observed in Saeftinghe.
- The bio-geomorphological models do show the characteristic sedimentation patterns on the vegetated tidal flats, i.e. levees alongside the tidal creeks.
- The bio-geomorphological models are capable of representing the characteristic flow velocities and the velocity pulses in the tidal creeks.

On the other hand, the models were not capable of predicting the exact locations of the channels, tidal creeks or tidal flats, nor the bed level elevation height of the tidal flats. The former appeared to be sensitive to the sediment grain size D_{50} . Moreover, the simulation results indicate that insufficient bed level elevation is the limiting factor for the amount of vegetated area, which is in turn affected by the shortage of sediment influx and/or accumulation. This shortage of sediment influx and/or sediment accumulation in the model could be due to taking only one sediment fraction into account in the model. Whilst Saeftinghe is a system where both sand and mud play a role in the sediment influx and accumulation. The bio-geomorphological modelling approach did not contribute to additional overall sediment accumulation either. However, the findings in the sensitivity analysis in chapter 5 suggests that this is sensitive to sediment grain size D_{50} variations.

Chapter 7

Discussion

The bio-geomorphological model improvements

In this research two vegetation models are adopted to represent the vegetation growth. The first model is the population dynamics model, which is based on the method developed by Temmerman et al. (2007) and the other model is the window of opportunity model, which is a newly developed method based on the window of opportunity concept (Balke et al., 2011).

The implementation of these models shows that the window of opportunity model does not show long-term results that are drastically different compared to the population dynamics model. This indicates that there is no significant improvement in the new vegetation method. On the other hand, the representation of the establishment process did improve, since the establishment height of the vegetation in the simulations shows a better approximation of reality. This improvement might be important to reproduce the middle to long-term vegetation patterns in salt marshes. In the long-term these differences are smoothed out due to the later expansion of the vegetation which leads to a similar equilibrium. Thus, possibly the differences between the vegetation methods mainly affect the time scales of the processes and only to a lesser extent the equilibrium situation. This could imply that the system is robust and has self-organizing properties. Therefore, an interesting step would be to assess the performance of the models regarding the representation of the time scales of the vegetation growth processes.

The types of salt marsh systems

The bio-geomorphological simulations suggest that two types of systems can be defined:

- Vegetation is leading
 - The morphological development follows the vegetation growth, as flow concentration due to vegetation leads to tidal creek formation
- Morphology is leading
 - The vegetation growth follows the morphological development and flow concentration due to vegetation enhances the channel and tidal creek pattern

The first type of system is observed in the sensitivity analysis (chapter 5) and shows that the influence of the vegetation on the morphology is dominant. This system is found for otherwise morphological inactive tidal flats where the vegetation growth experiences hardly any restriction from the hydrodynamic forcing or geometry. The random character of the vegetation growth together with these degrees of freedom for vegetation growth lead to an inherently unpredictable

development of the tidal creek pattern, although global morphological developments are less sensitive.

The other type of system is found in the Saeftinghe case study simulations (chapter 6); a morphologically active salt marsh where the morphology is leading the vegetation growth. The system shows a more robust vegetation pattern and tidal creek system, i.e. they are less sensitive to variations in the input parameters. This is because the hydrodynamic forcing and geometry determine the morphological development which restricts vegetation growth to locations where enough sediment accumulation has occurred. Hence, the degrees of freedom of the system are reduced, which suppresses to a great extent the random vegetation growth.

Finally, the types of systems identified could be considered as two extremities, since it is conceivable that there are also salt marshes where a combination of the two systems is found. To some extent, this is also the case in the Saeftinghe case study, since the vegetation growth on the tidal flats does lead to the morphological development of some small tidal creeks.

The predictability of the bio-morphological development in salt marshes

In general, the view on the long-term morphological predictability of these systems is diversified. According to Vriend et al. (1993), the morphological development is inherently unpredictable due to non-linear interaction between the morphology and the hydrodynamics. On the other hand, Dam (2013) states that the predictability depends among others on the degrees of freedom of a system, which can be restricted due to the tidal forcing and the geometry outlines.

As for the predictability of the bio-geomorphological development in terms of exact tidal creek patterns, it depends on the type of system. In systems where the vegetation is leading, it appears to be impossible to predict the tidal creek pattern due to the random vegetation establishment process. For systems where the morphology is leading this is potentially possible, because of less degrees of freedom in which the system can develop. On the other hand, when considering the predictability of the global morphological development, i.e. erosion/sedimentation amounts and global patterns, it is suggested that the results are rather robust for both systems. This implies that the bio-geomorphological modelling can be used for quantitative purposes, global development characteristics and to understand the system.

The practical applicability of the bio-geomorphological models

The primary reason for applying the bio-geomorphological models is to reproduce or predict the morphological development in salt marshes. Additionally, it can be applied to gain insight in the growth characteristics and vegetation patterns in salt marshes. Therefore, bio-geomorphological models should be used in systems where the vegetation is leading, since it determines the morphological development of, among others, the tidal creek system. In contrast, it is less important for systems where the morphology is leading, particularly if the sole purpose is to reproduce the global erosion/sedimentation patterns and the location of the tidal flats, channels and tidal creeks. However, it must be noted that the effect of bio-geomorphological modelling is not completely insignificant. It does enhance the sedimentation/erosion patterns and thus has an added value compared to solely a morphological model.

Hence, the need to apply bio-geomorphological modelling depends on the purpose of the user and the type of system under consideration. For the latter, it is important that the type of system can be pre-determined. It is hypothesised that important indicators for determining the type of system are the morphological activity in a system and the initial bed elevation, since the simulations suggests that:

- Vegetation is dominant on morphological inactive tidal flats without initial presence of tidal creeks
- Morphology is dominant in a morphologically active system with initial presence of tidal creeks.

Chapter 8

Conclusions and recommendations

8.1 Conclusions

The contribution of bio-geomorphological modelling

The bio-geomorphological modelling results show that the inclusion of vegetation in the morpho-hydrodynamic model is necessary to reproduce the salt marsh characteristic phenomena. However, the contribution to the long-term and global morphological prediction of salt marsh formation and succession depends on the type of system.

The first type of system, found in the sensitivity simulations, is defined as a system where the vegetation is leading the morphological development. This system is characterised by an inherently unpredictable development of the tidal creek pattern, which finds its origin in the random character of the establishment process in the vegetation methods.

The second type of system is observed in the Saeftinghe case study, a morphological active system where the morphology leads the vegetation growth. This system is characterised by a more robust vegetation pattern and tidal creek system. This is due to the fact that the geometry and the associated morphological development determine the final state of the vegetation patterns and tidal creek system.

The results of the Saeftinghe case study simulations demonstrate that the model is capable of reproducing the development of channels, tidal flats and tidal creek systems in Saeftinghe over a 100 year period (from non-existing to full grown salt marsh system), although not at the exact locations. Moreover, the simulations show characteristic overgrown vegetated marsh platforms dissected by tidal creek systems on the tidal flats. This is reflected in a positive Brier-Skill Score of around 0.8, which indicate that the model has a good skill in this case study.

To conclude, bio-geomorphological modelling is essential in the situation where the vegetation is leading, but when the vegetation follows the morphological development like in the 'Saeftinghe' case, the contribution is limited to enhancing the morphological development.

The vegetation growth models

The implementation of the vegetation growth models in the morpho-hydrodynamics modelling software FINEL2d reveals that both bio-geomorphological models are capable of reproducing the salt marsh characteristic morphological and hydrodynamic phenomena. The sensitivity analysis underlines that the vegetation growth characteristics, represented by the vegetation methods and the interaction with the morpho-hydrodynamics described by representative roughness and shear stress approach (Baptist, 2005), are able to reproduce the correct trend.

The representation of the vegetation growth processes in the population dynamics model based on the method developed by Temmerman et al. (2007) can introduce vegetation establishment at erroneous locations. This problem is addressed by development of a new vegetation growth method based on the theoretically more sound window of opportunity concept described by Balke et al. (2011). The results indicate that the window of opportunity concept leads to an improvement regarding the representation of the establishment characteristics and assures vegetation growth at favourable locations. However, no drastically different vegetation patterns are observed between the two vegetation methods.

The evaluation of the sensitivity results indicate that the establishment process representation and particularly the sediment grain size affect the large scale vegetation growth characteristics and the global patterns. This sensitivity to the sediment grain size is observed in the case study simulation as well. Although the sensitivity simulation shows that the tidal creek pattern is inherently sensitive to variations in the input parameters, the general tendency is that the large scale vegetation growth characteristics and the global patterns are robust.

To conclude, no significant improvement is observed for the new window of opportunity model compared to the population dynamics model. For the sensitivity of the model results it is concluded that the large scale vegetation growth characteristics and the global patterns are robust.

8.2 Recommendations

Recommendations regarding model development

- Discuss the representation of the growth processes and the choice of representative parameters with ecologists. This could lead to new insights regarding the ecological representation of the vegetation methods. In particular, attention could be given to represent the mechanism behind vegetation mortality.
- Reconsider the representation of the lateral expansion of vegetation. Although the current representation is considered to be independent of the grid cell size, the growth characteristics are affected by variations in grid cell size due to the lateral expansion. Although this effect on the overall growth characteristic is practically negligible, it could be improved (see section 5.1.2).
- Improve the approach that describes the influence of the vegetation on the morpho-hydrodynamics. The current approach developed by Baptist (2005) is not valid for sparse

vegetated situations, while these situations do arise in salt marsh modelling. In addition, the effect of the vegetation on morphology is only considered through the hydraulic roughness, i.e. influence on the flow velocity, while in reality this is a more complex process. Improving this aspect of vegetation modelling might require experimental tests and field measurements, but is considered a promising improvement.

- Simplify the establishment process of the window of opportunity model. From a more general point of view, it would be interesting to assess the additional value of the processes in the vegetation method. The purpose should be to develop a model with only the crucial processes without loss of accuracy. The window of opportunity concept applied for the representation of the establishment could perhaps be simplified.

Recommendations regarding the bio-geomorphological simulations

- Carry out a more comprehensive sensitivity analysis, where the influence of the vegetation parameter settings and morphological settings on the model results are assessed. This should be carried out for both types of systems. In particular for the influence of:
 - multiple sediment fractions, since salt marshes are systems where both sand and mud play a role in the sediment influx and accumulation.
 - the vegetation drag coefficient, since the influence of the vegetation on the morpho-hydrodynamics is an important aspect.
- Perform a comprehensive calibration and validation of the Saeftinghe case study. The calibration of the Saeftinghe model should focus on increasing the sediment accumulation. This might be achieved by taken multiple sediment fractions into account and/or by including the effect of the dredging activities in the case study, as the accumulated sand in front of the salt marsh can affect the influx of sediments. For the validation of the Saeftinghe case study a good next step would be to quantify and compare the tidal creek systems in more detail. For instance, by quantifying the channel and tidal creek density and proportions, which requires a proper quantification method. It is advisable to increase the grid resolution and the data resolution in order to obtain a better representation of the tidal creek system both in the model and in the data. Further calibration of the Saeftinghe case requires preferably additional measurements, for instance of flow velocities in channels, tidal creeks and within the vegetation.

Recommendations regarding further research

- Evaluate the additional value of long-term bio-geomorphological modelling of the formation and succession of salt marshes for sand mud morphological models. These models consider two sediment fractions and take into account the interaction between sand and mud, which can lead to cohesive behaviour of the bed. In general, salt marshes are systems where both sand and mud and the cohesive behaviour of the bed can play a role in the sediment influx and erosion/sedimentation patterns. Therefore, it is hypothesised that a sand-mud bio-geomorphological model can contribute to the long-term morphological predictions.

- Research the influence of waves and storms on the long term bio-geomorphological modelling of the formation and succession of salt marshes. In the Saeftinghe case study only an astronomical forcing is induced. Waves, particularly during storms, can induce cliff erosion at the marsh edge, which might lead to vegetation mortality and salt marsh destruction (Koppel et al., 2005). Further, the higher hydrodynamic forces during the storms may affect the long-term morphological development due to increased erosion in the channels and creeks. In addition, the water level set-up during storms can lead to inundation and thus additional sediment influx to the more elevated marsh platforms at the back. Therefore, this could be an important process that is necessary to describe the bio-geomorphological development of salt marshes.

- Assess the influence and value of the bio-geomorphological modelling for different case studies. These case studies can contribute to:
 - the validation of the bio-geomorphological models
 - the understanding of the morphological development of the salt marsh systems
 - the substantiation of the finding that there are different types of systems

Appendix A

Vegetation growth models

A.1 Rewriting the representative roughness equation

The representative roughness approach describes the influence of the vegetation on the depth average flow velocity. This approach, presented by Baptist (2005), consists of two separate equations, one to describe the flow through unsubmerged vegetation and a second equation to approximate the flow through and over submerged vegetation. This second equation is originally derived through genetic programming by Uthurburu (2004) to approximate the representative Chézy coefficient. In this thesis, this equation by Uthurburu (2004) is rewritten in terms of the dimensionless friction coefficient.

The original representative roughness equation for flow through and over submerged vegetation is given by,

$$C_{submerged} = \frac{\sqrt{g}}{\kappa} \cdot \log\left(\frac{h}{k}\right) + \sqrt{\frac{1}{(C_b^{-2}) + (\frac{1}{2g} \cdot C_{Dv} \cdot k \cdot \phi \cdot n_b)}} \quad \text{for } h \leq k \quad (\text{A.1})$$

Where,

$C_{submerged}$	=	Representative Chézy coefficient for submerged vegetation	$\left[\frac{m^{0.5}}{s}\right]$
C_b	=	Chézy coefficient bed	$\left[\frac{m^{0.5}}{s}\right]$
g	=	Gravitational acceleration	$[m \cdot s^{-2}]$
C_{Dv}	=	Drag coefficient vegetation	$[-]$
k	=	Uniform vegetation height	$[m]$
ϕ	=	Stem diameter	$[m]$
n_b	=	Stem density	$[m^{-2}]$
κ	=	Von karman constant	$[-]$
h	=	Water depth	$[m]$

This equation can be rewritten in terms of the dimensionless friction coefficient with the following relation,

$$C_b = \sqrt{\frac{g}{C_{fb}}} \quad (\text{A.2})$$

Where,

$$C_{fb} \quad = \quad \text{Bed friction coefficient} \quad [-]$$

Combining equations A.2 and A.1 gives,

$$\sqrt{\frac{g}{C_{fr, submerged}}} = \frac{\sqrt{g}}{\kappa} \cdot \log\left(\frac{h}{k}\right) + \sqrt{\frac{1}{\left(\frac{C_{fr, submerged}}{g}\right) + \left(\frac{1}{2g} \cdot C_{Dv} \cdot k \cdot \phi \cdot n_b\right)}} \quad \text{for } h \leq k \quad (\text{A.3})$$

Or,

$$\sqrt{\frac{1}{C_{fr, submerged}}} = \frac{\sqrt{1}}{\kappa} \cdot \log\left(\frac{h}{k}\right) + \sqrt{\frac{1}{C_{fr, submerged} + \left(\frac{1}{2} \cdot C_{Dv} \cdot k \cdot \phi \cdot n_b\right)}} \quad \text{for } h \leq k \quad (\text{A.4})$$

This can be simplified to the equation that is presented in this thesis,

$$C_{fr, submerged} = \left(\frac{1}{\frac{1}{\kappa} \cdot \log\left(\frac{h}{k}\right) + \sqrt{\frac{1}{C_{fb} + \frac{1}{2} \cdot C_{Dv} \cdot n_b \cdot \phi \cdot k}}} \right)^2 \quad \text{for } h \geq k \quad (\text{A.5})$$

Appendix B

Numerical implementation

B.1 Vegetation decay processes, population dynamics model

This section evaluates the coupling between the hydrodynamics and the vegetation decay processes. For the vegetation mortality due to inundation, this coupling is represented by:

$$\left(\frac{dn_b}{dt}\right)_{inund} = \max\{(h - h_{crit}), 0\} \cdot PE_h \quad (\text{B.1})$$

Where,

n_b	=	Stems per surface area	$[m^{-2}]$
h_{crit}	=	Critical inundation water level	$[m]$
PE_h	=	Plant mortality rate for inundation stress	$[m^{-3} \cdot s]$

The coupling of this vegetation decay equation with the hydrodynamics can be carried out using different approaches. The approach applied by Temmerman et al. (2007) is coupling of the vegetation growth model with the hydrodynamics after each tidal cycle, also known as offline coupling. However, in this research an online coupling approach is applied, meaning that the hydrodynamic output is used as input for the vegetation growth model at every computational time step. The difference between these approaches is illustrated in figure B.1.

This figure indicates that using the online coupling approach leads to less vegetation mortality. This difference between these approaches can be reduced by increasing the mortality coefficients and reducing the critical inundation height for the online method. These adjustment are assessed in a simple single point simulation, where the water level is varied harmonically. The parameter selection for this simulation is presented in table B.1.

TABLE B.1: Numerical example, online and offline coupling vegetation inundation mortality

Approach	Forcing	PE_h	h_{crit}
Off-line	M2-tide, amplitude 2 [m]	300 $[m^{-3} \cdot yr^{-1}]$	1.1 [m]
On-line	M2-tide, amplitude 2 [m]	1200 $[m^{-3} \cdot yr^{-1}]$	1.0 [m]

Figure B.2 presents the results of this single point simulation, which shows that the differences in vegetation mortality are insignificant in the region between 0 m and 0.9 m relative to MWL. However, below 0 m the online method starts to calculate significantly more mortality, but this can be justified by stating that vegetation growing below mean sea level should not be able to survive. Thus, these adjustments to the mortality coefficients and the critical inundation height for the online method are more or less equivalent to the values used by Temmerman et al. (2007) for the offline approach. A remark to this conclusion is that this is only tested for a simple harmonic M2 tide, the equivalent online parameter might be different under a more complex tidal signal.

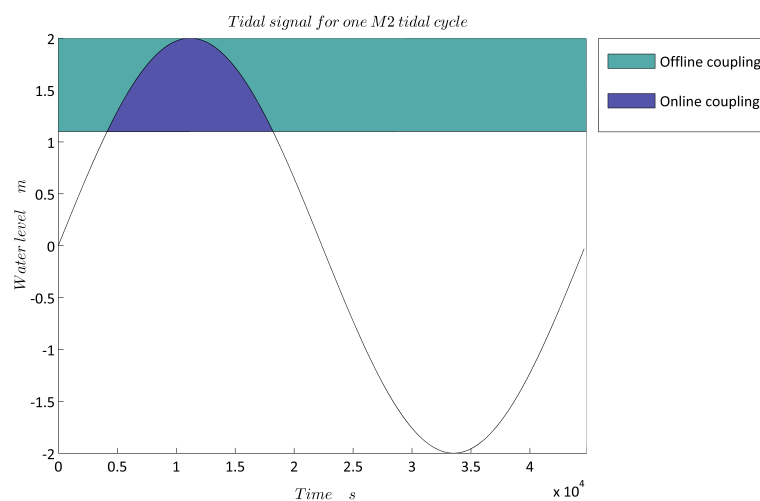


FIGURE B.1: Difference between the online and offline coupling approach

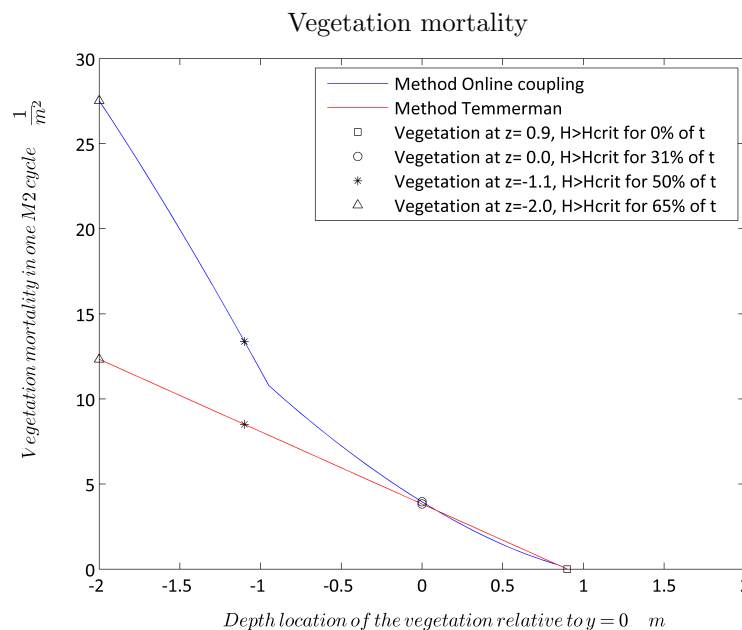


FIGURE B.2: Adjusted mortality coefficient for the online coupling method. Vegetation mortality accumulated for a M2 cycle for different establishment depths

A similar adjustment could be applied to the vegetation mortality due to shear stress, since the representation is similar to the vegetation mortality due to inundation, see equation B.2. However, this is not necessary, as the shear stress mortality coefficient PE_τ used by Temmerman et al. (2007) is chosen such that the vegetation dies instantly when the shear stress threshold is exceeded, i.e. $PE_\tau = 30 [N^{-1} \cdot s^{-1}]$, while $PE_h = 300 [m^{-3} \cdot yr^{-1}]$.

$$\left(\frac{dn_b}{dt}\right)_{flow} = \max\{(\tau_b - \tau_{b, crit}), 0\} \cdot PE_\tau \quad (\text{B.2})$$

Where,

τ_b	= Measured bed shear stress	$[N \cdot m^{-2}]$
$\tau_{b, crit}$	= Critical bed shear stress resistance vegetation	$[N \cdot m^{-2}]$
PE_τ	= Plant mortality rate for shear stress	$[N \cdot s^{-1}]$

Appendix C

Case study results

C.1 Development of Saeftinghe, window of opportunity model

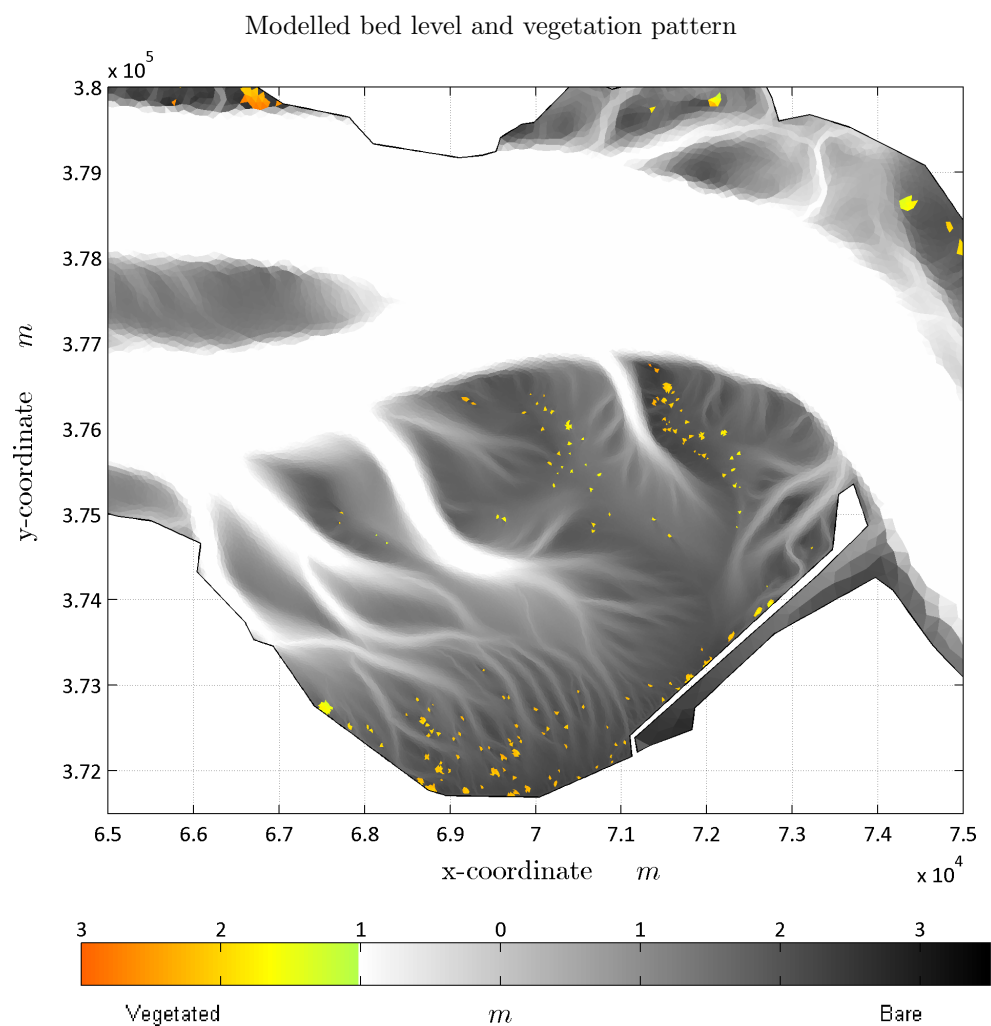


FIGURE C.1: Bed level and vegetation pattern for Saeftinghe after 26 years (in 1931), window of opportunity model

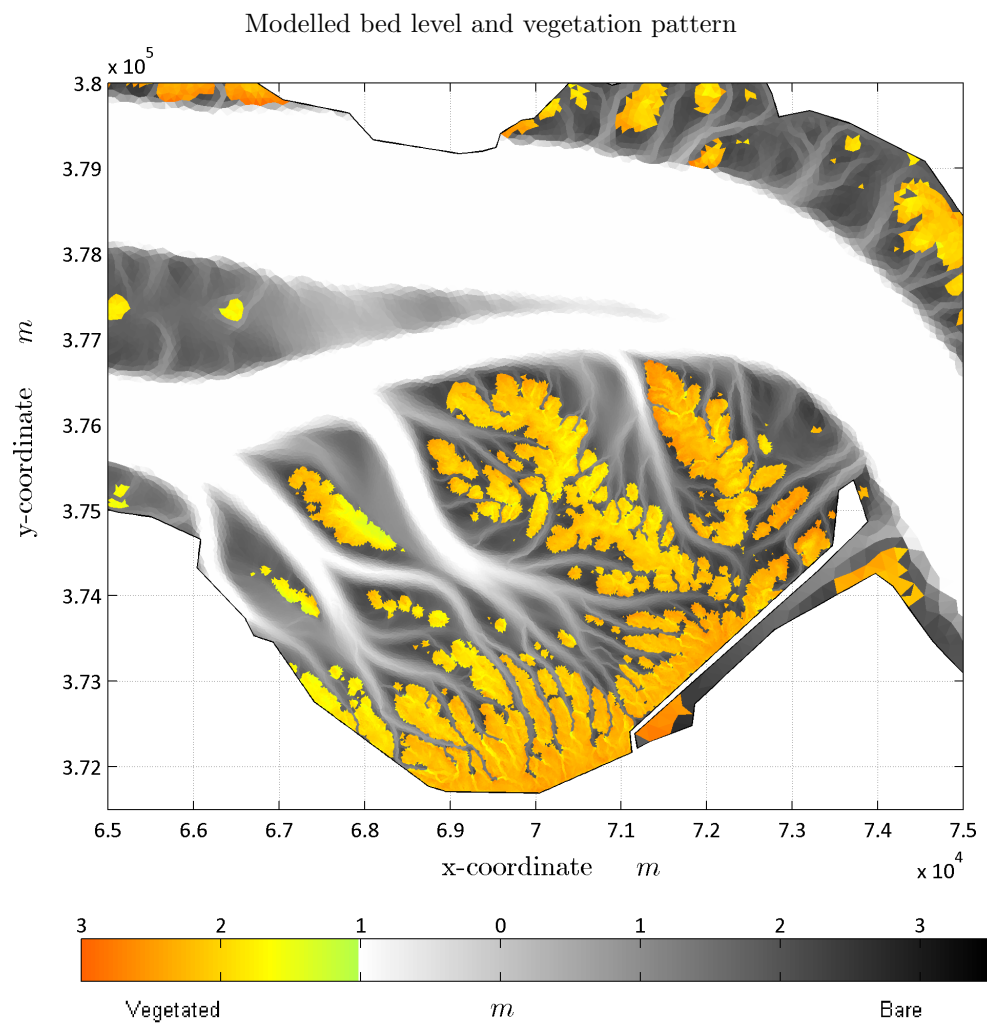


FIGURE C.2: Bed level and vegetation pattern for Saeftinghe after 58 years (in 1963), window of opportunity model

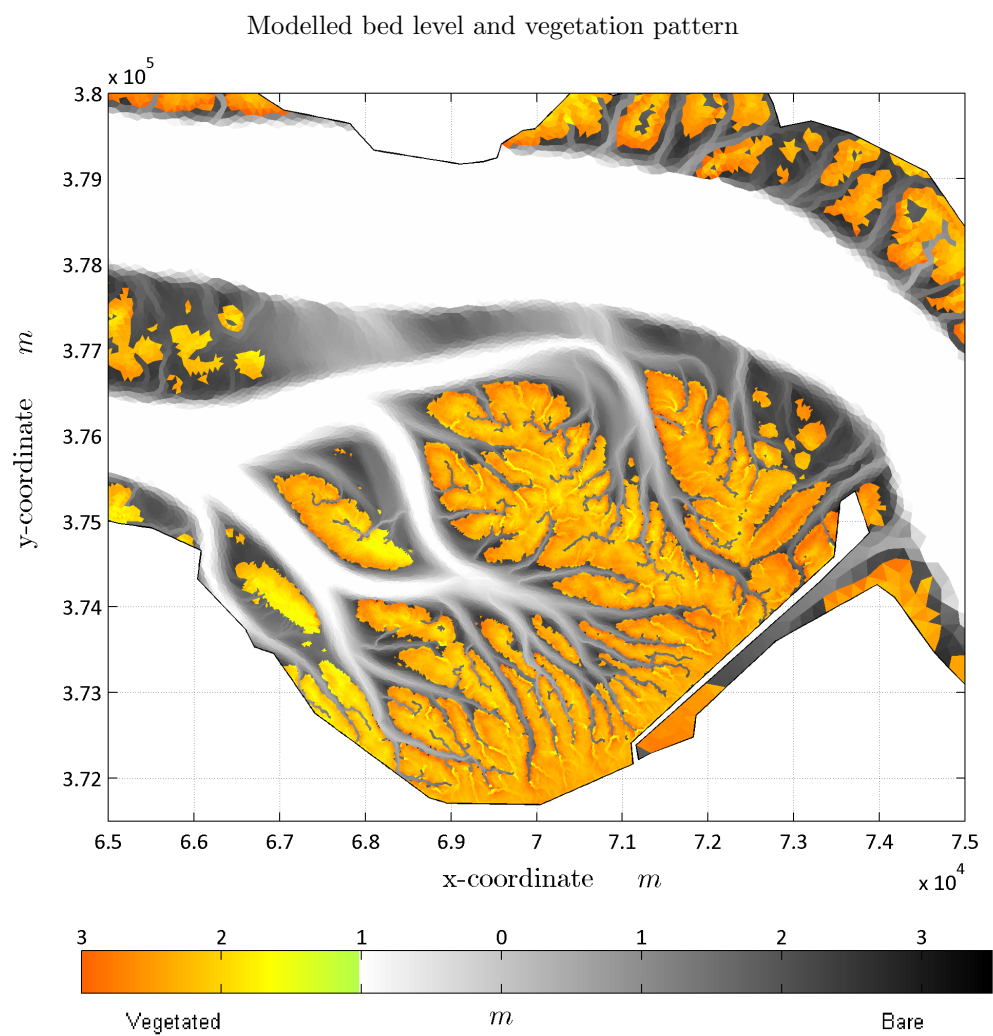


FIGURE C.3: Bed level and vegetation pattern for Saeftinghe after 87 years (in 1992), window of opportunity model

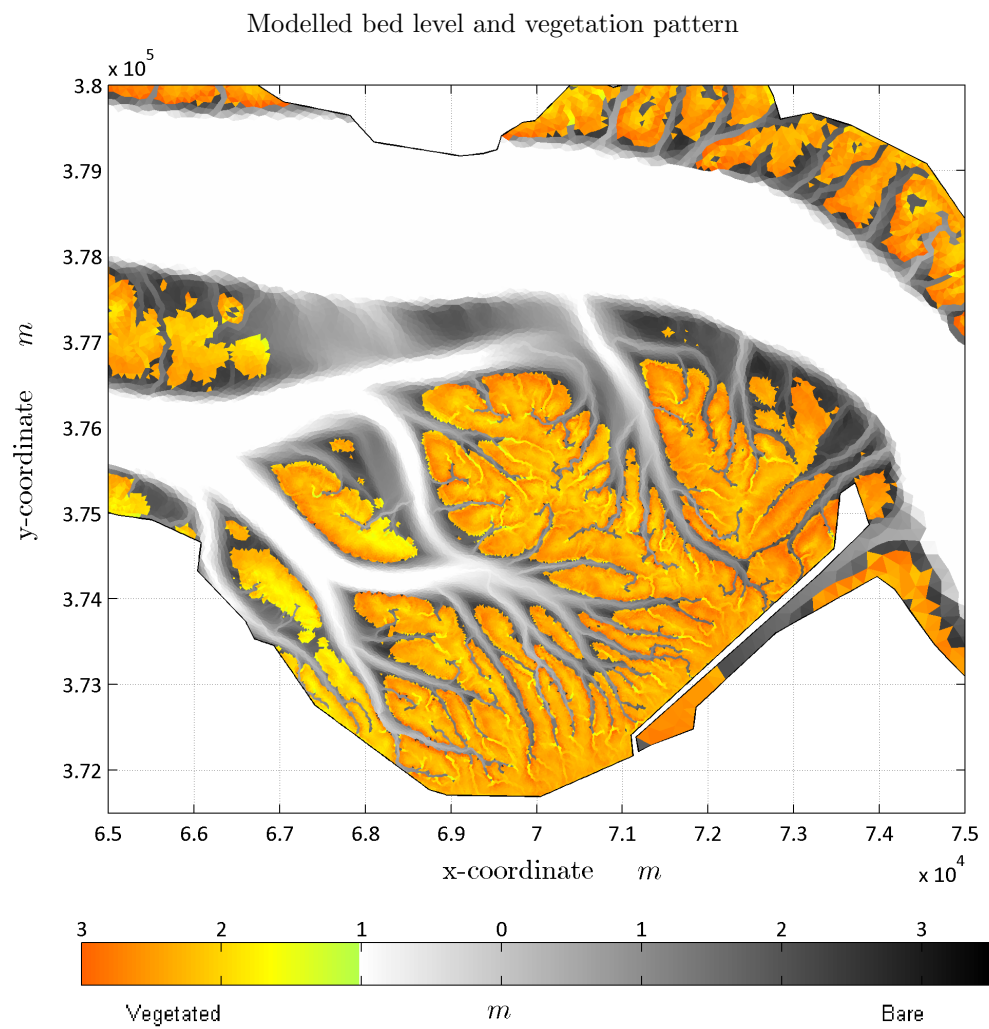


FIGURE C.4: Bed level and vegetation pattern for Saeftinghe after 99 years (in 2004), window of opportunity model

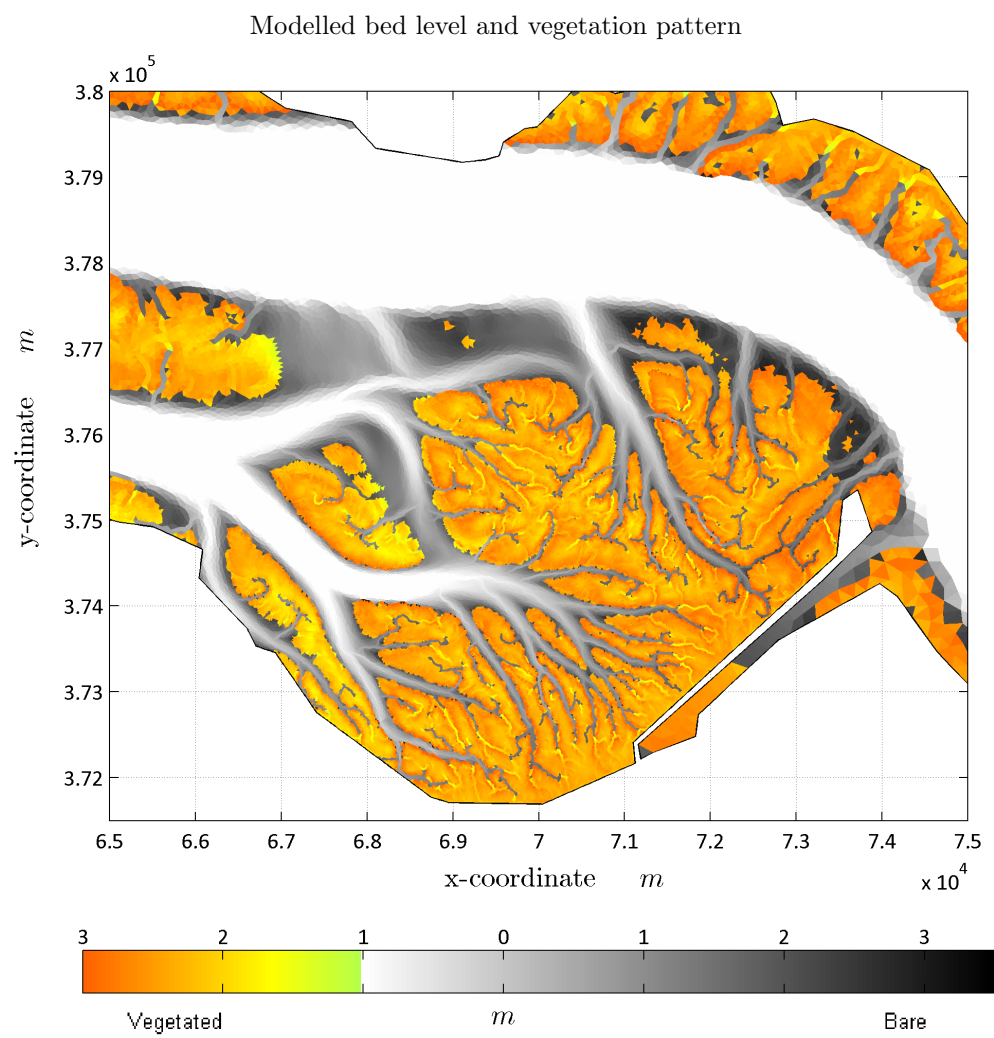


FIGURE C.5: Bed level and vegetation pattern for Saeftinghe after 122 years (in 2027), window of opportunity model

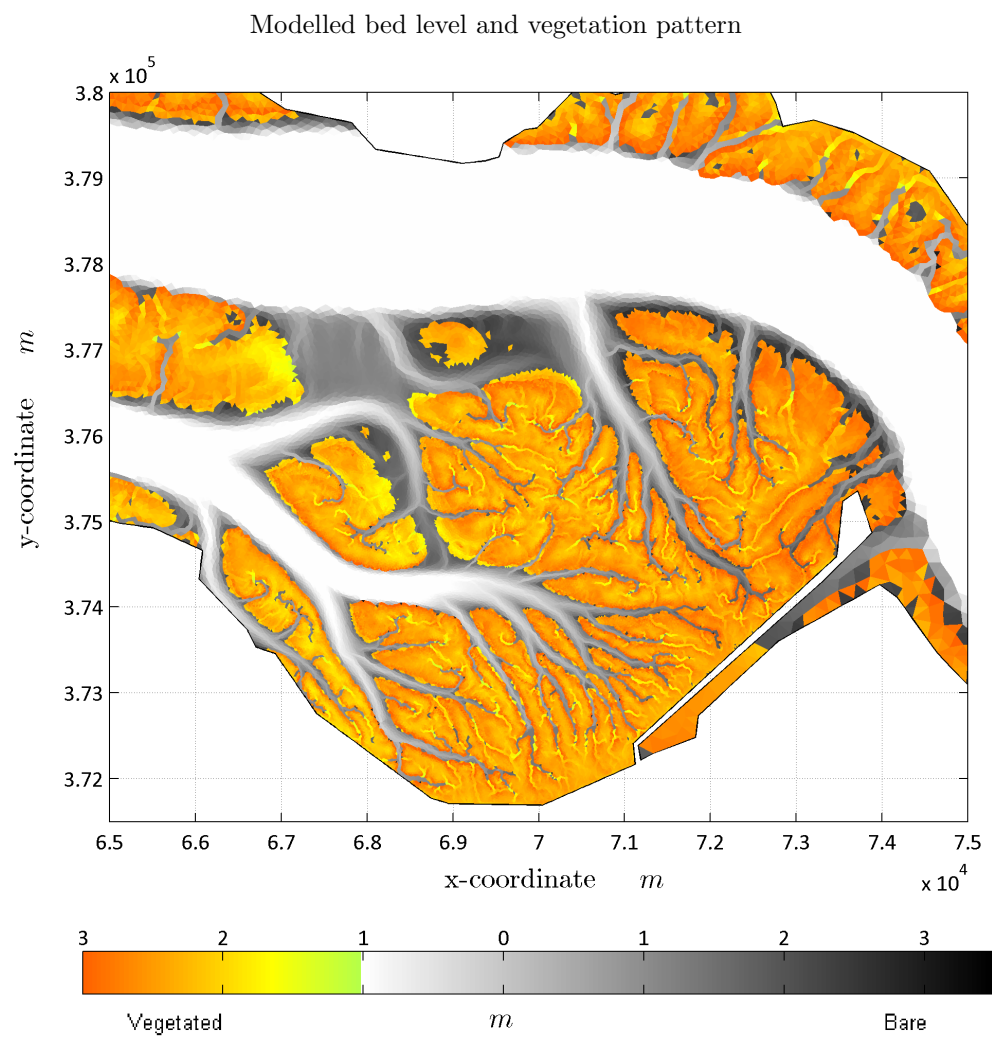


FIGURE C.6: Bed level and vegetation pattern for Saeftinghe after 148 years (in 2053), window of opportunity model

C.2 Development of Saeftinghe, population dynamics model

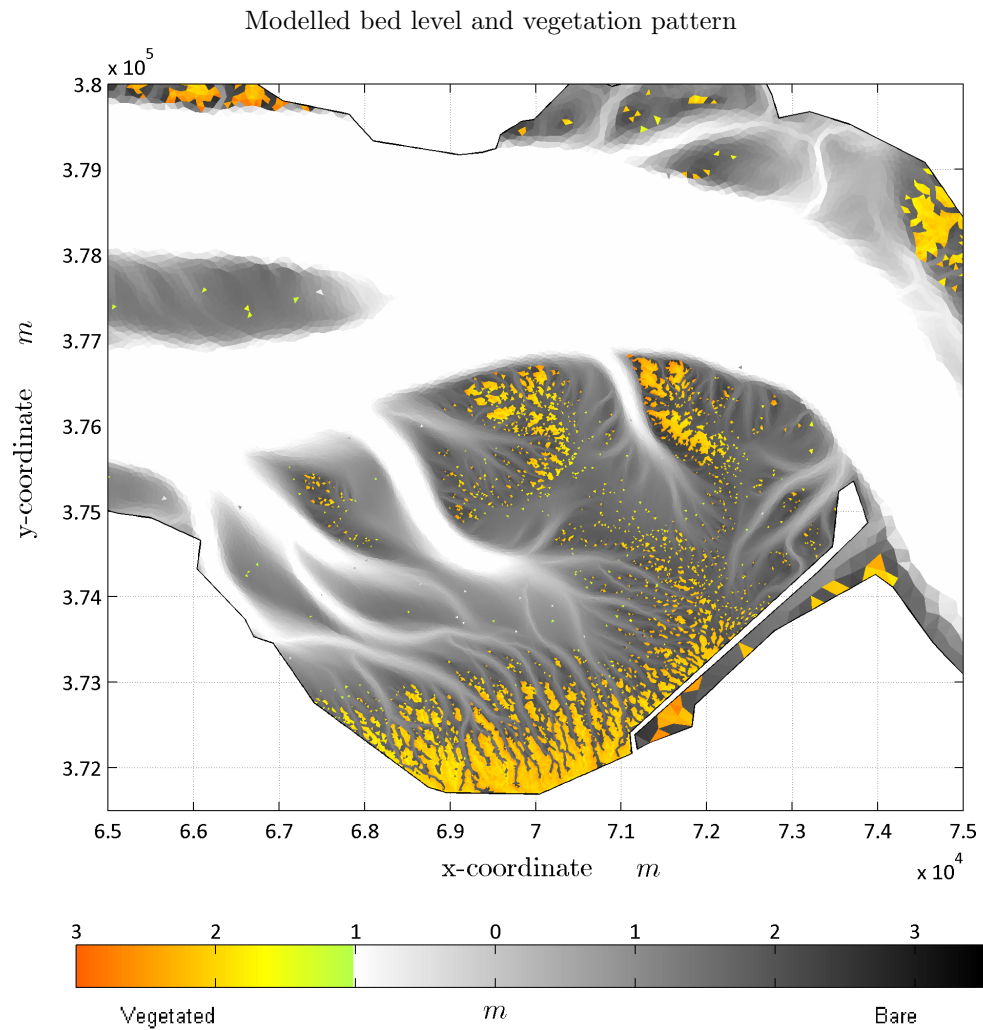


FIGURE C.7: Bed level and vegetation pattern for Saeftinghe after 26 years (in 1931), population dynamics model

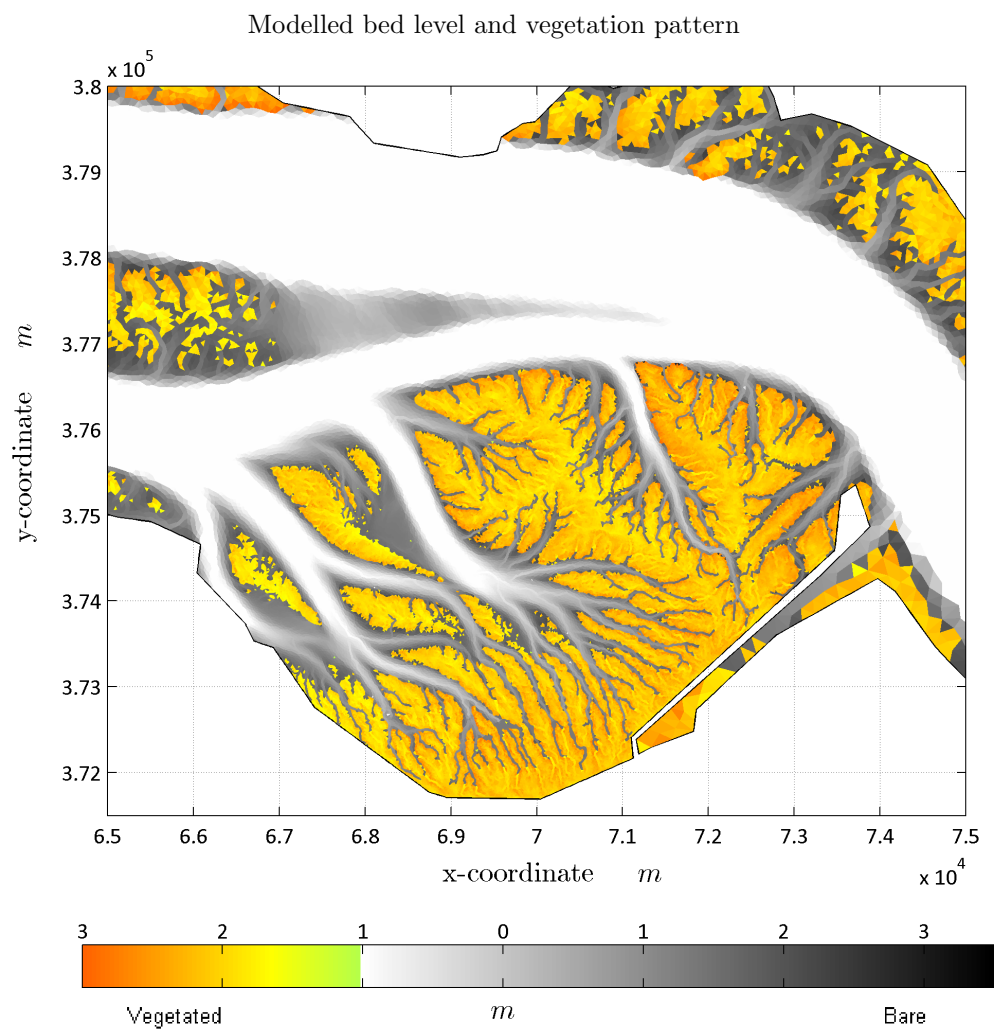


FIGURE C.8: Bed level and vegetation pattern for Saeftinghe after 58 years (in 1963), population dynamics model

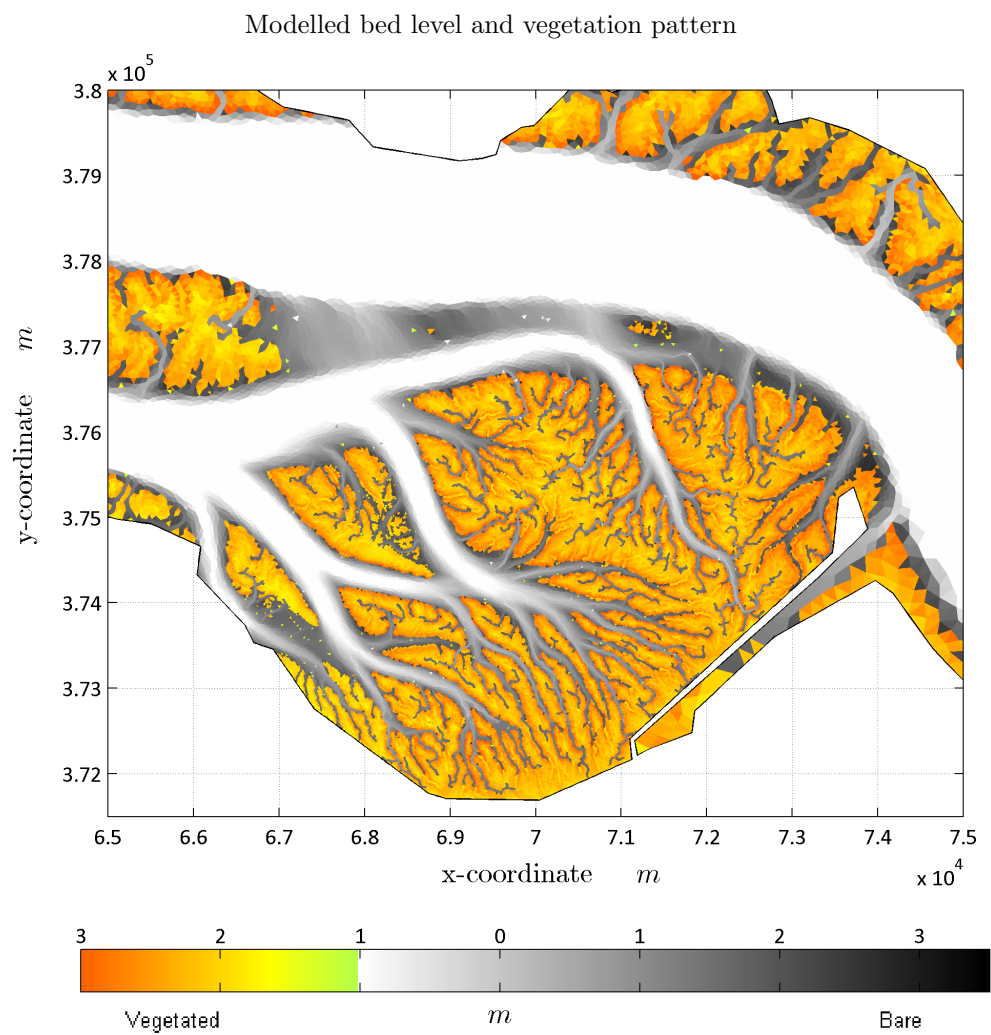


FIGURE C.9: Bed level and vegetation pattern for Saeftinghe after 87 years (in 1992), population dynamics model

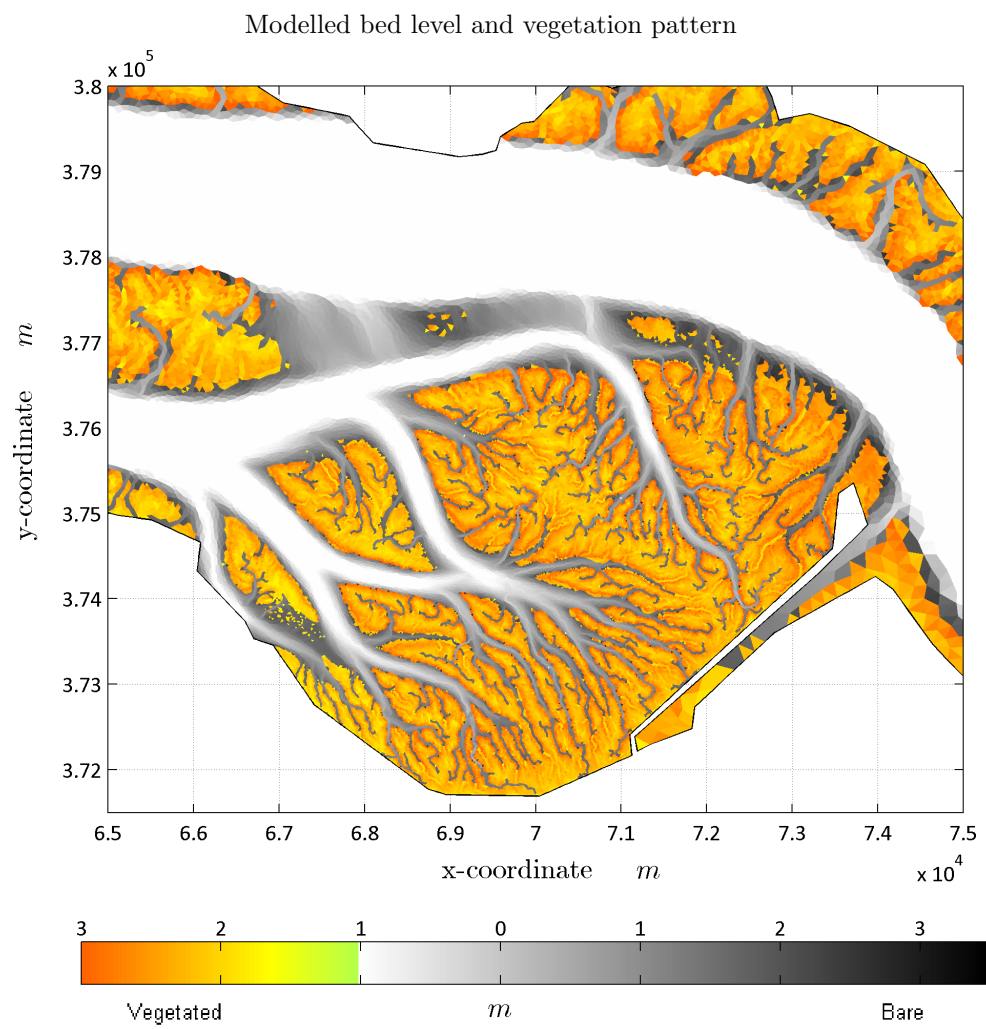


FIGURE C.10: Bed level and vegetation pattern for Saeftinghe after 99 years (in 2004), population dynamics model

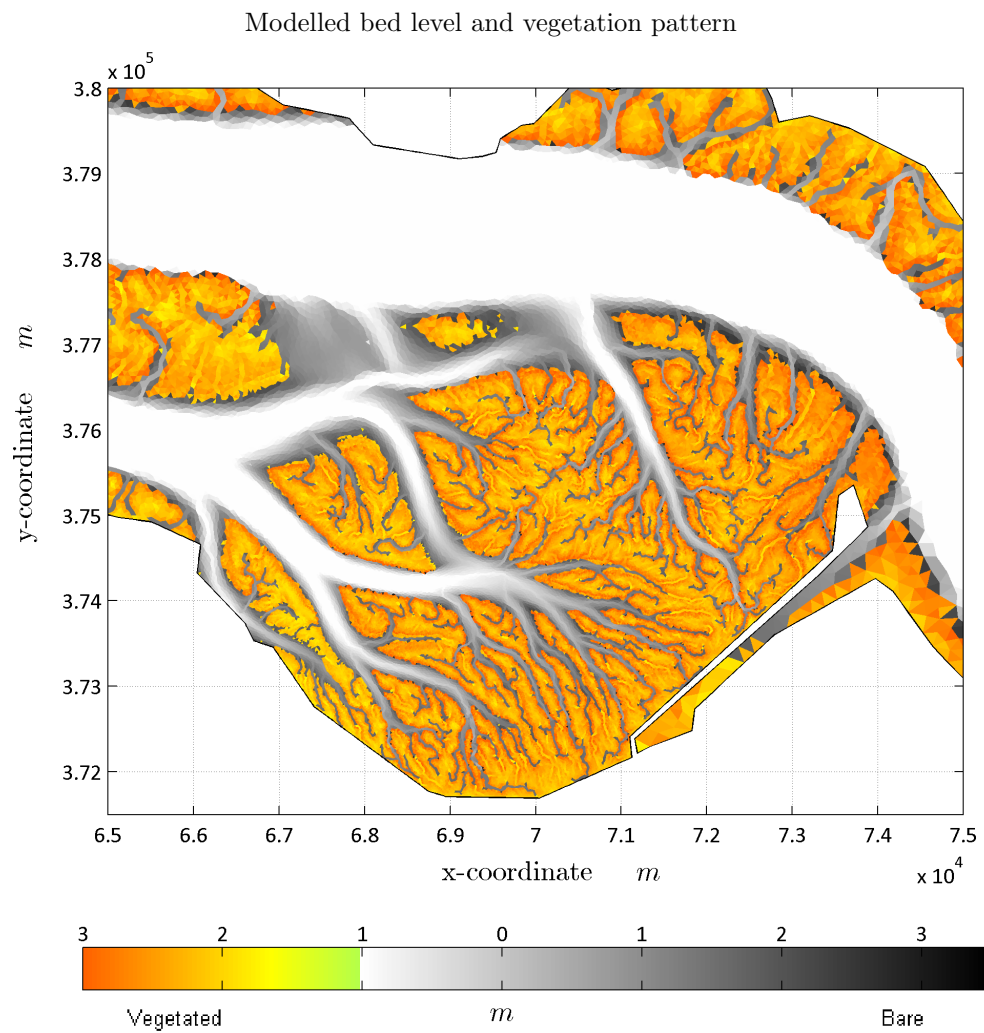


FIGURE C.11: Bed level and vegetation pattern for Saeftinghe after 122 years (in 2027), population dynamics model

C.3 Development of Saeftinghe, measured

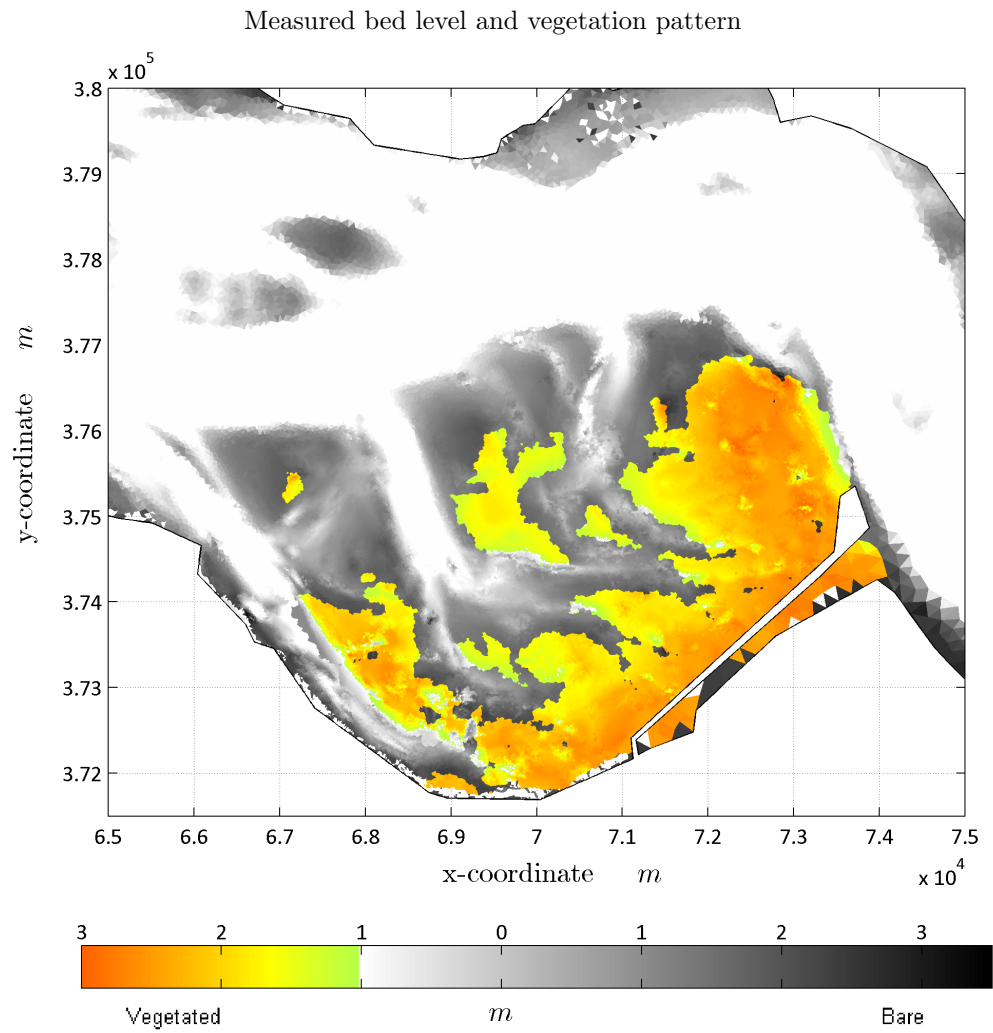


FIGURE C.12: Measured bed level and vegetation pattern for Saeftinghe after 26 years (in 1931)

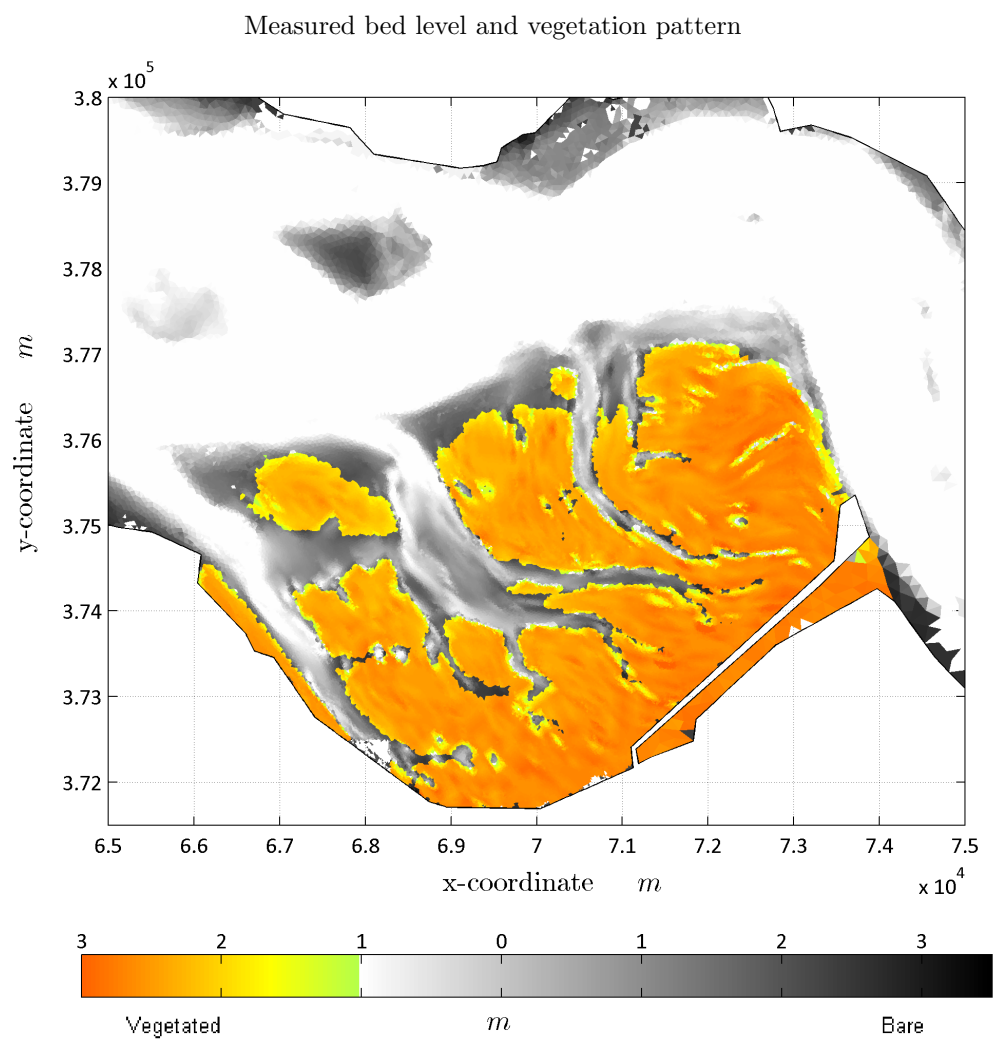


FIGURE C.13: Measured bed level and vegetation pattern for Saeftinghe after 58 years (in 1963)

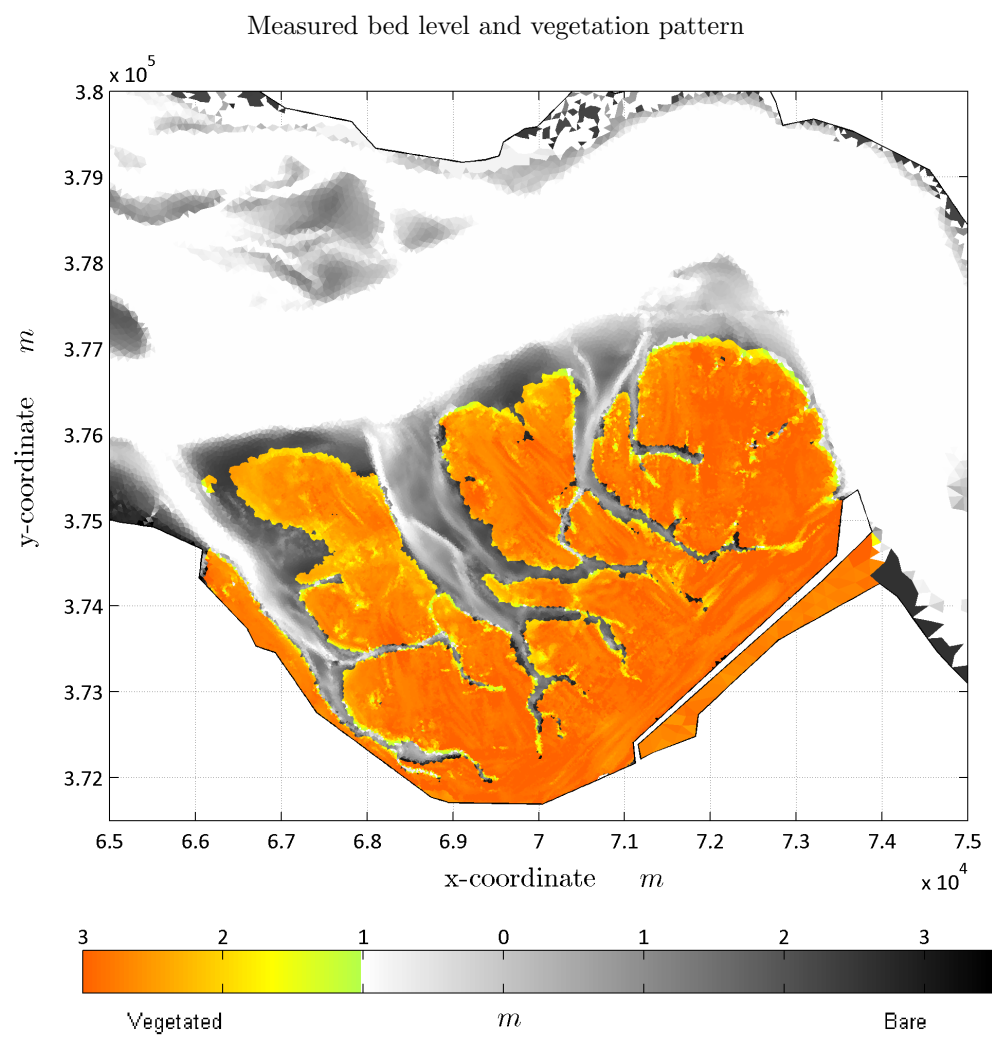


FIGURE C.14: Measured bed level and vegetation pattern for Saeftinghe after 87 years (in 1992)

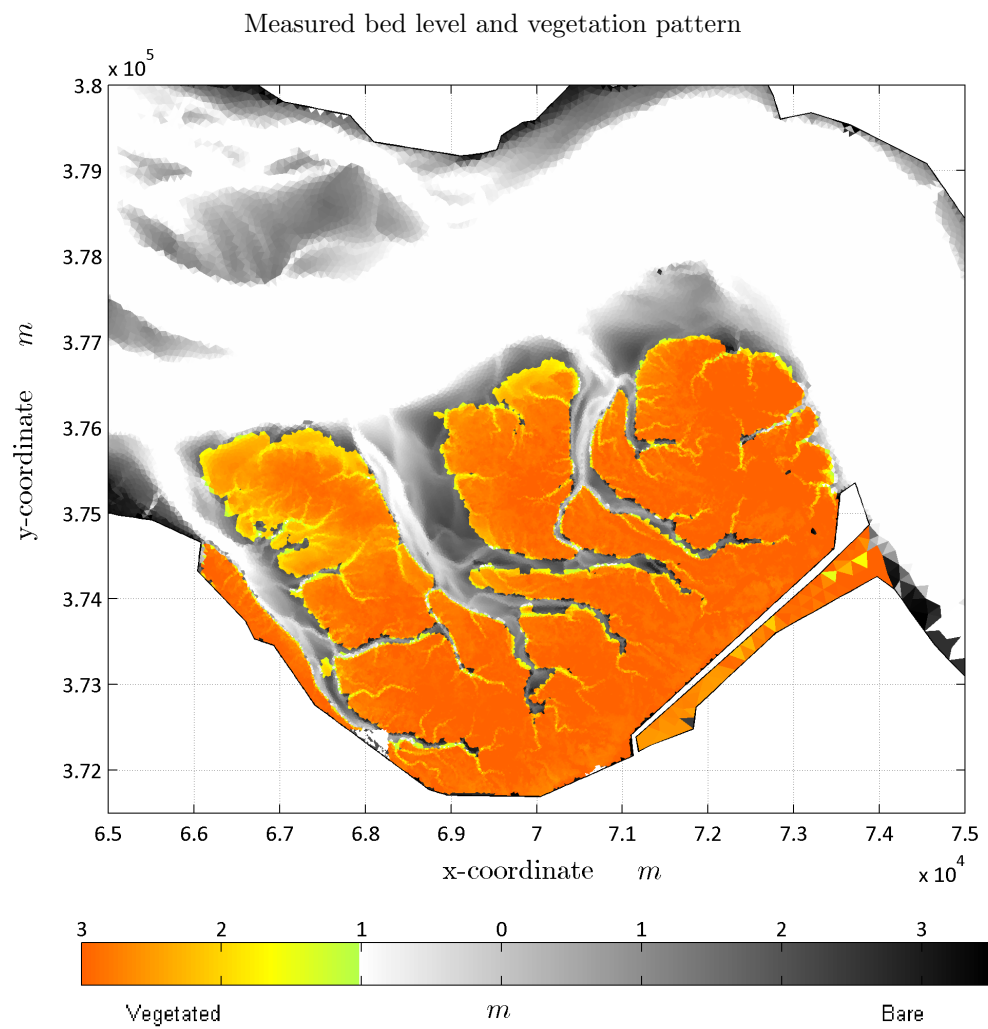


FIGURE C.15: Measured bed level and vegetation pattern for Saeftinghe after 99 years (in 2004)

C.4 Saeftinghe results for different sediment grain sizes, window of opportunity

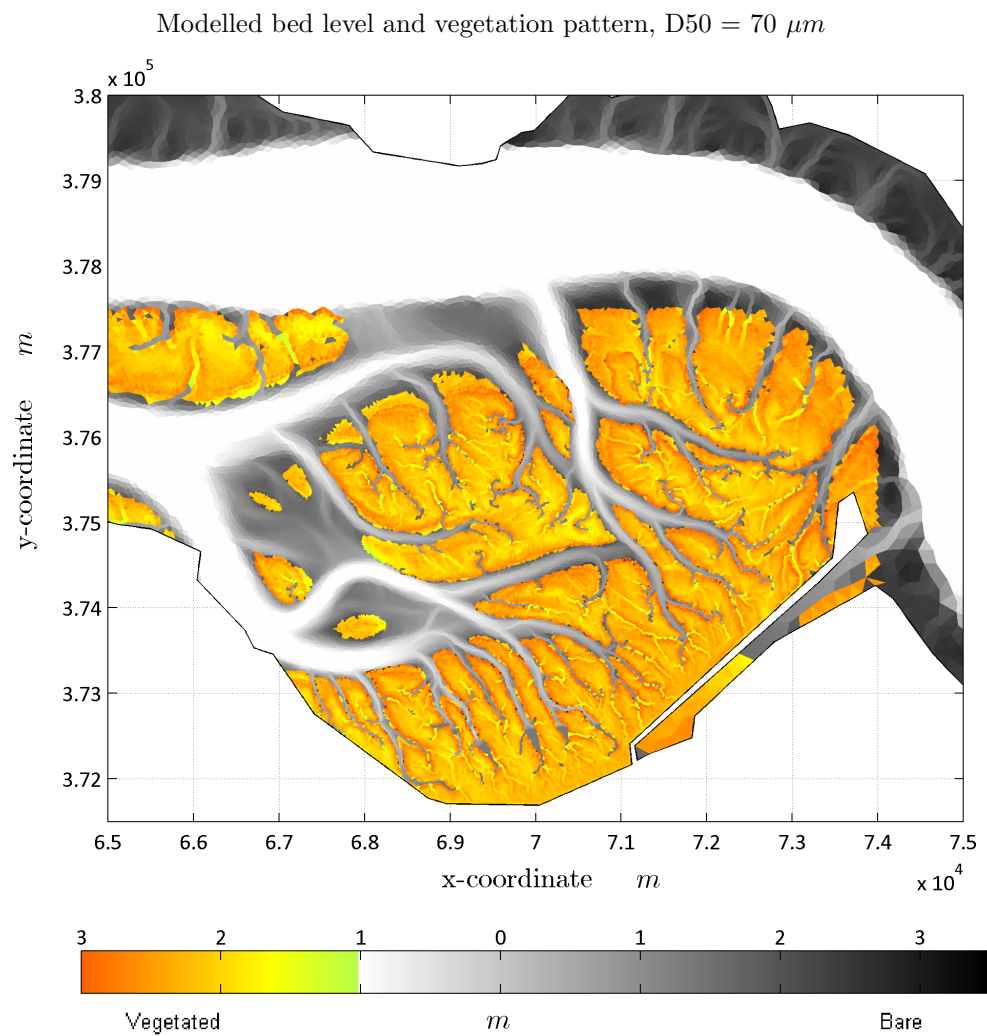


FIGURE C.16: Bed level and vegetation pattern for Saeftinghe after 148 years (in 2053), window of opportunity model

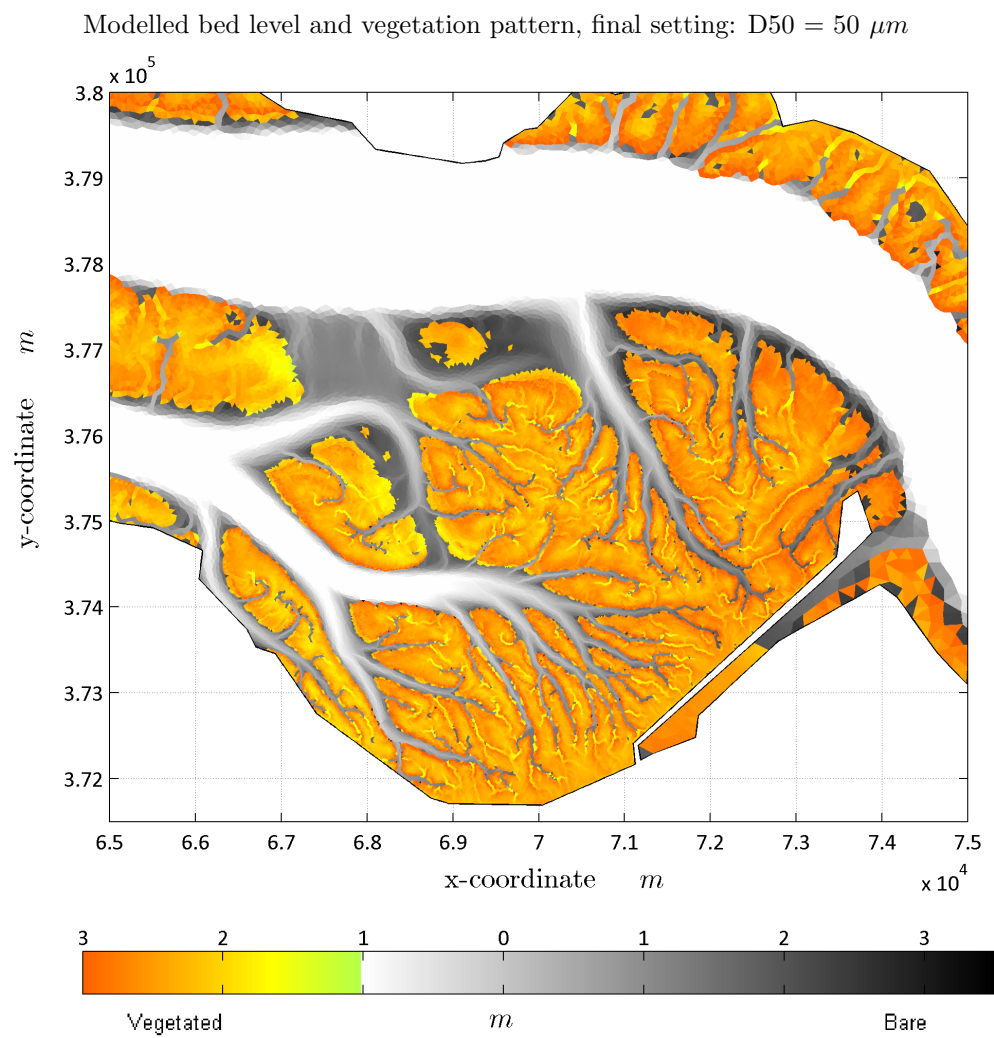


FIGURE C.17: Bed level and vegetation pattern for Saeftinghe after 148 years (in 2053), window of opportunity model

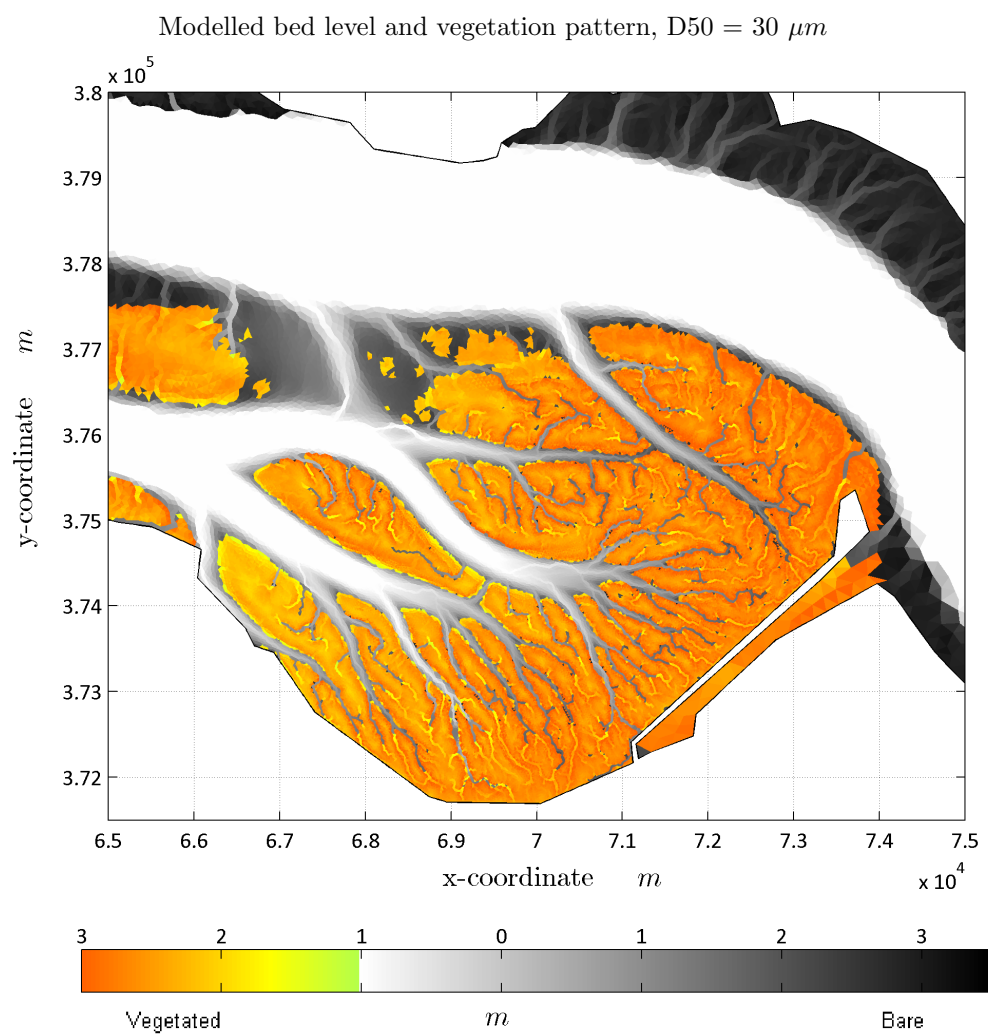


FIGURE C.18: Bed level and vegetation pattern for Saeftinghe after 148 years (in 2053), window of opportunity model

Bibliography

- Balke, T., T.J. Bouma, E.M. Horstman, E.L. Webb, P.L.A. Erftemeijer, and P.M.J. Herman (2011). “Windows of opportunity: thresholds to mangrove seedling establishment on tidal flats”. In: *Marine Ecology Progress Series* 440, pp. 1–9.
- Baptist, M.J. (2005). “Modelling floodplain biogeomorphology”. Phd Thesis. Delft University of Technology.
- Beeftink, W.G. (1965). “De zoutvegetatie van ZW-Nederland beschouwd in Europees verband”. In:
- Bouma, T.J., L.A. van Duren, S. Temmerman, T. Claverie, A. Blanco-Garcia, T. Ysebaert, and P.M.J. Herman (2007). “Spatial flow and sedimentation patterns within patches of epibenthic structures: Combining field, flume and modelling experiments”. In: *Elsevier. Continental Shelf Research* 27, pp. 1020–1045.
- Bouma, T.J., M. Friedrichs, B.K. van Wesenbeeck, S. Temmerman, G. Graf, and P. M. J. Herman (2009). “Density-dependent linkage of scale-dependent feedbacks: a flume study on the intertidal macrophyte *Spartina anglica*”. In: *Oikos* 118, pp. 260–268.
- D’Alpaos, A., Stefano Lanzoni, and Marco Marani (2005). “Tidal network ontogeny: Channel initiation and early development”. In: *Journal of Geophysical Research* 110.
- D’Alpaos, A., S. Lanzoni, M. Marani, and A. Rinaldo (2007). “Landscape evolution in tidal embayments: Modeling the interplay of erosion, sedimentation, and vegetation dynamics”. In: *Journal of Geophysical Research* 112.
- Dam, G. and B. van Prooijen (2006). “Morfodynamische berekeningen van de Westerschelde met behulp van ”FINEL2d”. In: *Eindrapport, GD/06119/1339. Svasek Hydraulics*.
- Dam, G., A.J. Bliet, R.J. Labeur, S. Iides, and Y. Plancke (2007). “Long term process-based morphological model of the Western Scheldt Estuary”. In:
- Dam, Gerard (2013). “Long-term process-based modelling of the morphology of estuaries”. Phd Thesis proposal. UNESCO-IHE Institute for Water Education.
- Dijkema, K.S., A. Nicolai, J. De Vlas and C. Smit, H. Jongerius, and H. Nauta (2001). “Van Landaanwinning Naar Kwelderwerken”. In: *Rijkswaterstaat directie Noord-Nederland*.
- Engelund, F. and E. Hansen (1967). “A monograph on sediment transport in alluvial channels”. In: *Teknik Forlag. Copenhagen*.
- Fagherazzi, S., M.L. Kirwan, S.M. Mudd, G.R. Guntenspergen, S. Temmerman, A.D’Alpaos, J. Van de Koppel, J.M. Rybczyk, E. Reyes, C. Craft, and J. Clough (2011). “Numerical models of salt marsh evolution: ecological, geomorphic and climatic factors”. In: *Review of geophysics* 49.
- Gallapatti, R. and C.B. Vreugdenhil (1985). “A depth-integrated model for suspended sediment transport”. In: *Journal of hydraulic research* 23, pp. 981–999.

- Glaister, P. (1993). "Flux difference splitting for open-channel flows". In: *Int. J. Num. Meth. Fluids* 16, pp. 629–654.
- Hughes, T.J.R. (1987). "The finite element method". In: *Prentice-Hall. Englewood Cliffs, N.J.*
- Hulzen, J.B. van, J. van Soelen, and T.J. Bouma (2007). "Morphological Variation and Habitat Modification are Strongly Correlated for the Autogenic Ecosystem Engineer *Spartina anglica* (Common Cordgrass)". In: *Estuaries and Coasts* 30.1, pp. 3–11.
- Jones, C.G., J.H. Lawton, and M. Schachak (1994). "Organisms as ecosystem engineers". In: *Ecology* 78, pp. 1946–1957.
- Keijzer, M., M. Baptist, V. Babovic, and J.R. Uthurburu (2005). "Determining Equations for Vegetation Induced Resistance using Genetic Programming". In: *GECCO*, pp. 25–29.
- Koppel, J van, D van de Wal, J.P. Bakker, and P.M.J Herman (2005). "SelfOrganization and Vegetation Collapse in Salt Marsh Ecosystems". In: *The American Naturalist* 165.1.
- LVT (2013). "LTV Veiligheid en Toegankelijkheid, Actualisatierapport Finel 2D Schelde-estuarium". In: *Achtergrondrapport A-26*.
- Rinaldo, A., S. Fagherazzi, S. Lanzoni, M. Marani, and W.E. Dietrich (1999). "Tidal networks: 2. Watershed delineation and comparative network morphology". In: *Water Resources Research* 35.(12).
- Temmerman, S., T.J. Bouma, G. Govers, Z.B. Wang, M.B. De Vries, and P.M. J. Herman (2005a). "Impact of vegetation on flow routing and sedimentation patterns: Three-dimensional modelling for a tidal marsh". In: *Journal of geophysical research* 110.
- Temmerman, S., T. J. Bouma, G. Govers, and D. Lauwaet (2005b). "Flow Paths of Water and Sediment in a Tidal Marsh: Relations with Marsh Developmental Stage and Tidal Inundation Height". In: *Estuaries* 28.(3), pp. 338–352.
- Temmerman, S., T.J. Bouma, J. Van de Koppel, D. Van der Wal, M.B. De Vries, and P.M.J. Herman (2007). "Vegetation causes channel erosion in a tidal landscape". In: *The Geological Society of America* 35.(7), pp. 631–634.
- Uthurburu, R.J. (2004). "Evaluation of physically based and evolutionary data mining approaches for modelling resistance due to vegetation in SOBEK 1D-2D". In: *M.Sc. thesis H.H.485. Unesco IHE, Delft*.
- Vreugdenhil, C.B. (1994). "Numerical methods for shallow water flow". In: *Institute for Marine and Atmospheric Research Utrecht (IMAU). Utrecht University, The Netherland*.
- Vriend, H.J. De, M. Capobianco, T. Chesher, H.E. de Swart, B. Latteux, and M.J.F. Stive (1993). "Approaches to long-term modelling of coastal morphology: A review". In: *Coastal Engineering* 21, pp. 225–269.
- Wang, C. and S. Temmerman (2013). "Does biogeomorphic feedback lead to abrupt shifts between alternative landscape states?: An empirical study on intertidal flats and marshes". In: *Journal of Geophysical Research. Earth Surface* 118, pp. 229–240.
- Wesenbeeck, B.K. van (2007). "Thresholds and shifts: consequences of habitat modification in salt-marsh pioneer zones". Phd Thesis. University of Groningen.
- Ye, Qinghua (2012). "An approach towards generic coastal geomorphological modeling with applications". Phd Thesis. UNESCO-IHE Institute for Water Education.